Grant Agreement: 814966

CARES

CITY AIR REMOTE EMISSION SENSING

D3.4 – Summary report on partner cities' measurements campaigns

WP 3
Task 3.1, 3.2, 3.3

April 2023

This project has received funding from the European Union's Horizon 2020 research and innovation program under grant agreement No 814966.

CARES website: www.cares-project.eu

Document history and validation

When	Who	Comments
August 2022	Yoann Bernard, ICCT	Definition and structure of the deliverable
April 24th 2023	Yoann Bernard, ICCT	First partial draft
April 25th 2023	Yoann Bernard, ICCT	Second draft
April 26th 2023	Åke Sjödin, IVL, Simone Casadei, Innovhub, Bartosz Piłat, KAS, Michal Vojtisek, CTU	Review of the deliverable
April 29th 2023	Yoann Bernard, ICCT	Final drafting
April 30th 2023	Åke Sjödin, IVL	Submission

Authors:

Section 1.1 : Yoann Bernard, Kaylin Lee, Rohit Nepali (ICCT), Uwe Tietge (ICCT), Marco Bedogni (AMAT).

Section 1.2 : Rebecca Wagner, David Carslaw, and Naomi Farren (University of York).

Section 1.3 : Markus Knoll (TUG), Martin Penz (TUG), Alexander Bergmann (TUG), Denis Pöhler (Airyx), Christina Schmidt (Airyx), and Hannes Juchem (Airyx).

Section 1.4 : Markus Knoll (TUG), Martin Penz (TUG), Alexander Bergmann (TUG), Simone Casadei (Innovhub SSI) and Tommaso Rossi (Innovhub SSI).

Section 1.5 : Silvia Moroni, Francesco Cruz Torres, Ramon Pedrini, Silvia Belmuso, Paolo Palomba and Marco Bedogni (AMAT), Simone Casadei, Gabriele Migliavacca, Tommaso Rossi (Innovhub SSI).

Section 2.1 : Yoann Bernard, Kaylin Lee, Rohit Nepali (ICCT), Uwe Tietge (ICCT), Peter Mock (ICCT).

Section 2.2 : Markus Knoll (TUG), Martin Penz (TUG), Alexander Bergmann (TUG), Denis Pöhler (Airyx), Christina Schmidt (Airyx), and Hannes Juchem (Airyx).

Section 3.1 : Yoann Bernard, Kaylin Lee, Rohit Nepali (ICCT), Uwe Tietge (ICCT), Michal Vojtisek (CTU).

Section 3.2 : Markus Knoll (TUG), Martin Penz (TUG), Alexander Bergmann (TUG), Denis Pöhler (Airyx), Christina Schmidt (Airyx), and Hannes Juchem (Airyx), Michal Vojtisek (CTU).

Section 3.3 : Denis Pöhler (Airyx, University of Heidelberg), Christina Schmidt (Airyx, University of Heidelberg), and Hannes Juchem (University of Heidelberg), Michal Vojtisek (CTU).

Section 4.0 : Yoann Bernard, Kaylin Lee, Rohit Nepali (ICCT), Markus Knoll (TUG), Martin Penz (TUG), Alexander Bergmann (TUG), Uwe Tietge (ICCT).

Section 5.0 : Yoann Bernard, Kaylin Lee, Markus Knoll (TUG), Martin Penz (TUG), Alexander Bergmann (TUG), Uwe Tietge (ICCT).

Section 6.0 : Yoann Bernard, Kaylin Lee

Contact: Yoann Bernard

Email: y.bernard@theicct.org

Deliverable No. D.3.4: Public report

Summary

This report summarizes the results from cities' measurement campaigns conducted in Milan, Krakow, and Prague. Covid-19 restrictions impacted the original schedule; however, the three campaigns successfully took place in each city and demonstrated the feasibility of various Remote Emission Sensing (RES) technologies. Cross-road and overhead commercial instruments, point sampling, and plume chasing were compared with reference instruments such as PEMS. As part of the Milan campaign, a good correlation was found between advanced air quality sensors and reference instruments. In addition, the positive effect of street cleaning on pollutant concentrations was established. Plume chasing was used in Prague to collect emissions from thousands of vehicles, and to conduct a tampering enforcement campaign in collaboration with the police.

The CARES city campaigns demonstrated that remote emission sensing technologies can be successfully deployed in urban settings and that the various techniques can complement each other. Commercial open-path instruments can measure various gaseous pollutants ratioed to CO_2 in relatively high traffic conditions. Point sampling, mobile sampling and plume chasing were used to successfully measure pollutants to CO_2 ratios such as for NO_x, BC, PN and speciated VOCs. Point sampling was conducted in less dense traffic flow to distinguish individual plumes. Those techniques were found to be promising approaches to further analyse emission sources and were effective in detecting highly emitting vehicles. The data confirmed the highest NO_x and PM emissions from pre-Euro 5 diesel light-duty vehicles, but significant progresses with the latest emission standards. NO_x emissions from pre-Euro 5 petrol vehicles were found to be higher than expected compared to the trend from handbook emission factors. In the winter ambient temperatures of Krakow, petrol PM emissions were higher than in the warmer campaigns of Milan and Prague. LPG-compatible vehicles were found to emit more pollutant emissions than their petrol equivalent. Finally, a small share of vehicles was responsible for significantly increasing average pollutant emission factors. Those vehicles were suspected to have a defective after-treatment system (e.g., three-way catalyst, SCR, DPF) that in some cases were tampered.

RES techniques employed during the CARES campaigns offer promising solutions to identify high-emitting vehicles or groups of vehicles and to develop effective policies for reducing emissions from transport. RES could complement periodical technical inspection of vehicles in the European Union, by providing a fast, contactless, and undetectable method of screening emissions from the fleet.

Attainment of the objectives and explanation of deviations

Description of work related to deliverable as given in DoW

The objectives were to conduct remote sensing testing in Krakow, Milan and Prague and employ commercial RES instruments, as well as point sampling and plume chasing systems further developed in WP1. The target was to use the results to identify high individual emitters or group of emitters, track policy effectiveness and well as steer new policies.

Time deviation from original DoW

According to the last amendment to the Grant Agreement the delivery date for D3.4 was 31 October 2022. The date could not be met as the vehicle specification dataset for the last campaign in Prague were first received in early 2023 from the Czech Minister of Transport. The delay is 6 months.

Content deviation from original DoW

None.

Table of Contents

1. Milan campaign

Mainly due to the pandemic, initially planned as the last campaign, the Milan demonstration was completed first among the three cities. The remote sensing testing was conducted at three locations within the city of Milan to monitor the performance of innovative systems helping to strengthen the city's low emission zone (LEZ), which bans most polluting vehicles. Two of the locations were situated in the Area C of the LEZ and Congestion Charge (city center), and one location in the surrounding Area B of the LEZ. Running from September 23 to October 18, 2021, the campaign used remote sensing technology installed at the restricted traffic zones to collect real-world vehicular emissions data and evaluate the direct impact on local air quality.

Within the scope of the measurement campaign, researchers tested newly developed remote sensing technology as part of WP1. Specifically, CARES partners evaluated, for the first time in real urban conditions, the precision and the accuracy of these sensors collocated along with a commercial system and an air quality monitoring station. The remote sensing systems were validated by using emissions data obtained by testing vehicles equipped with Portable Emissions Measurement Systems (PEMS).

The campaign was run in partnership with the Municipality of Milan and its Mobility, Environment and Territory Agency (AMAT). It was carried out with the contribution from Hager Environmental & Atmospheric Technologies (H.E.A.T.), Graz University of Technology, University of York, and Airyx. Innovhub-SSI managed the campaign with on-board emission measurements with the contribution also from the European Commission DG JRC (Joint Research Center).

The campaign was successfully carried out despite covid restrictions, last-minute change of plans, and practical difficulties encountered during the preparation. As an example, the main location we had selected during months encountered some major building renovations with scaffolding preventing us from setting up the measurement. A new site was agreed on around 2 months before the campaign started. The main hurdle during the preparation was to secure access to the electricity grid to power the point sampling systems and the two EDAR units, in compliance with the technical and safety regulations. Other problems were related to obtaining the public soil occupation permissions, to guarantee safety for pedestrians, drivers, CARES technicians, researchers and instruments and the General Data Protection Regulation compliance in relation to the data collection activities and management (number plates),

Three sampling locations were identified with the objectives to 1) collocate point sampling, one of the EDAR unit and air quality monitoring, 2) maximize the number of measurements, and 3) measure in the two areas B and C of the low-emission zone (Figure 1).

Figure 1. Testing sites in Milan. Area C: via Madre Cabrini for instrument collocation and via Bazzoni for point sampling alone. Area B: via Cilea with EDAR system alone.

Graz University of Technology (TUG) conducted together with Airyx and University of Heidelberg point sampling measurements in via Madre Cabrini (Figure 2) and via Bazzoni (Figure 3).

A van was equipped with several particle and gas analyzers detecting emissions of the passing vehicles. Light barriers were used to detect the vehicle pass time, vehicle speed and acceleration. An Automatic number-plate recognition (ANPR) camera identified the license plates of the passing vehicles for technical vehicle characteristics and statistics.

The following characteristics were measured in the point sampling van:

- Particle number concentration (PN) – TUG diffusion charger
- Black carbon (BC) mass concentration – Black Carbon Tracker, Magee Aethalometer AE33
- NO_x (NO, NO_2) – Airyx ICAD
- CO_2 – Black Carbon Tracker, Airyx ICAD

The point sampling van was co-located with an EDAR unit for remote emission sensing for more than 10 days in Madre Cabrini. In addition, to get more insights into the point sampling methodology, measurements with test vehicles equipped with PEMS were conducted both in via Madre Cabrini and in via Cilea. Innovhub-SSI conducted more than 60 vehicle passes with a DPF tampered vehicle (Volkswagen Golf, Euro 4, diesel), a high NO_x emitter (Renault Clio, Euro 6b diesel) and a bi-fuel car (Fiat Panda, Euro 4 petrol/CNG). In addition, JRC drove by the locations with two PEMS equipped vehicles (Volkswagen Transporter diesel, Euro 6d-TEMP-EVAP-ISC, and a Ford Puma Euro 6d-ISC-FCM, mild hybrid gasoline).

Figure 2. PEMS-equipped high emitting vehicle passing by the overhead remote-sensing unit and point sampling in Madre Cabrini, Milan.

The second site was via Bazzoni, a two-lane road with traffic in both directions originally assumed as a difficult measurement spot for point sampling.

Figure 3. Point sampling in via Bazzoni, Milan.

HEAT used two of their EDAR units to measure in Milan. One system was collocated in via Madre Cabrini (Area C), the second was set up in via Cilea (Area B), in a residential area with presumed higher traffic than in the city center (Figure 4).

Figure 4. PEMS-equipped bi-fuel vehicle passing by the overhead remote-sensing unit in via Cilea, Milan.

All in all, more than 37,000 vehicle passes could be identified from the EDAR units and point sampling that were matched with the detected vehicles' characteristics, obtained by Innovhub-SSI from the Italian Ministry of Transport Data Center with a deep and complete detail, reaching a significant and complete traffic emissions database useful for AMAT and the Municipality of Milan.

1.1. Analysis of the overhead EDAR remote-sensing measurements

1.1.1. Composition of the measured fleet

The overhead EDAR systems deployed in Milan collected 35,568 measurements from 19,217 unique vehicles. More measurements were available from via Madre Cabrini, located in Area C or the city center, with almost 20,000 measurements from over 10,000 vehicles, than via Cilea located in Area B, where a total number of around 15,000 measurements from 8,500 vehicles was collected. In both sites, some vehicles were measured more than once.

Vehicle classes of measured vehicles were first assessed to characterize the Milan fleet, as shown in Figure 5. Passenger car was the predominant vehicle class, representing 83% of all measured vehicles, followed by light commercial vehicle (10%). Vehicle class of a sizable share (4%) of vehicles was not identifiable, which likely indicates that they are foreign vehicles or there is a gap in the registration database. Bus and light 2/3/4 wheeler, comprising mostly of motorcycles, each accounted for 2% of the measured vehicles.

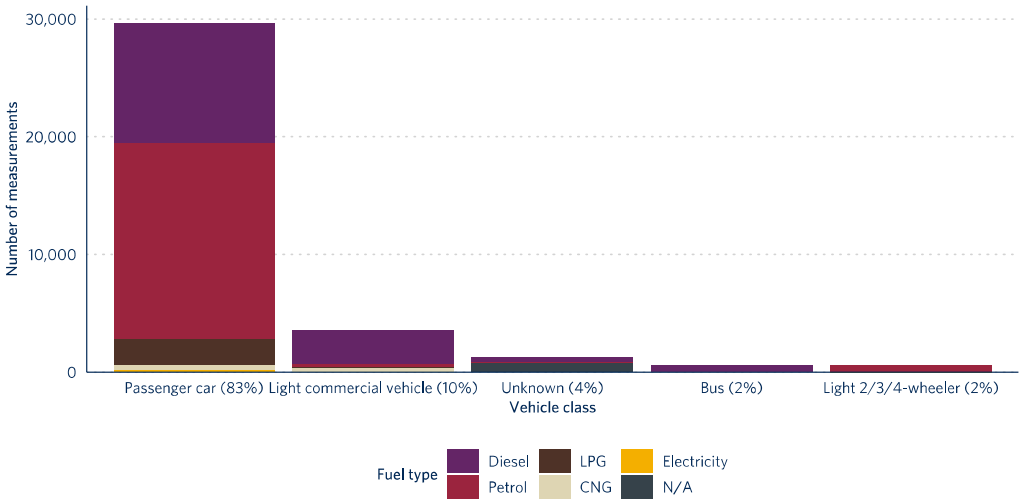

Figure 5. Distribution of vehicle classes and fuel types for all vehicles measured by the EDAR systems during the Milan demonstration campaign.

Over half of the measured passenger cars were powered by petrol and diesel, but a significant share of them were bi-fuel vehicles using liquified petroleum gas (LPG), along with petrol. Light commercial vehicles, as well as buses, were mainly diesel-powered, as it is typically the case for heavy-duty vehicles. Motorcycles and mopeds were primarily using petrol.

The composition of passenger cars, the most common vehicle class from the measurements, was further investigated. Almost 30,000 vehicle passes were collected from around 16,000 unique vehicles, with some vehicles measured by the EDAR system more than once. Similar numbers of measurements were collected from the two sites, Cilea (13,500) and Madre Cabrini (16,000). All vehicle passes from both sites, including both valid and invalid emissions measurements, were used to characterize the overall passenger car activity in Milan.

The measured passenger cars in Milan were predominantly petrol-powered (56%), followed by diesel (34%) and LPG (7%), as shown in Figure 6. Vehicles certified to the oldest available standards, such as Euro 2 and 3, and the newest ones, such as Euro 6d-TEMP and 6d, were primarily petrol vehicles. This trend is likely attributable to the longer lifespan of petrol vehicles that tend to remain in the fleet longer than vehicles of other fuel types and the decreasing popularity of diesel vehicles in the aftermath of the

"Dieselgate" scandal from Euro 6d-TEMP vehicles. Diesel vehicles represented 45% of the Euro 6 vehicles but this share fell down to 35% with Euro 6d-TEMP and 28% with Euro 6d vehicles.

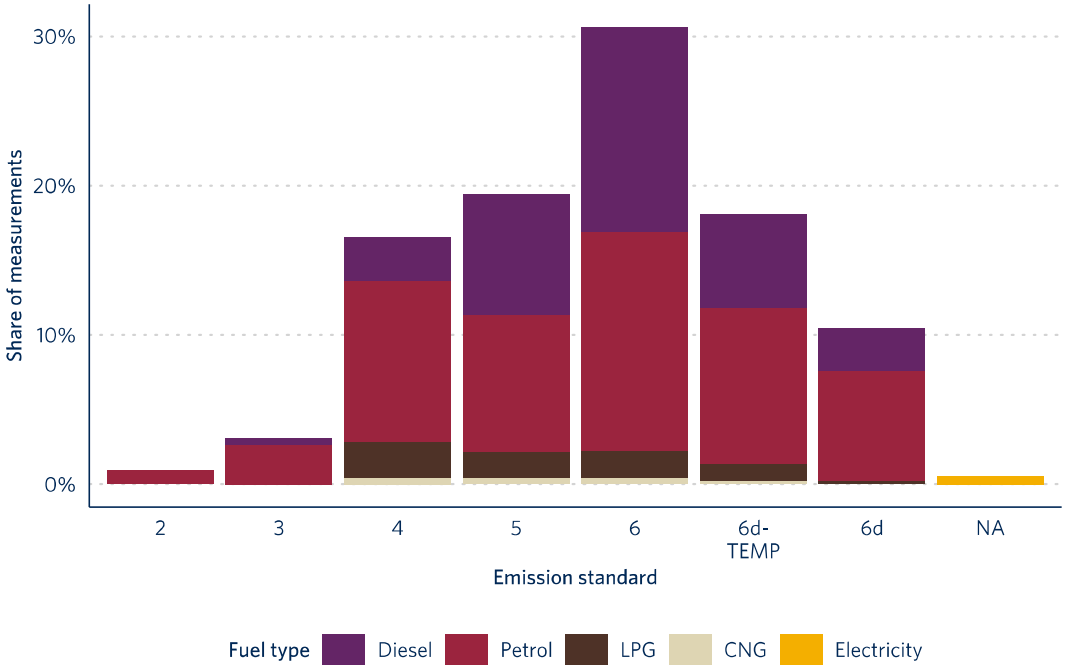

Figure 6. Composition of measured passenger cars in Milan by fuel type and emission standard.

The EDAR systems deployed in Milan notably collected a sufficient number of LPG vehicles which enables the definition of emission factors and their comparison with those of conventional fuel types, like petrol or diesel. Most of the LPG vehicles were certified from Euro 4 to 6d-TEMP. A few electric vehicles are also measured but their share was not significant.

1.1.2. Vehicle dynamic characteristics

As parameters of driving conditions are important determinants of emission performance, this section explores the driving conditions of vehicles measured in Milan. Driving conditions of all measured vehicles are summarized in Table 1. Ambient temperature has an influence on the warming of the engine and aftertreatment system, while speed, acceleration, and vehicle specific power (VSP) are good indicators of the engine load, which determines the levels of emissions.

Table 1. Average ambient temperature, vehicle specific power (VSP), speed, and acceleration of all vehicle measurements in Milan and their standard deviations.

	Ambient temp (℃)	VSP (kW/t)	Speed (km/h)	Acceleration (km/h/s)
Average	22.0	4.6	33.0	0.8
Standard deviation	3.5	6.7	13.5	2.1

At the time of the measurements in September 2021, the ambient temperature in Milan was mild, at 22℃. The average speed and acceleration were at levels representative of urban driving conditions. Speed and acceleration are used to calculate vehicle specific power in combination with the road slope information. The average VSP of all measured vehicles in Milan, whose area is entirely flat, was 4.6 kW/t, which can be considered as mild and well within the range of VSPs typically seen at type-approval emissions testing.

Vehicles measured in Cilea and Madre Cabrini showed similar distributions of ambient temperature and vehicle power demand (VSP). Speed, however, drew different pictures, as shown in Figure 7. Vehicles in via Madre Cabrini had an average speed slightly lower than those from Cilea because the street was

located in the city center. The difference in speed is later revisited to explain the difference in emission levels seen between the two sites.

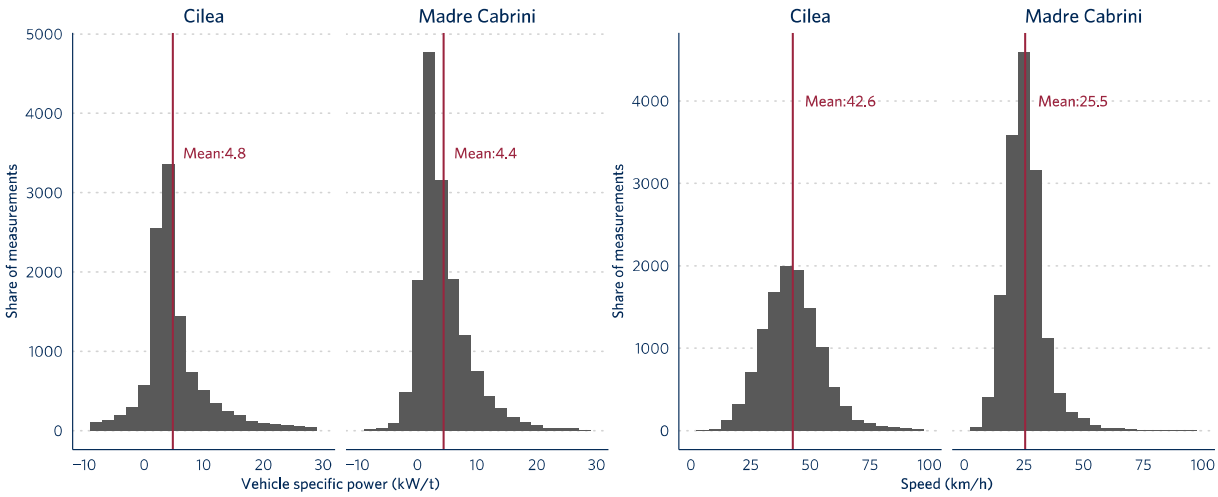

Figure 7. Distributions of vehicle specific power and speed of all measured vehicles in Milan by sites.

1.1.3. Measurement validity

Not all vehicle passes have valid emission measurements, as the detection of emissions by the EDAR instrument requires certain conditions, such as sufficient plume size or clear distinction of the vehicle plume from that of others. This section assesses the rate at which the EDAR instruments successfully measure emissions from different classes and powertrain types of vehicles.

The validity rate of emissions measurements by vehicle type is given in Figure 8. Vehicle types, such as passenger car, light commercial vehicle, and bus, had relatively high validity rates; emissions from over 70% of all passing vehicles were detected by the EDAR instruments. Light 2/3/4-wheeler, like mopeds and motorcycles, that is commonly found in Milan, however, showed a lower validity rate of 29%. The difficulty of emissions detection from mopeds and motorcycles can be attributable to the fact that they drive closer to the side of the road, farther from the EDAR set up and have relatively small plumes, especially under the flat road conditions of Milan.

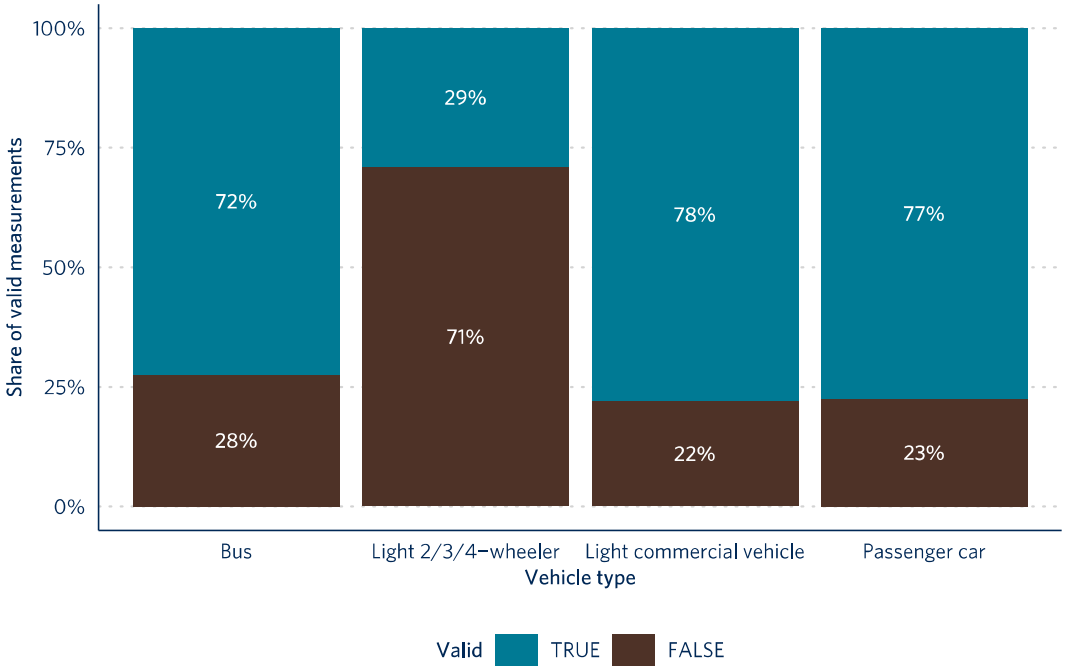

Figure 8. Validity rate of emissions measurements by vehicle class. Only vehicle types with more than 50 measurements are presented.

The emissions validity was also assessed for vehicles of different powertrain types. As it is expected from remote sensing measurements, the share of valid emissions in all measurements diminished with increasing levels of electrification. The results, however, demonstrated that commercial remote sensing instruments can be used to detect emissions from hybrid vehicles as well. As shown in Figure 9, vehicles with internal combustion engines, which made up the majority of the vehicles measured, had the highest validity rate of 79%. Conventional hybrid vehicle (HEV) and plug-in hybrid followed with respective validity rates of 69% and 64%. The latter indicated that plug-in hybrids were emitting tailpipe emissions, or using internal combustion engines, at least 64% of the time. The results also highlight the potential usage of remote sensing in the emission assessment of plug-in hybrid vehicles, as well as ICE vehicles.

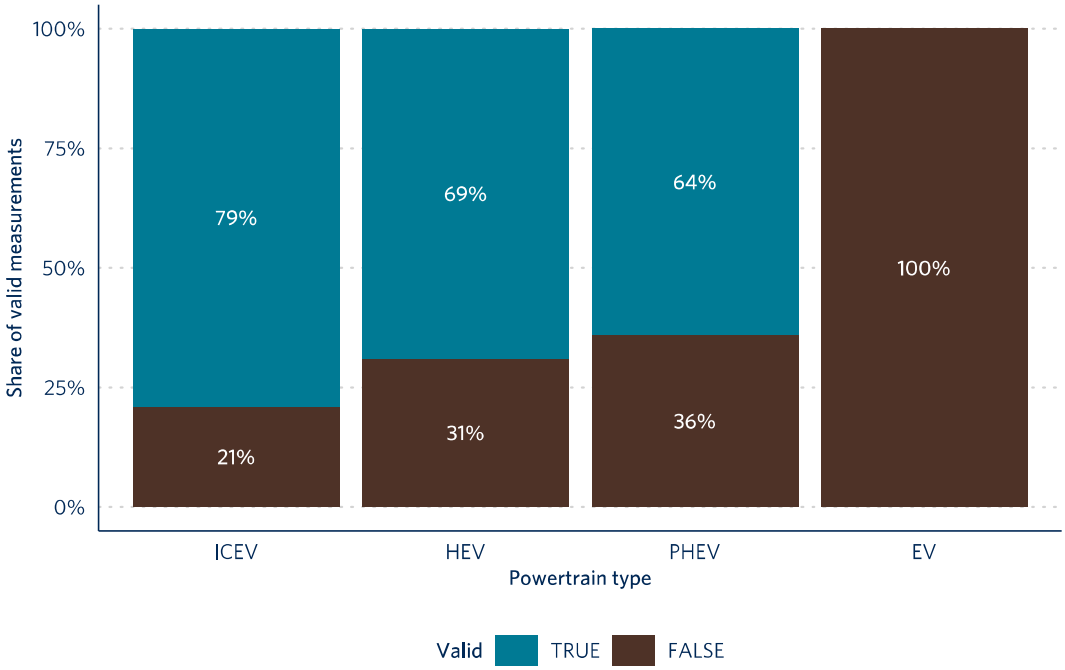

Figure 9. Validity rate of emissions measurements by powertrain type. Only powertrain types with more than 50 measurements are presented.

1.1.4. Emissions

The following section examines the pollutant emissions from passenger cars measured in Milan, as they constituted the largest sample. Emissions of all pollutants detectable by the EDAR systems, namely NO_x, PM, CO, and HC were investigated for the two main conventional fuels, diesel, and petrol. The results from the EDAR data reiterated previous study findings that diesel passenger cars emit significantly higher NO_x emissions than petrol counterparts prior to the introduction of the 6d-TEMP emission standard (Figure 10). Euro 6d-TEMP diesel vehicles, from which standard additional on-road emissions testing has been required, achieved a 75% reduction in NO_x emissions compared to its preceding standard, Euro 6. Petrol vehicles showed a steady improvement in NO_x emission performance over time with newer standards like Euro 6d-TEMP and Euro 6d emitting average NO_x emissions below 1 g/kg.

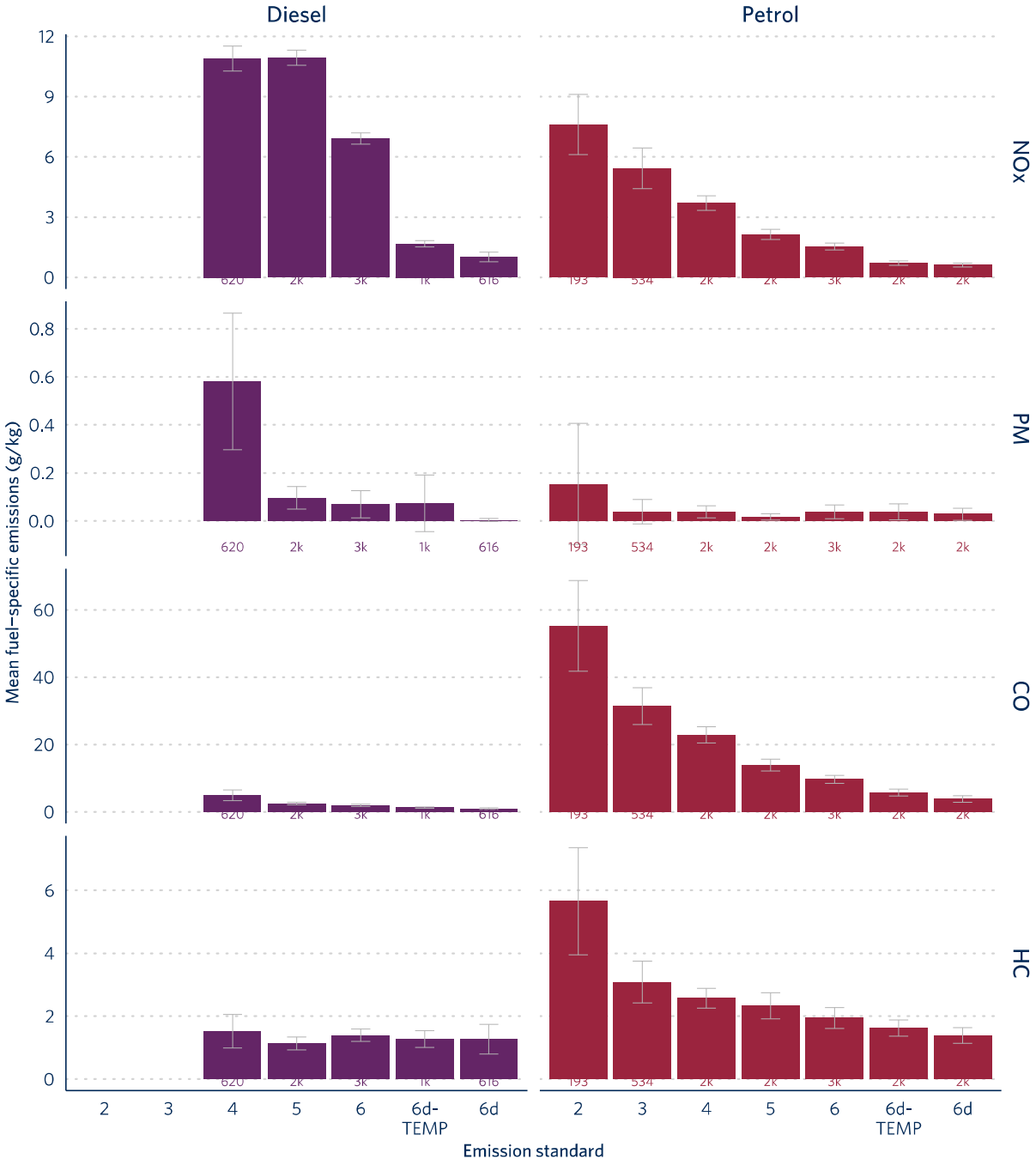

Figure 10. Fuel-specific emissions from diesel and petrol passenger cars measured in Milan with the two EDAR units. Only results from 100 or more measurements are presented.

Diesel vehicles were also mostly responsible for PM emissions in Milan. Particularly, the average PM emissions from Euro 4 diesel vehicles were notably high compared to the rest of the vehicles. Average PM levels from post-Euro 4 diesel vehicles, however, are reduced by over 80% from the Euro 4 level owing to the introduction of diesel particulate filters. The results show variable PM emissions from newer standards, which is further addressed later in this report.

CO and HC emissions were predominantly emitted by petrol vehicles as a result of incomplete combustion of petrol fuels. Both CO and HC emission performance of petrol vehicles, however, improved significantly with the introduction of newer standards. The average HC emissions from the newest Euro 6d petrol vehicles were on par with those from the diesel counterparts.

Despite the low number of LPG- and CNG-powered cars, preliminary results suggested that they are not performing better in terms of emissions than their petrol equivalents (Figure 11). NO_x emissions from LPG and CNG were higher across all emission standards than petrol vehicles, debunking the conventional belief that these alternative fuels are cleaner. Also, significantly elevated levels of CO

emissions from LPG vehicles were found. Additionally, a glimpse at methane (CH_4) measurements showed that CNG vehicles were emitting significantly higher levels of methane than petrol or LPG vehicles. These results are particularly important for Milan, as the current low-emission zone exempts LPG and CNG vehicles from its restrictions, due to the current national laws.

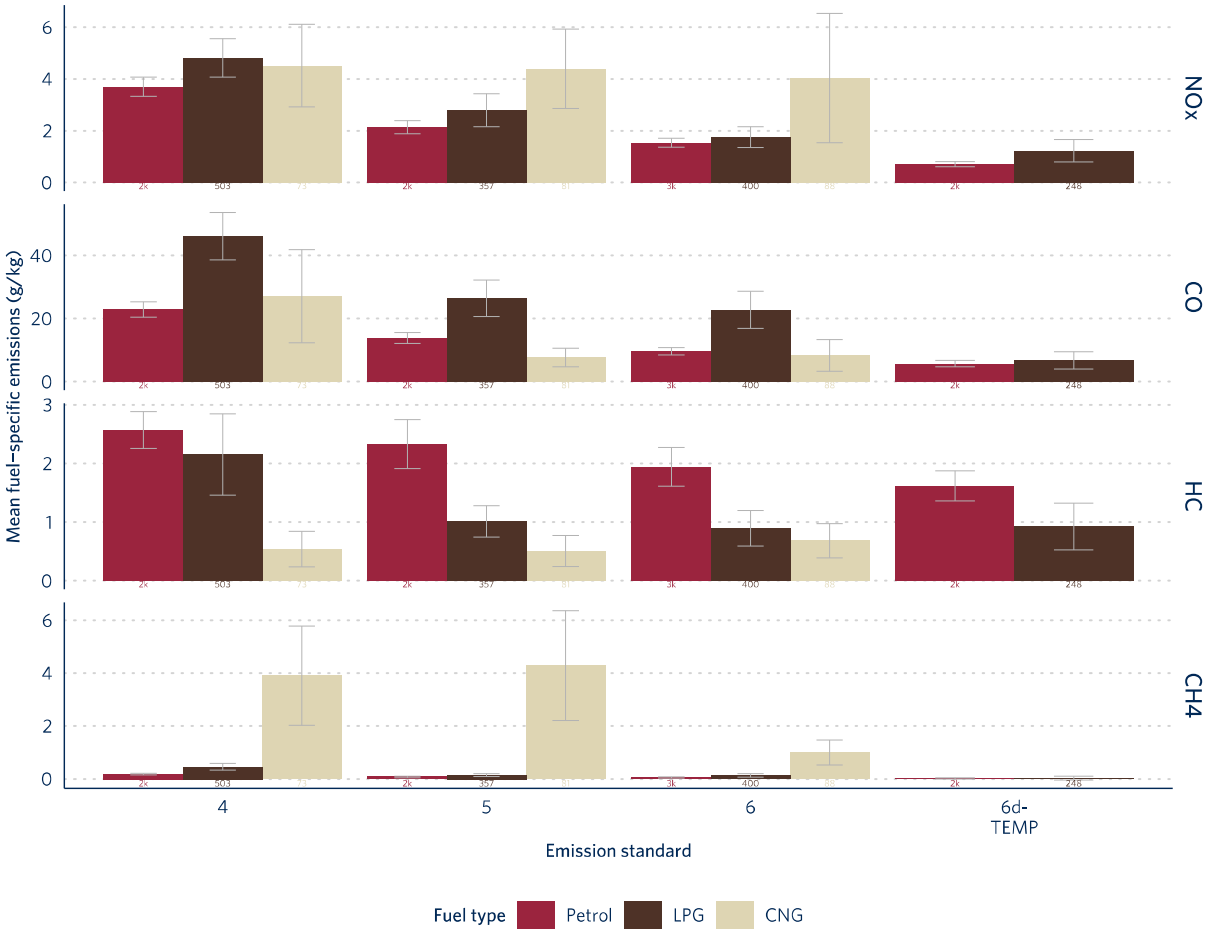

Figure 11. Fuel-specific emissions from petrol, LPG, and CNG passenger cars measured in Milan with the two EDAR units. Only results from 50 or more measurements are presented.

Fuel-specific NO_x emissions were converted to distance-specific NO_x emissions to enable the NO_x performance comparison across different fuel types. This was done using type-approval CO_2 information available from the registry data and relevant adjustment factor for real-world CO_2 emissions.[1] Such comparison across fuel types demonstrated the outsized NO_x emissions from diesel vehicles compared to other fuel types (Figure 12). It also reemphasizes the importance of limiting the use of LPG and CNG vehicles as well as diesel and petrol vehicles in Milan.

[1] Yoann Bernard et al., "Determination of Real-World Emissions from Passenger Vehicles Using Remote Sensing Data" (Washington, D.C.: TRUE Initiative, June 5, 2018), https://theicct.org/publication/determination-of-real-world-emissions-from-passenger-vehicles-using-remote-sensing-data/.

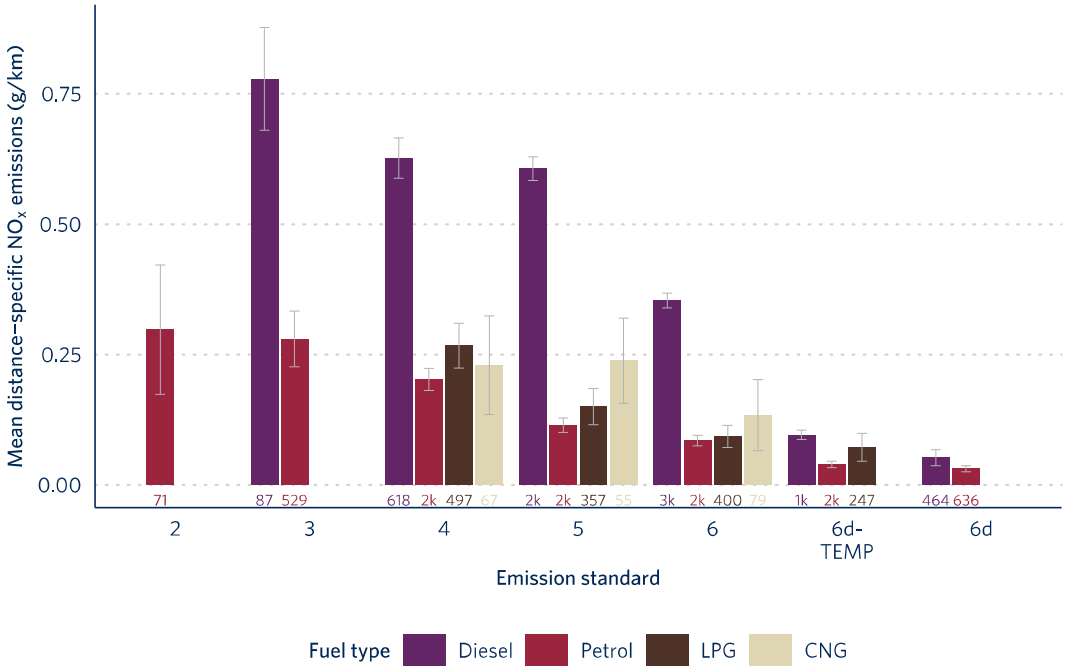

Figure 12. Distance-specific emissions from passenger cars of all fuel types measured in Milan with the two EDAR units. Only results from 50 or more measurements are presented.

Distance-specific NO_x emissions from vehicles measured in two testing sites are shown in Figure 13. When compared with type-approval limits (although the comparison is indicative, given that the limits refer to standard cycles performed in laboratory), diesel vehicles certified to below Euro 6d-TEMP showed real-world emissions multiple times the limits. Petrol and LPG vehicles certified to below Euro 6 also showed exceedances of regulatory limits in real-world operation. Newer vehicles subject to on-road testing, Euro 6d-TEMP and Euro 6d, however, were emitting NO_x at levels below on-road (RDE) limits.

NO_x emissions from diesel vehicles older than Euro 6d-TEMP in Madre Cabrini were 45% - 58% higher than those measured in Cilea. This difference in NO_x emissions between the two sites suggests that emission performance of vehicles could be influenced by the different driving conditions. Vehicles measured in Madre Cabrini had a slower average speed which is characteristic of urban driving conditions. Via Madre Cabrini is located in the city center and therefore the cars measured on via Madre Cabrini were more likely to have cold engines than those in via Cilea, due to the short driving distances urban drivers typically drive. However, this hypothesis does not explain the lower NO_x emissions in via Cabrini for newer diesel and most petrol and LPG vehicles, although the difference between the two sites diminished with newer standards.

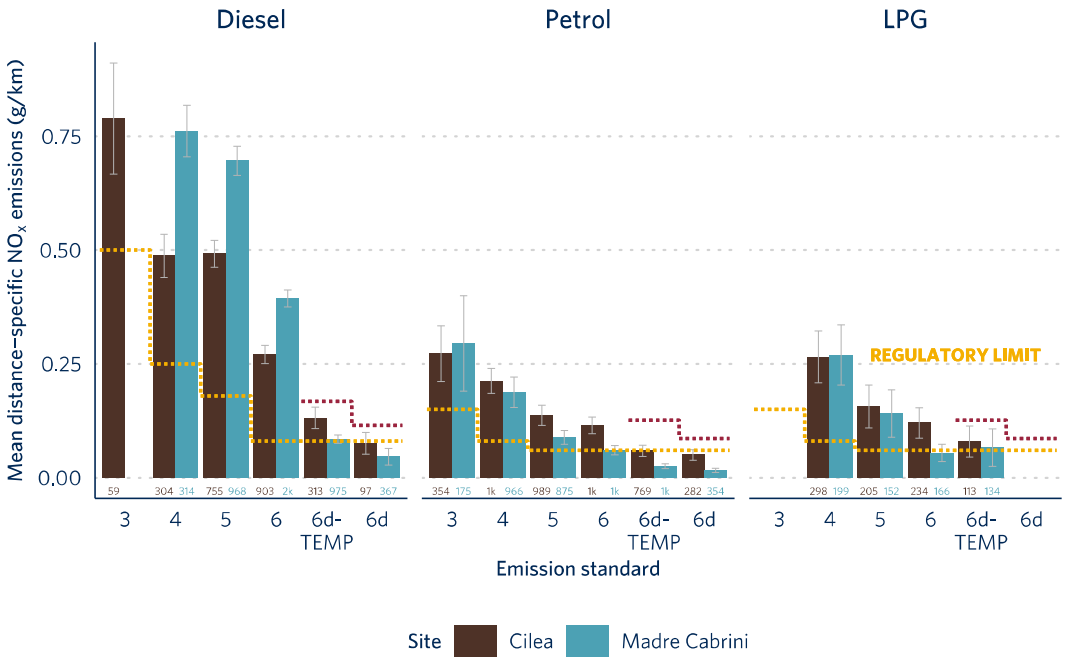

Figure 13. Distance-specific NO_x emissions from passenger cars measured in Milan broken down by site. Only results from 50 or more measurements are presented.

Average NO_x levels of petrol and diesel cars measured in Milan were further compared with EEA emission factors (EEA air pollutant emission inventory guidebook 2019 - Passenger cars, light commercial trucks, heavy-duty vehicles including buses and motorcycles –Updated October 2021) calculated according to the following main assumptions (most of them agreed with AUTH / EMISIA):

- mean ambient Temperature: 20 °C

- trip length for passenger cars: 12 km

- mean speed: 20 km/h

- cumulative activity: total mileages provided by the Italian Ministry, excepting for Euro 3 diesel (set equal to 200,000 km because the experimental total mileage is higher than 200,000 km, but the EEA methodology for the degradation calculation is valid up to 200,000 km) and for Euro 6d-TEMP / Euro 6d (the total mileages provided by the Italian Ministry are not representative for these two classes because the first regulatory inspections are done after four years from the car's first registration).

The following Table summarizes the total mileages used for the EEA emission factors calculation.

Table 2. Total mileages used for the EEA emission factors calculation.

	Euro 2	Euro 3	Euro 4	Euro 5	Euro 6	Euro 6d-TEMP	Euro 6d
diesel		200,000	175,910	130,464	85,691	50,000	20,000
petrol	142,896	135,123	119,351	91,586	61,887	25,000	10,000

The obtained NO_x EEA emission factors were compared to those measured in Milan by the EDAR units. To avoid discrepancies due only to the g/kg to g/km conversion, the comparison of the two datasets was not carried out on the absolute values, but on the base of the relative variations referring to a specific "reference" technology, in particular to Euro 5 that was well known when the EEA methodology update was released. In other words, the two datasets were normalized to the respective Euro 5 Emission Factor: the EDAR values normalized on the base of the EDAR's Euro 5 EF, and the EEA values normalized on the base of the EEA's Euro 5 EF.

The following two Figures show the percentage variation of NO_x emission factors, separately for petrol and diesel cars. In order to examine the sensitivity of the EEA degradation factor, the calculated EEA

emission factors are provided for two cases: with a degradation estimated using the total mileages provided by the Italian Ministry, and with a "maximum degradation factor" estimated using 200,000 km for all technologies before Euro 6 and 50,000 km for all Euro 6 technologies.

The pictures show that, for example, the petrol cars EF variations for Euro 3/4 vs Euro 5 measured by EDAR units are higher than those provided by EEA and lower for Euro 6, suggesting that maybe some more investigations could be useful to analyze possible discrepancies for technologies before Euro 6d-TEMP, whose NO_x emissions could be underestimated. As for diesel cars, the discrepancy for Euro 6 only suggests that the NO_x emission estimations carried out in the city of Milan could overestimate the contribution of that category.

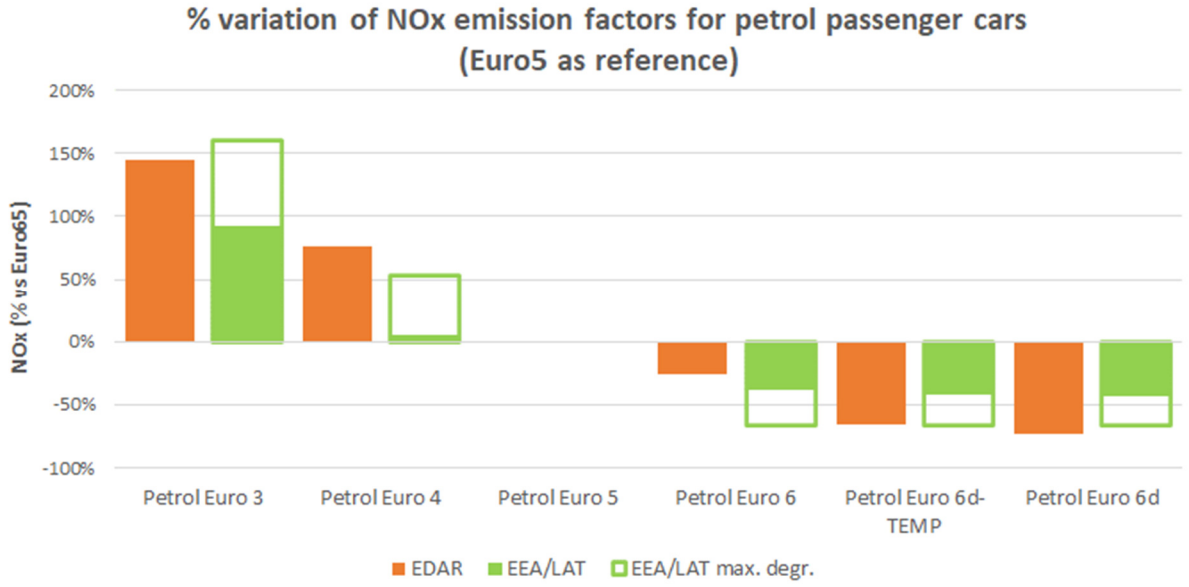

Figure 14. Percentage variation of NO_x emission factors for petrol passenger cars.

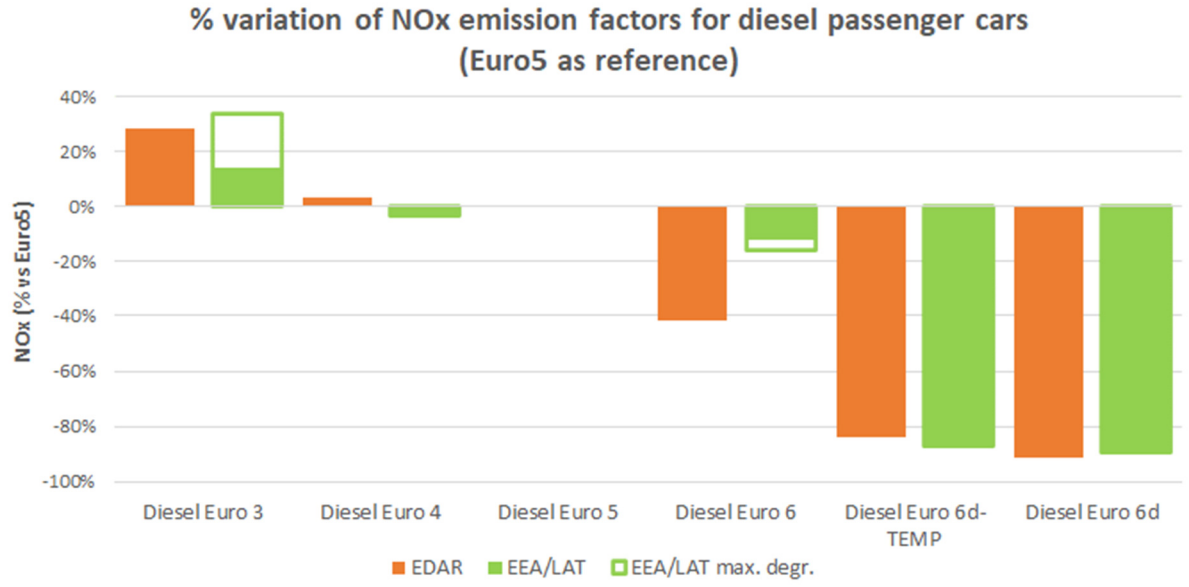

Figure 15. Percentage variation of NO_x emission factors for diesel passenger cars.

PN results

A supplementary analysis was conducted to troubleshoot the PM trend exhibited by the passenger cars measured in Milan by the EDAR. To do that, the raw data expressed in particulate number per CO_2

(nanomole per moles) was further analyzed.[2] The PN results were converted to distance specific emissions to allow a comparison with the Euro 5b/6 emission standard limits (although the comparison is indicative, given that the limit refer to standard cycles performed in laboratory).

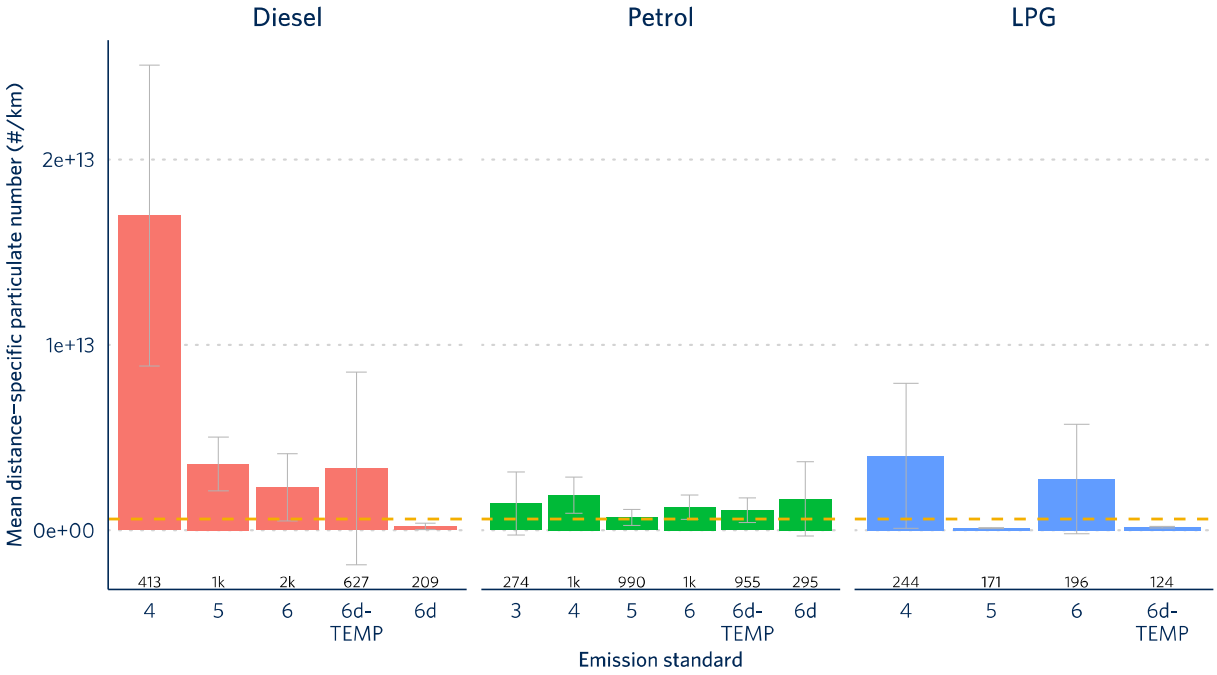

Figure 16. Passenger cars distance-specific PN emissions by fuel type and emission standard.

Figure 16 shows the improvement on diesel PN emissions with the successive emissions standards and especially the introduction of DPF with Euro 5. The results on petrol and LPG are highly variable in some cases (e.g., LPG Euro 4 and Euro 6) due to the presence of high emitters.

Overall, PN emissions measured by the EDAR tend to exceed the Euro 5b/6 limit for PN (6×10^{11}). The EDAR remote sensing reportedly captures PN with volatile compounds, which may explain the high levels of emissions shown in the results. Other reasons may include the presence of malfunctions and regeneration events for DPF equipped vehicles.

PN high-emitters and percentiles

[2] The EDAR scales up the PN to PM using a fixed molar mass.

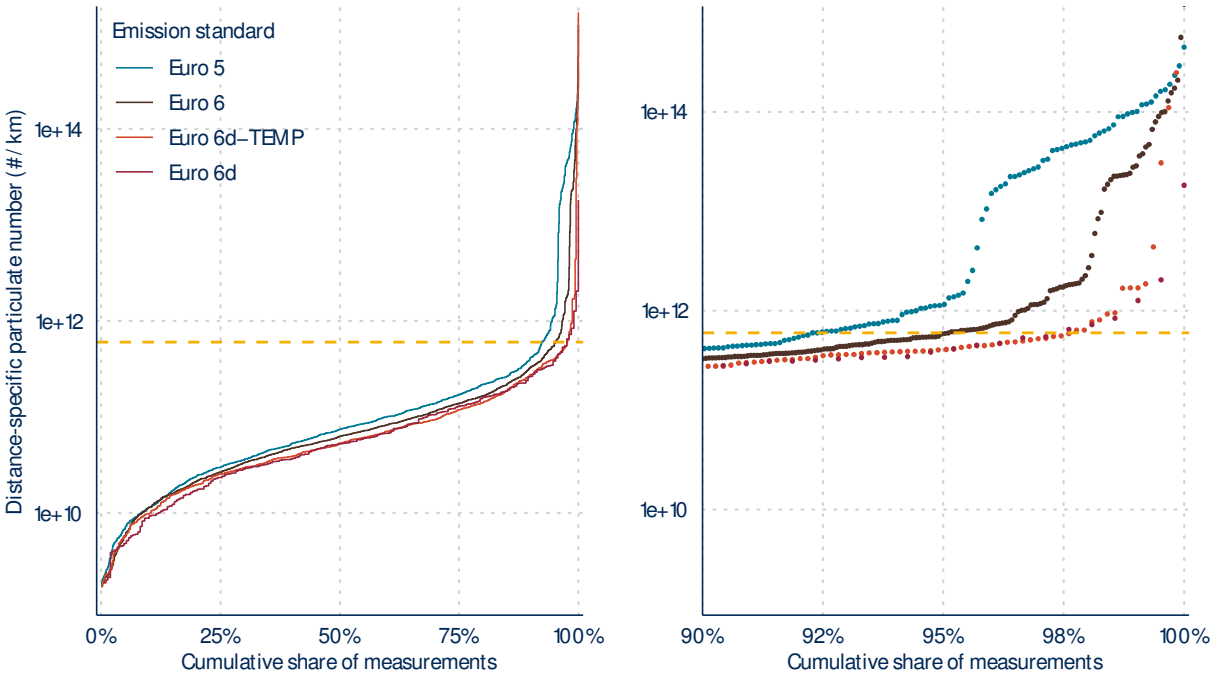

Figure 17. Cumulative share of distance-specific PN emissions from diesel Euro 5 and newer

Figure 17 shows the cumulative share of PN for diesel passenger cars equipped with DPF. The results indicate that the PN records from the EDAR are over the emission standard limit for 8% of the measurements for Euro 5, but for a lower share for successive standards.

1.2. Point and mobile sampling of Volatile Organic Compounds (VOC) monitoring

The University of York carried out a combination of both point sampling and mobile measurements of VOCs and other trace gas species. High time resolution measurements of multiple species were carried out using the University of York mobile laboratory.[3] The mobile laboratory contains a Selected-Ion Flow-Tube Mass Spectrometer (SIFT-MS) for measurements of speciated VOCs and an Iterative Cavity enhanced Differential Optical Absorption Spectrometer (ICAD) for measurements of CO_2 and NO_x.

The aim of the point sampling measurements was to test the new method of vehicle emissions measurements and to also investigate if the SIFT-MS could be used to derive VOC emission ratios of vehicles. The aim of the mobile measurements was to complement the point sampling measurements and to demonstrate that the SIFT-MS in the mobile laboratory can be used to obtain spatial VOC measurements in an urban area. An overview of the point sampling and mobile measurements will be discussed below.

Point sampling measurements were carried out at Via Madre Cabrini. The sample inlet for the mobile laboratory was placed underneath the HEAT remote sensing equipment and vehicle information was recorded using an automatic number plate recognition camera placed on the dashboard of the TUG/Airyx van. A total of 108 hours of point sampling measurements were conducted (4.5 days), between 27/09/2021 and 02/10/2021. The point sampling data collection was paused between approximately 09:00 and 16:00 local time on 30/09/2021 and 01/10/2021 to conduct the mobile measurements.

[3] Rebecca L. Wagner et al., "Application of a Mobile Laboratory Using a Selected-Ion Flow-Tube Mass Spectrometer (SIFT-MS) for Characterisation of Volatile Organic Compounds and Atmospheric Trace Gases," *Atmospheric Measurement Techniques* 14, no. 9 (September 16, 2021): 6083–6100, https://doi.org/10.5194/amt-14-6083-2021.

Mobile measurements were carried out between 10AM to 4PM on the 30th of September and the 1st of October 2021 during daytime hours (09:00-15:00). The measurement route is shown in section 1.2.2. The total distance is 13.2 km, covering a variety of areas of Milan- including inside and outside of the low emissions zone and inside and outside of the city center. There are a series of ring roads surrounding the city of Milan which form an expanding circle from the center (Area C) outwards into Area B. Area B is a Low Emission Zone (LEZ) with no access for the most polluting vehicles and Area C is a combined Urban Toll Road and LEZ. The measurement route was designed to capture a `slice' of the circular ring roads, to capture potential changes in vehicle fleet, congestion levels and other emission sources. The route was driven a total of 7 times, resulting in ~13 hours of mobile measurements.

The SIFT-MS was operated at a time resolution of 1 Hz for point sampling measurements and 2 Hz for mobile measurements. A range of speciated VOCs were measured by the SIFT-MS, including toluene, benzene, m-xylene, ethanol, trimethylbenzene, 1,3-butadiene, propane, acetaldehyde, and acetone.

1.2.1. Point sampling of VOCs

Alignment of species

Point sampling measurements are used to determine emissions of pollutants from road vehicles, and this is typically done by calculating ratios between pollutants (emission ratios). Combustion-related emissions are determined by calculating the ratio of a pollutant to CO_2 as this represents the amount of a pollutant emitted per unit of fuel burnt.[4,5] It is therefore important that measurement data is aligned to a vehicle pass and that pollutants are aligned to one another.

Figure 18 shows an example of two vehicle passes and corresponding pollutant peaks measured by the SIFT-MS and the ICAD after the data has been aligned manually using lighter tests. The lighter tests were conducted daily to determine the lag time between the sample inlet and the different instruments. Increases in CO_2 and NO_x are shown for both of the vehicle passes and increases in the selected VOC compounds are shown for the first vehicle pass. The pollutant peaks associated with the first vehicle reach a maximum slightly before the vehicle pass time, however, pollutant peaks associated with the second vehicle pass reach a maximum slightly after the vehicle pass time.

[4] Claudia S. Hak et al., "A New Approach to In-Situ Determination of Roadside Particle Emission Factors of Individual Vehicles under Conventional Driving Conditions," *Atmospheric Environment* 43, no. 15 (May 1, 2009): 2481–88, https://doi.org/10.1016/j.atmosenv.2009.01.041.

[5] Å M. Hallquist et al., "Particle and Gaseous Emissions from Individual Diesel and CNG Buses," *Atmospheric Chemistry and Physics* 13, no. 10 (May 27, 2013): 5337–50, https://doi.org/10.5194/acp-13-5337-2013.

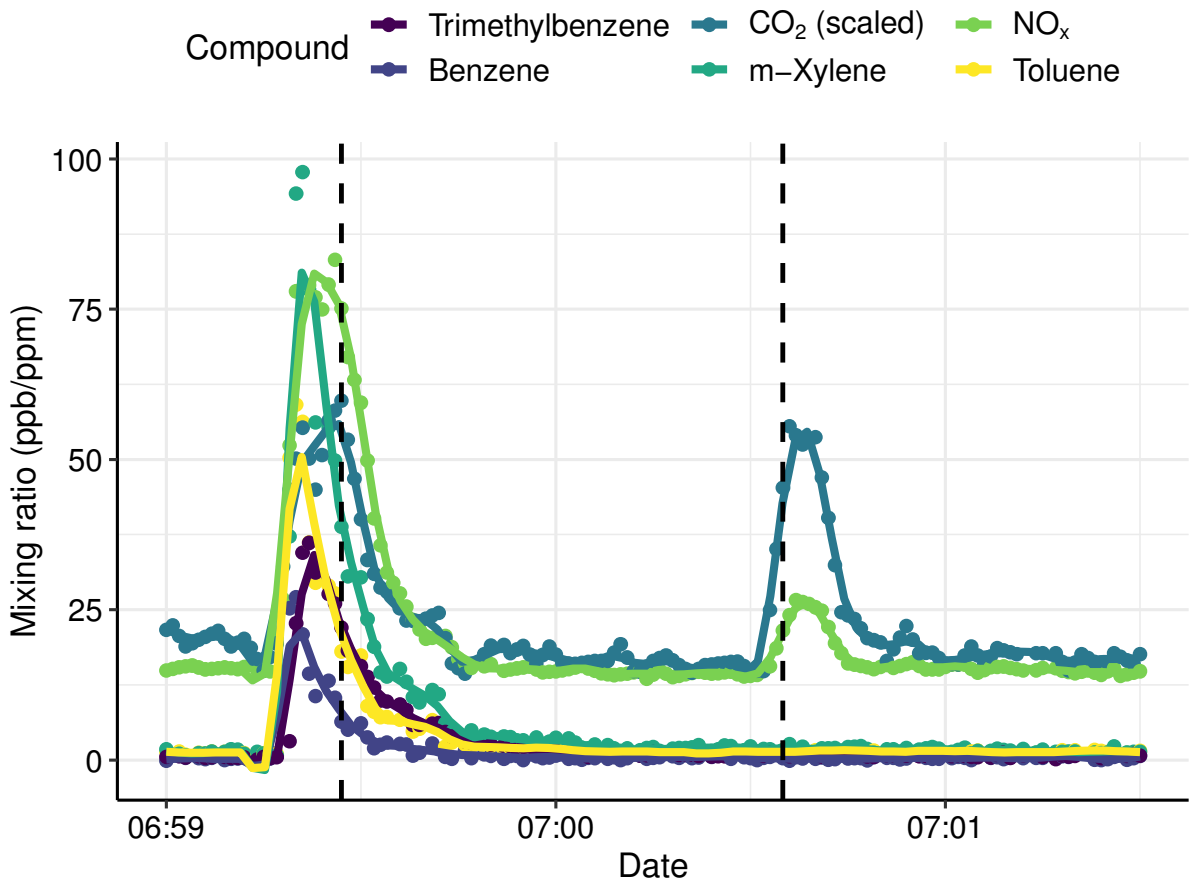

Figure 18. An example of pollutant peaks from the SIFT-MS (trimethylbenzene, benzene, m-xylene, and toluene (all in ppb)) and the ICAD (CO_2 (in ppm) and NO_x (in ppb)) with vehicle passes (dashed lines). CO_2 has been scaled by -525 ppm for data visualization.

An example of pollutant peaks from the SIFT-MS (trimethylbenzene, benzene, m-xylene, and toluene (all in ppb)) and the ICAD (CO_2 (in ppm) and NO_x (in ppb)) with vehicle passes (dashed lines). CO_2 has been scaled by -525 ppm for data visualization.

There are a multitude of reasons as to why the pollutant measurements associated with the vehicle passes show different behavior. These reasons include meteorological effects, such as varying wind speed and direction which can affect the vehicle plumes. Another reason could be varying vehicle speeds along the measurement road as the sample inlet and ANPR camera were placed slightly apart, so the time of the vehicle taken to travel between the inlet and the camera would vary with vehicle speed. Therefore, in order to calculate accurate emission factors and associate them with individual vehicles, it is important that any differing response times in pollutant measurements and vehicle passes are considered.

A further challenge that is important to address is ensuring that combustion-only emissions related to vehicles are extracted from point sampling measurements, which are being carried out in a highly complex emissions area. The point sampling measurements for this study were carried out in Milan and in a highly populated urban environment where it is possible that there is a broad range of emission sources, particularly for VOCs. Therefore, it is important that only vehicle-related emissions are extracted from the data before further analysis is performed and emission ratios are calculated.

An analysis method has been developed to overcome these problems by considering the differing response times for individual vehicle measurements and ensuring the alignment of measurement data related to a particular vehicle pass. All measurement species for each vehicle pass are aligned to give the best correlation to CO_2. The analysis method also includes identification of a combustion plume, by using a requirement of a delta CO_2 change of 20~ppm, which ensures that combustion-related vehicle emissions are extracted from a complex source area. The analysis method also uses a short time window associated with a vehicle pass and the emission ratio is calculated with a regression, which overcomes complex background determination.

Emission ratios of VOCs

Real-world and on-road measurements of VOCs from individual vehicles are limited. During the measurement campaign in Milan, VOCs from passing vehicles were measured using the point sampling measurement technique. Emission ratios of VOCs were then calculated for individual vehicles using the analysis method described above. Average VOC to CO_2 ratios have been extracted from the point sampling measurements for different vehicle categories, including vehicle type, fuel type and euro class (shown in Figure 19).

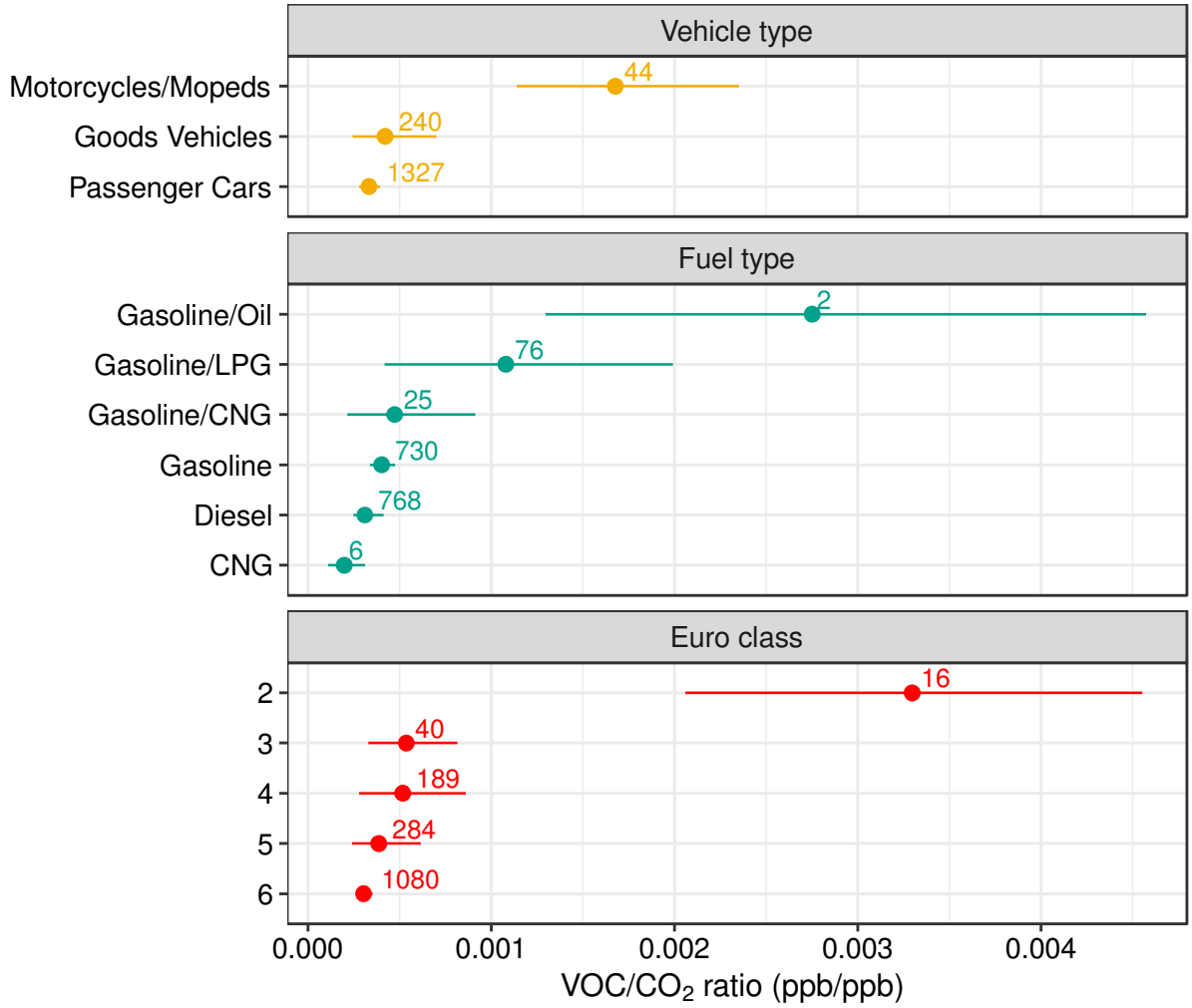

Figure 19. Average VOC/CO_2 ratios (ppb/ppb) calculated for different vehicle categories, including vehicle type, fuel type and Euro class. The variables in each category are ordered by their corresponding ratio values. The numbers associated with each point represent the number of vehicles used to calculate each average. The error bars represent the 95% confidence interval calculated for each mean value.

Average VOC/CO_2 ratios (ppb/ppb) calculated for different vehicle categories, including vehicle type, fuel type and euro class. The variables in each category are ordered by their corresponding ratio values. The numbers associated with each point represent the number of vehicles used to calculate each average. The error bars represent the 95% confidence interval calculated for each mean value.

The vehicle type with the highest VOC/CO_2 ratio are motorcycles and mopeds, which have a significantly higher ratio than other fuel types. Motorcycles/mopeds have an average ratio of approximately 4 times higher than goods vehicles and 5 times higher than passenger cars. The significantly higher ratio for motorcycles and mopeds is likely due to the composition of the vehicle fleet in Milan as a higher percentage of motorcycles and mopeds are older vehicles compared to passenger cars and goods vehicles. Older vehicles are likely to have higher emissions due to higher emission limits or due to deterioration of emission controls (catalytic converters). In addition, motorcycles and mopeds are certified under the L-category standard which is about 10 years lagging behind the light-duty vehicle

regulation in term of stringency.[6] The VOC/CO_2 ratio associated with motorcycles and mopeds could also be influenced by the fuel type ratios, as the highest is seen for gasoline/oil bi-fuels and this fuel type was only observed in motorcycles and mopeds.

Gasoline/oil fuel vehicles have the highest VOC/CO_2 ratio 6.8 times higher than the average ratio associated with standard gasoline fuel vehicles. Gasoline/oil bi-fuel is associated with motorcycles and mopeds with 2-stroke engines, which require a small percentage volume of oil to be added to the fuel due to the absence of a lubricating system. The gasoline/LPG fuel type has an average ratio of 2.8 times higher than the average ratio associated with the standard gasoline fuel type. Gasoline/LPG vehicles are bi-fuel vehicles with two separate fuel tanks, where the engine can run on one fuel or the other. LPG is a mixture of hydrocarbon gases, including propane, propylene, butylene, isobutane and n-butane, and the higher ratio for this fuel type could be a result of evaporative emissions from the LPG fuel. Gasoline fuel type has a slightly higher VOC/CO_2 ratio than diesel, this could be due to the selected VOC compounds, which were lower-weight hydrocarbons and therefore more likely to be emitted from gasoline vehicles.

Figure 19 also shows that the average VOC/CO_2 ratio decreased with increasing Euro class. As Euro classes increase, emission limits for pollutants become more stringent and new emissions reductions technology is introduced. Therefore, reducing hydrocarbon/VOC emissions are likely to be a consequence of this.

Overall, motorcycles and mopeds and some of the gasoline bi-fuel fuel types could be significant VOC sources in Milan due to their high VOC/CO_2 ratios, which represent a high amount of VOC emitted per unit of fuel burnt. Typically, motorcycles and mopeds and bi-fuel fuel types are not regulated in low emissions zones, particularly in Europe, and therefore low emission zones may be less effective in improving air quality. The gasoline/oil fuel type is likely to become less important as it will be difficult for 2-stroke engines to meet increasingly stringent emissions limits, however, they could become important in areas with higher usage. Furthermore, it is likely that the number of motorcycles and mopeds were underestimated as they typically drive close to each other and to other vehicles and therefore may not be captured by the ANPR camera.

Comparison to EDAR

The emission ratios of species extracted from point sampling measurements and analysis can be compared to the same ratios measured using the EDAR remote sensing instrument. The EDAR instrument calculates background corrected ratios of NO_x and total hydrocarbons (HC) to CO_2 directly from the vehicle exhaust. Figure 20 shows the comparison of the average VOC/CO_2 ratios for different vehicle categories calculated from the EDAR and point sampling measurements. For the comparison, only the vehicles that were recorded by both the EDAR and Graz ANPR cameras were included, therefore measurements of the same vehicles could be compared.

[6] EU: MOTORCYCLES: EMISSIONS. https://www.transportpolicy.net/standard/eu-motorcycles-emissions/

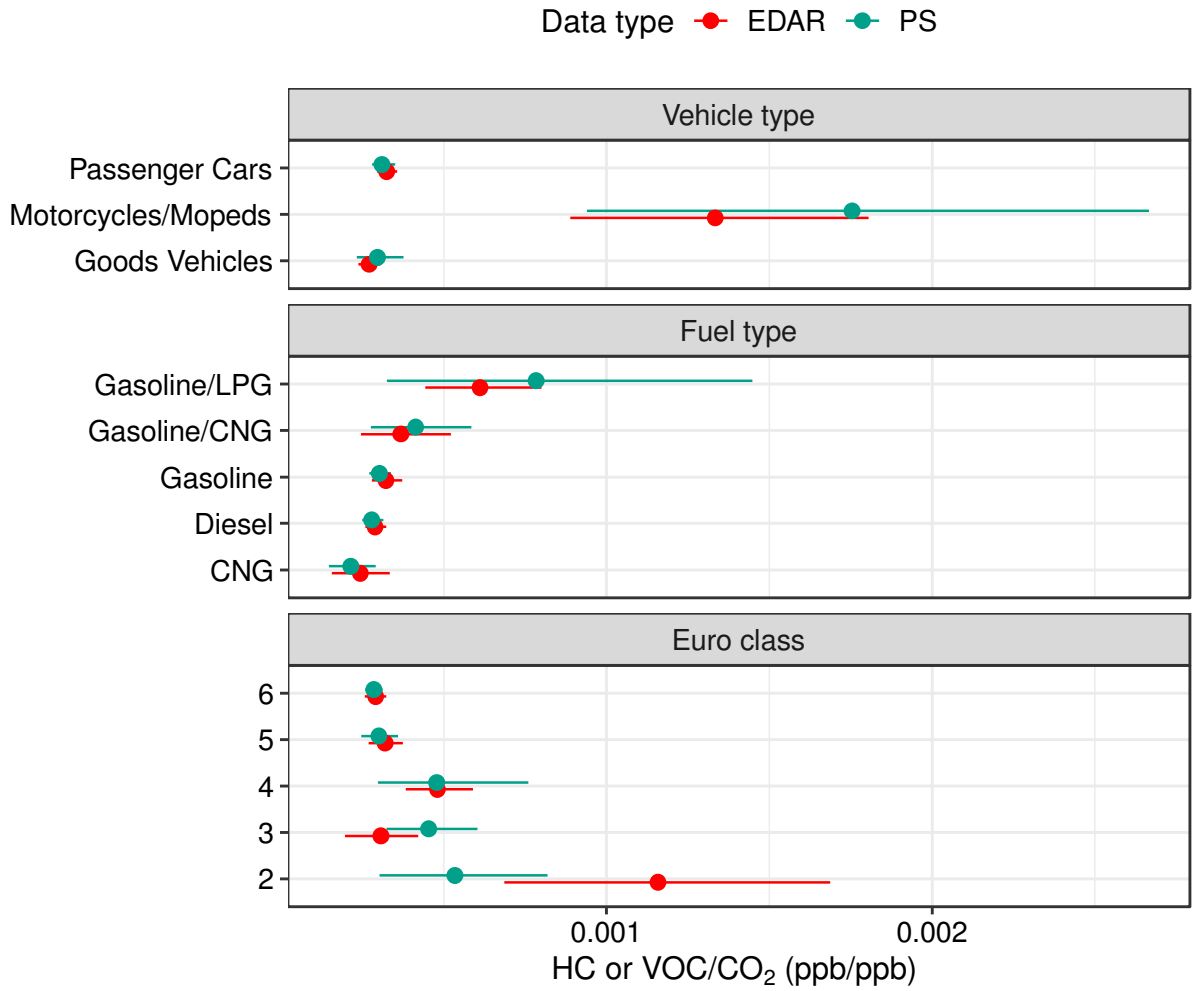

Figure 20. Comparison of average total HC or VOC/CO_2 ratios extracted from EDAR remote sensing (red) and point sampling (blue) for vehicle categories: vehicle type, fuel type and euro class. The error bars represent the 95% confidence interval calculated for each mean value.

Figure 20 shows the comparison of average total HC (EDAR) or VOC (point sampling) to CO_2 ratios calculated from the different measurement methods for vehicle categories, including vehicle type, fuel type and Euro class. The measurement methods agree well, with all of the values being within error of the other measurement method. The trends in each vehicle category group also shown the same pattern between the two measurement methods, for example motorcycles and mopeds and gasoline/LPG fuel type vehicles have the highest ratios. The EDAR HC measurement is calibrated against propane and is used as a basis of representing total HCs. Therefore, remote sensing is limited for measurement of HCs and point sampling can be used to provide a breakdown of individual VOC species. An improvement is using the point sampling measurement technique alongside a mass spectrometer, which can provide information on speciated VOC emissions. Quantification of speciated VOC emissions is useful for the determination of possible health effects or ozone forming potential from vehicular VOC emissions.

Overall, the good agreement between EDAR remote sensing and point sampling indicates that point sampling is a useful measurement technique for determining road vehicular emissions of NO_x and VOCs. An advantage of the point sampling measurement technique compared to remote sensing is that point sampling is less limited in measurement location. A suitable measurement location for point sampling requires a space to park the mobile laboratory, whereas cross-road remote sensing requires a location in which measurement can be performed across the road. A further advantage of point sampling is that targeted measurement compounds can be expanded, provided that measurement of air pollutants can be performed at a high enough time resolution.

1.2.2. Mobile sampling of VOCs

Spatial mapping of pollutants

To spatially map concentrations or ratios between pollutants, a Gaussian kernel smoother is used. This avoids arbitrarily dividing the road network into road segments which down-weights the contribution from less frequent, higher concentrations and potentially leads to important information and intermittent sources being missed.

Gaussian kernel weights represent geographical weights, which is a distance decay function and determines how quickly weights decrease as distance increases. A Gaussian weighting scheme never reaches zero and therefore every measurement contributes to the model result, but more weight is given to data close to the location of interest, while down-weighting data collected further away and reducing the influence of outliers or measurements with a high uncertainty.

The approach also avoids arbitrarily dividing the road up into sections, whereby it can be difficult to determine an appropriate section length. Instead, the spatial scale over which the original data is aggregated can be controlled by varying the width of the kernel, which is determined by the sigma (σ) value. A small σ (100~m) can be used to focus on localised effects at a fine spatial scale. A larger value of σ (1000~m) extends the range over which measurements influence the result and would therefore be useful in studying patterns on a broader, regional scale.

To apply the distance-weighted model to the mobile measurement data, firstly the road network was split into equally spaced 10 m points. This was selected as an appropriate resolution, given that at an average speed of 20 mph the monitoring platform would cover a distance of 9 m in each 1 Hz measurement. The distance-weighted mean was computed at every point within 10 m of any observations.

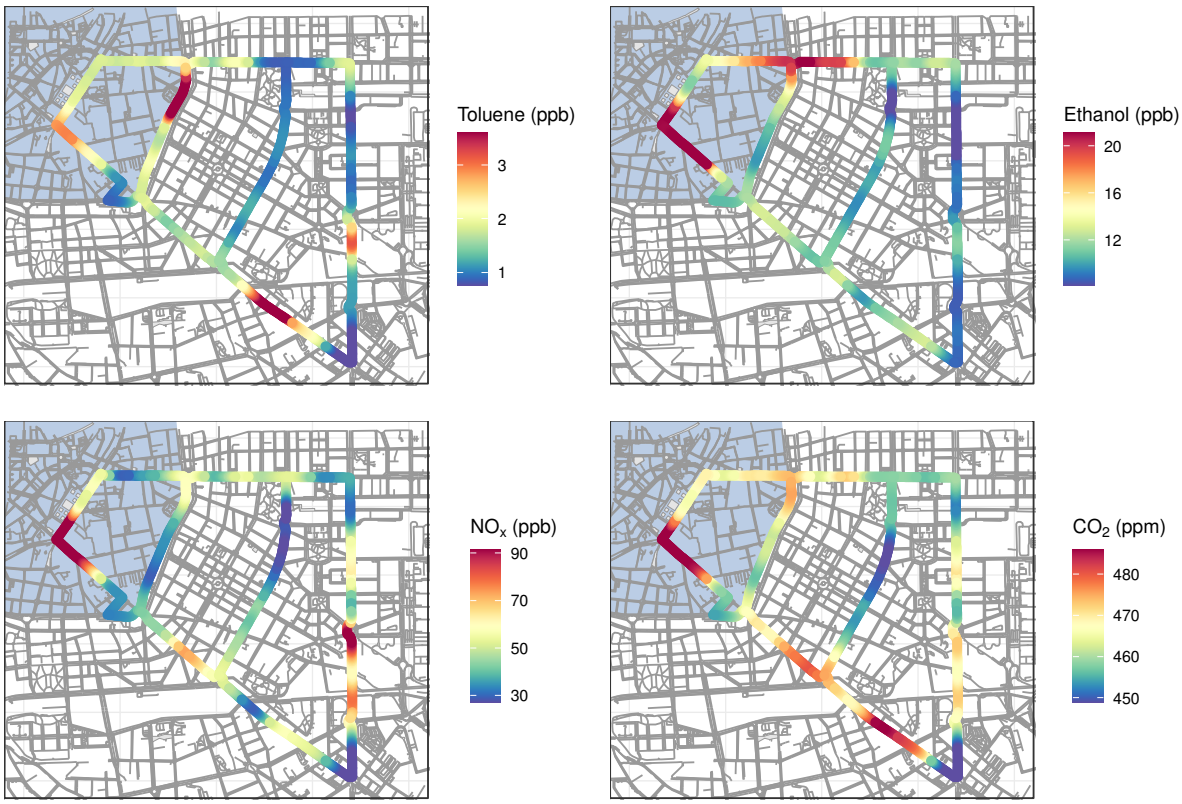

Figure 21. Spatial mapping of median values of Toluene (ppb), Ethanol (ppb), NO_x (ppb) and CO_2 (ppm) from mobile measurements around Milan. The blue shaded region shows Area C, the combined Urban Toll Road and Low Emission Zone. Maps created using a σ of 100 m. Legend lower and upper limits represent the 5th and 95th percentile of the pollutant mixing ratio. © OpenStreetMap.

Figure 21 shows the distance-weighted mean mixing ratios of toluene, ethanol, NO_x, and CO_2 along the Milan mobile measurement route. The maps show some contrasting differences between the different compounds. Toluene mixing ratios are fairly low for the majority of the route, but elevated levels are seen at the top of the road second in from the left and the bottom right of the map. The elevated levels

at the bottom right correspond with elevated levels in CO_2, which is indicative of emissions from road vehicles. However, the other area with elevated toluene mixing ratio does not seem to correspond to any of the other mapped compounds and this elevated level occurs outside of a road vehicle fuelling station, suggesting that the elevated toluene is detected due to evaporative emissions.

There is an area in inner Milan which shows elevated levels of ethanol, NO_x, and CO_2 (red in the bottom left of the maps) and this area has a variety of possible emission sources including hotels, shops, restaurants, and bakeries. It is likely that the elevated levels here are due to businesses in this area and not vehicle emissions due to lower mixing ratios of toluene, which is a good indicator for vehicle emissions. There is an additional area of elevated NO_x observed on the right-hand side of the map, which occurs near a roundabout on the outer-side of Milan. It is likely that this elevated level is due to vehicle emissions as there are also slightly elevated levels of toluene and CO_2 observed.

Spatial representativity of a point measurement

Both point sampling and mobile measurements were carried out in Milan, and this provides the opportunity for comparison between the two measurement techniques. By comparing the results obtained from the different measurement techniques, the spatial representativity of a point measurement and the contribution of vehicle emissions to air quality in an urban area can be determined.

Combustion-related emission ratios of NO_x and VOCs have been extracted from mobile measurements and then compared to corresponding emission ratios calculated from point sampling. Emission ratios of NO_x and VOCs were extracted using the rolling regression analysis method, which allows for extraction of combustion-related plumes (method described in the footnote cited paper).[7] Emission ratios from point sampling are also extracted as combustion-related plumes and therefore the results from the two measurement methods can be compared.

[7] Naomi J. Farren et al., "Emission Ratio Determination from Road Vehicles Using a Range of Remote Emission Sensing Techniques," *Science of The Total Environment* 875 (June 1, 2023): 162621, https://doi.org/10.1016/j.scitotenv.2023.162621.

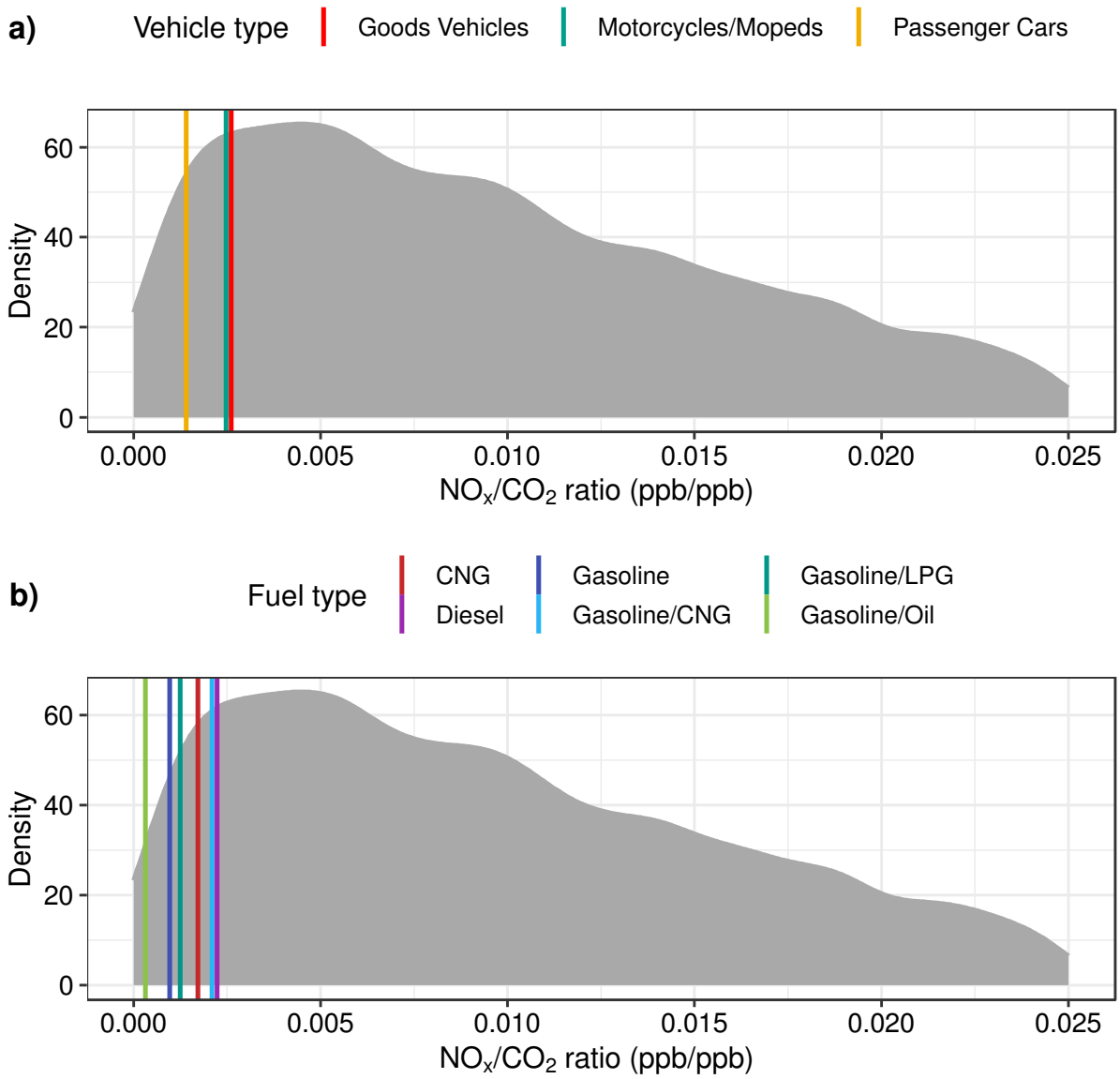

Figure 22. Comparison of NO_x/CO_2 ratios (ppb/ppb) extracted from mobile and point sampling measurements carried out in Milan. The density plot shows the distribution of the NO_x/CO_2 ratios extracted from mobile measurements using rolling regression. The vertical lines represent the average NO_x/CO_2 ratios calculated from point sampling for different a) vehicle types and b) fuel types.

Figure 22 shows the comparison between NO_x/CO_2 ratios extracted from mobile and point sampling measurements. The distribution of NO_x/CO_2 ratios from mobile measurements are shown by the density curve in Figure 22 and the vertical lines represent different NO_x/CO_2 ratios for grouped vehicle categories extracted from point sampling. Both Figure 22 a and b show that NO_x/CO_2 ratios agree relatively well between the two measurement techniques and that ratios from mobile measurements are slightly higher. In fact, the average NO_x/CO_2 ratio extracted from mobile measurements was 15 times higher than point sampling ratios. Higher NO_x emissions detected during mobile measurements could be evidence that the sample of vehicles spatially are much higher emitters of NO_x. This could be due to higher numbers of vehicles that emit higher levels of NO_x, such as diesel vehicles or heavy goods vehicles, or that after-treatment systems are not working well. Furthermore, during mobile measurements a wider variety of driving conditions were sampled compared to point sampling, which experienced more straightforward operating conditions. Therefore, relying on point measurements could give a limited, then distorted view of vehicular NO_x emissions.

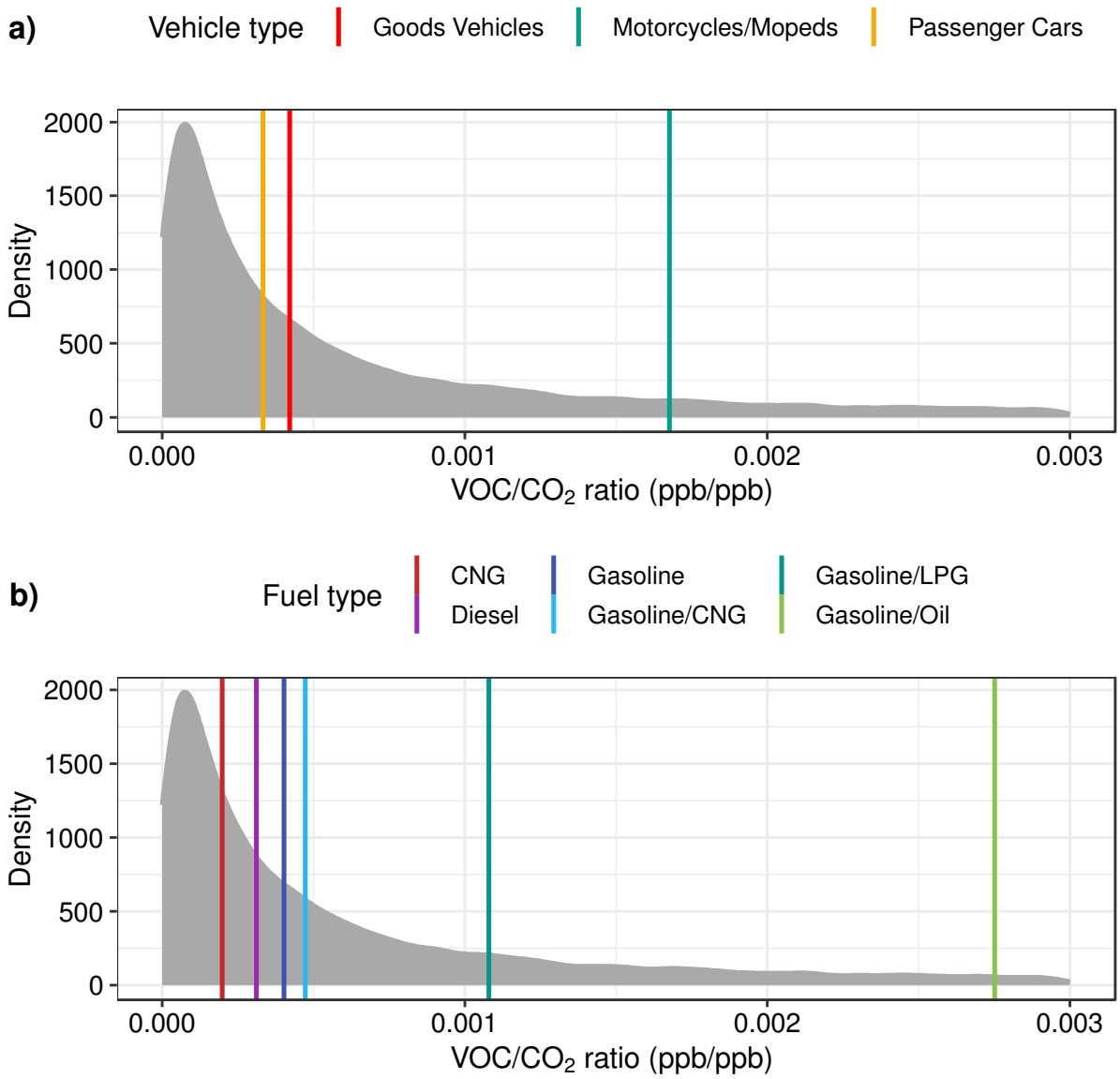

Figure 23. Comparison of VOC/CO_2 ratios (ppb/ppb) extracted from mobile and point sampling measurements carried out in Milan. The density plot shows the distribution of the VOC/CO_2 ratios extracted from mobile measurements using rolling regression. The vertical lines represent the average VOC/CO_2 ratios calculated from point sampling for different a) vehicle types and b) fuel types.

Figure 23 shows the comparison of VOC/CO_2 ratios extracted from mobile and point sampling measurements. In both Figure 23 a and b the VOC/CO_2 ratios from mobile measurements appear to be lower than the ratios extracted from point sampling. However, the average VOC/CO_2 ratio extracted from mobile measurements was 16 times higher than point sampling. Higher VOC/CO_2 ratios measured during mobile measurements are likely due to sampling of high VOC emitting vehicles, such as motorcycles and mopeds, or variation in operating conditions.

Higher average NO_x and VOC emission ratios extracted from mobile measurement compared to point sampling are likely a result of emission events from high-emitting NO_x and VOC vehicles, such as motorcycles and mopeds or natural gas fuel vehicles (as shown in Figure 19) This indicates that these vehicle types could play an important role in spatial emissions of NO_x and VOCs. Furthermore, the emission ratios extracted from point sampling are likely to be lower as the vehicle fleet was dominated by Euro class 6 passenger cars.

1.3. Point sampling of NO_x, NO_2, BC and PN emissions

1.3.1. Measurement Setup

For the CARES city measurement campaigns an automated system was planned that is able to record the passing times, recognise the number plates and perform the emission measurements over long time periods without permanent human supervision (see Figure 24).

The three main components are the ANPR camera for number plate recognition, a light barrier for the detection of the vehicle passing times, speed and acceleration and the measurement system consisting of the sample line, the corresponding emission measurement instruments and the data management system. A newly developed black carbon tracker (BCT) was used for black carbon (BC) and CO_2 measurement,[8] besides a custom developed diffusion charger for PN[9] and an ICAD[10] which measures NO_2, NO_x and CO_2. In addition, an Aethalometer AE33 (Magee Scientific) was used for additional BC measurement and source appointment. In the first part of the campaign, PN (D_{50} cut-off at 23 nm) measurements were conducted without catalytic stripper also including the volatile particle fraction. A more detailed description of the setup and the measurement principle can be found in Knoll et al.[11]

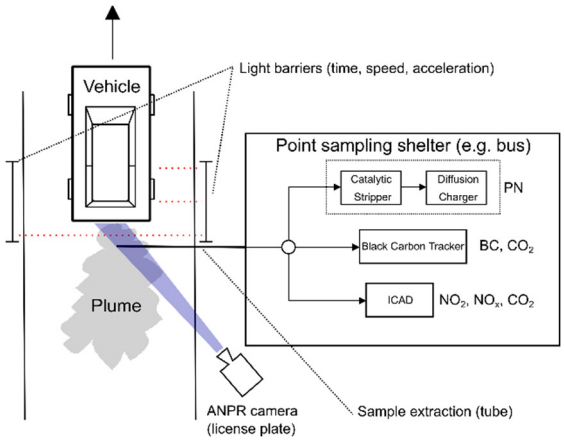

Figure 24. Schematic of the PS setup

Table 3. Used instrumentation during the CARES city measurement campaigns.

Instruments	Measured Species
Black Carbon Tracker	BC, CO_2
Aethalometer	BC, Brown Carbon
Diffusion Charger	PN
ICAD	NO_2, NO_x, CO_2

1.3.2. Results

Prior to the detailed emission specific results, we give a short overview on the captured vehicle fleet during the performed measuring campaigns. In Figure 26, the share of the captured emission factors from PS of the different vehicle types is shown. The majority of the measurements (82.7 %) stems from passenger cars. This is followed by captured emission factors from light commercial vehicles (12.1 %), light duty vehicles (2 %) and heavy-duty vehicles (0.8 %). In case of fuel type, most of the vehicles were

[8] Knoll, M. Lang, B., Bergmann, A. Performance of Black Carbon Instruments for Extractive Remote Emission Sensing. AAAR conference. https://aaarabstracts.com/2021/AbstractBook.pdf. 2021.

[9] M. A. Schriefl et al., "Characterization of Particle Number Counters Based on Pulsed-Mode Diffusion Charging," *Aerosol Science and Technology* 54, no. 7 (July 2, 2020): 772–89, https://doi.org/10.1080/02786826.2020.1724257.

[10] Martin Horbanski et al., "The ICAD (Iterative Cavity-Enhanced DOAS) Method," *Atmospheric Measurement Techniques* 12, no. 6 (June 26, 2019): 3365–81, https://doi.org/10.5194/amt-12-3365-2019.

[11] Knoll, M., Penz, M., Juchem, H., Schmidt, C., Pöhler, D., Bergmann, A. Point Sampling as Roadside Vehicle Emission Screening Technique. Submitted to Atmospheric Measurement Techniques. 2023.

operated by diesel only (Figure 25). But also, a substantial share of hybrid (12.7 %) and LPG (4.1 %) vehicles were captured. The following emission results focus on passenger cars (vehicle category: M1).

Captured Vehicle Fleet:

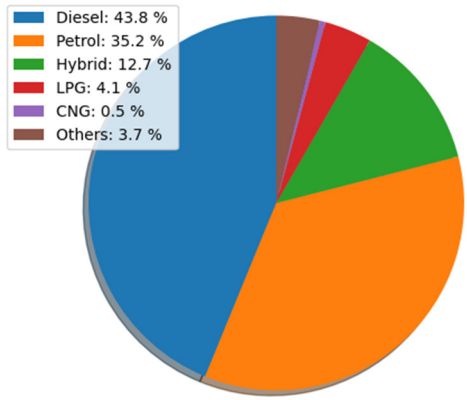

Figure 25. Milan - Captured vehicles according to fuel type.

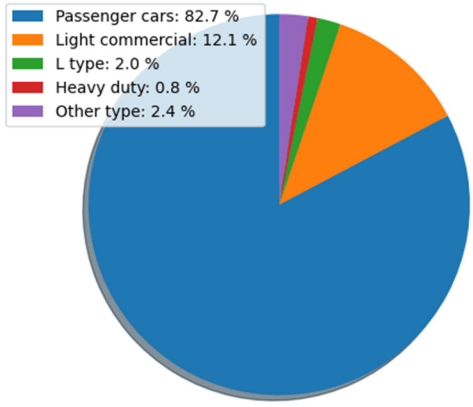

Figure 26. Milan. Captured vehicles according to vehicle type.

Emission measurement results:

Distance-specific emissions were derived from emissions ratios to CO_2 using the same method as in section 1.1. The black carbon emissions were measured with the usage of the BCT. A significant decrease in BC emissions for diesel cars can be noticed with successive development of the emissions legislations. Mean and median values for Euro 6 vehicles (Euro 6, Euro 6d-TEMP, Euro 6d) for BC are below the Euro norm limits for PM. It is also remarkable that variance is also decreasing with newer cars (N_{Euro4}: 189, N_{Euro6}: 2292) while the number of outliers is strongly increasing. This comes along with the larger number of measured vehicles. Causes for the outliers can be considered to be defective exhaust aftertreatment systems (e.g., defective DPF) or regeneration events. For petrol cars, on the contrary, this strong variance decreasing effect is not visible tough the absolute values are on a far lower level. BC emissions of Euro 6 petrol and diesel vehicles are in a similar scale (diesel Euro 6 mean: 2.9 mg/km, median: 0.8 mg/km; petrol Euro 6 mean: 2.8 mg/km, median: 1.0 mg/km). Despite the increasing amount of petrol cars with fuel direct-injection over time, the BC mass emissions stayed quite stable over the emission standards.

The particle number emissions show similar tendencies as the BC emission results above. In the first part of the Milan measurement campaign, PN (D_{50} cut-off at 23 nm) was measured without removal of the volatile particle fraction (Figure 29 and Figure 30). In the second part of the campaign the catalytic stripper was added and solid particle number (SPN) was measured, where the results can be seen in Figure 31 and Figure 32. The impact of volatiles can both be seen for diesel and petrol passenger cars for the high emitters. Mean values increase for Euro 4 and Euro 5 between 50 % and 300 % if the volatiles fraction is included and is even more pronounced for Euro 6 emission standards. Median values of diesel Euro 6 emission standards cars are below the PN RDE limit (9 e11/km including the on-road conformity factor), in contrast to Euro 5 vehicles were also the median is above the limit. Measured NO_x emissions from Euro 3 up to Euro 5 diesel cars don't show the same trend as the reduction of the corresponding type-approval emission limits. For Euro 6d-TEMP and Euro 6d vehicles a significant reduction is identifiable (mean and median values below limit). This comes along with the introduction of more stringent type approval regulations mandating on-road testing. As expected, NO_x emissions from petrol vehicles are generally lower compared to their diesel counterparts. For petrol passenger cars a slow but steady reduction of real driving emissions is noticeable.

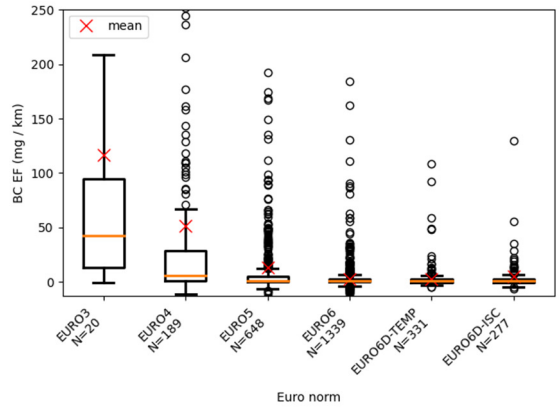

Figure 27. Milan - BC emissions of diesel passenger cars for different Euro norms.

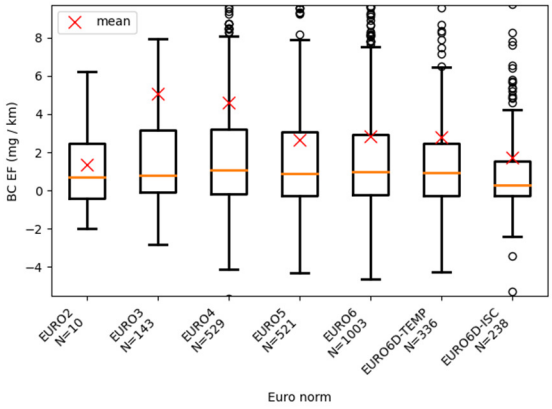

Figure 28. Milan - BC emissions of petrol passenger cars for different Euro norms.

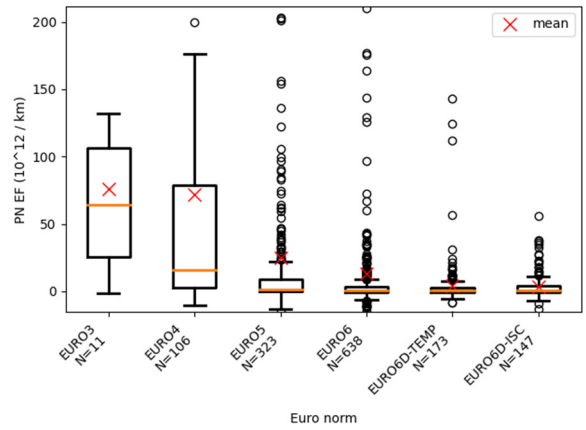

Figure 29. Milan – PN (including volatiles) emissions of diesel passenger cars for different Euro norms

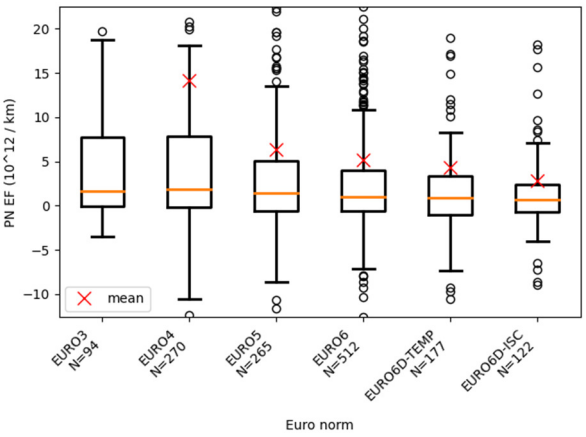

Figure 30. Milan – PN (including volatiles) emissions of petrol passenger cars for different Euro norms

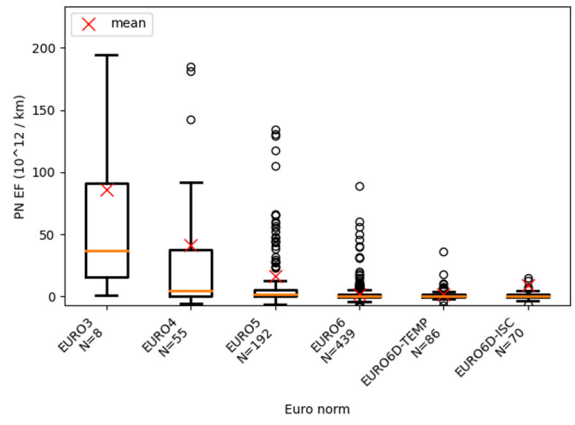

Figure 31. Milan - SPN (without volatiles) emissions of diesel passenger cars for different Euro norms

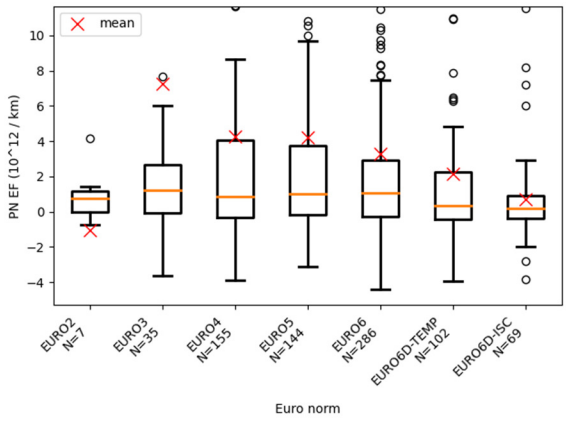

Figure 32. Milan - SPN (without volatiles) emissions of petrol passenger cars for different Euro norms

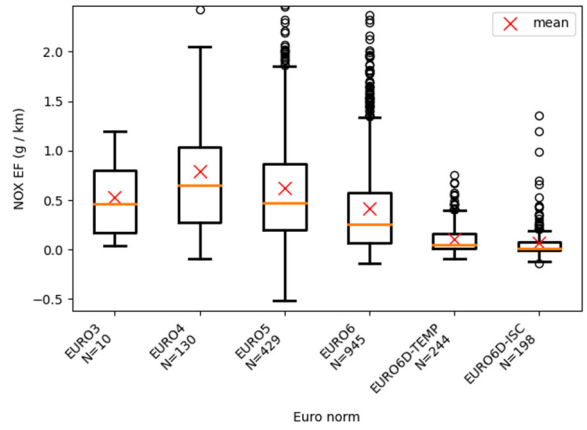

Figure 33. Milan - NO_x emissions of diesel passenger cars for different Euro norms

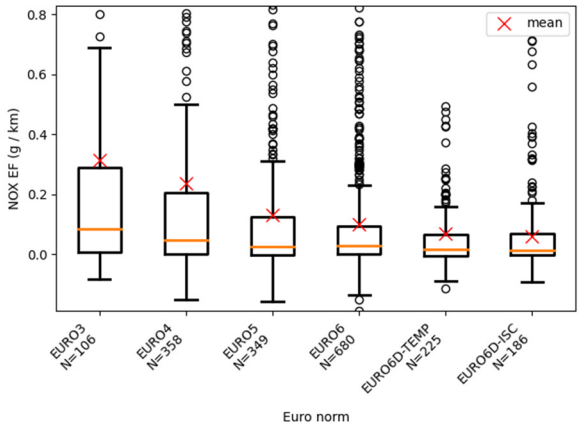

Figure 34. Milan - NO_x emissions of petrol passenger cars for different Euro norms

1.4. Validation Measurements and RES Intercomparison

An important step of Milan analysis is to compare results from the various instruments. Figure 35 presents a comparison of passages for Airyx and TUG point sampling, compared to valid and invalid (outliers) measurements from the EDAR unit in Madre Cabrini. Some of the differences are due to the EDAR instrument configuration in Milan which was not allowing measurement during rain events.

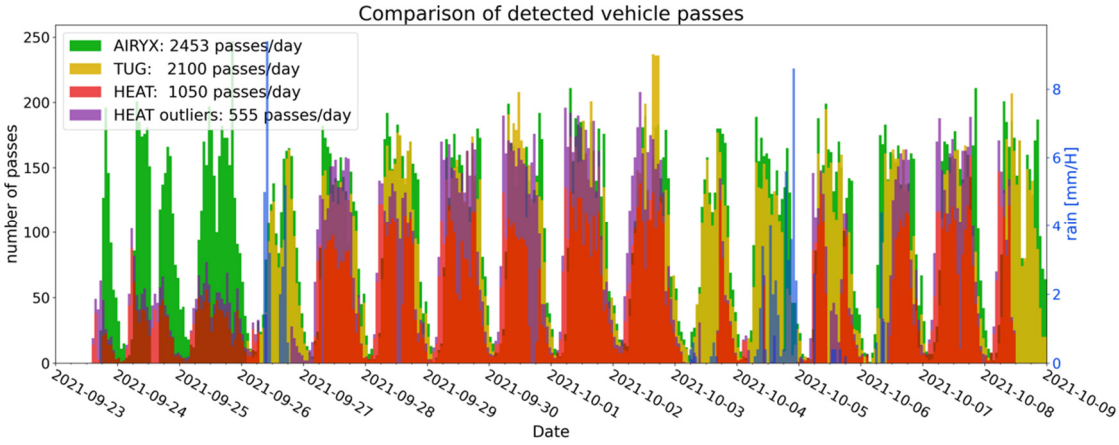

Figure 35. Comparison of passages per day for the different instruments. The HEAT/EDAR instrument configuration in Milan which was not allowing measurement during rain events.

The following sections compare emission ratios from the different remote sensing technologies with PEMS.

1.4.1. Emission comparison between EDAR and PEMS

Introduction

During the Milan campaign, evaluation measurements were conducted with test vehicles equipped with portable emission measurement systems (PEMS). The PEMS measurements served as a reference in comparison to the EDAR and PS systems, which were co-located at the measurement spot in Madre Cabrini.

Selected test vehicles and instrument set-up

For the PEMS measurement three different vehicles were selected. A Volkswagen (VW) Golf (Euro 4, diesel) was selected as representative vehicles for high particle emitters. Therefore, the equipped diesel particulate filter (DPF) was tampered in an official garage. A Renault Clio (Euro 6b, diesel) served as high NO_x emitter. The third vehicle - a Fiat Panda (Euro 4, petrol/CNG) – was chosen to cover the representativeness of gasoline vehicles and contemporarily to test and represent bi-fuel cars that can often be found in daily usage in Northern Italy .

For the evaluation measurements, two different AVL Move PEMS were used. For testing the two diesel vehicles the AVL 492 iS GAS PEMS and the AVL 496 PN PEMS were used. For the test drives with the bi-fuel (gasoline/CNG) vehicle the AVL 493 iX GAS PEMS was used. The PN module was included, as for the two diesel cars PN values were of big interest. For the FIAT Panda (bi-fuel) the Total Hydrocarbon (THC) and CH_4 concentrations were from interest and therefore a FTIR PEMS was included in the measurement system instead of the PN PEMS. A picture of the PEMS equipped Renault Clio Sporter is shown in Figure 36.

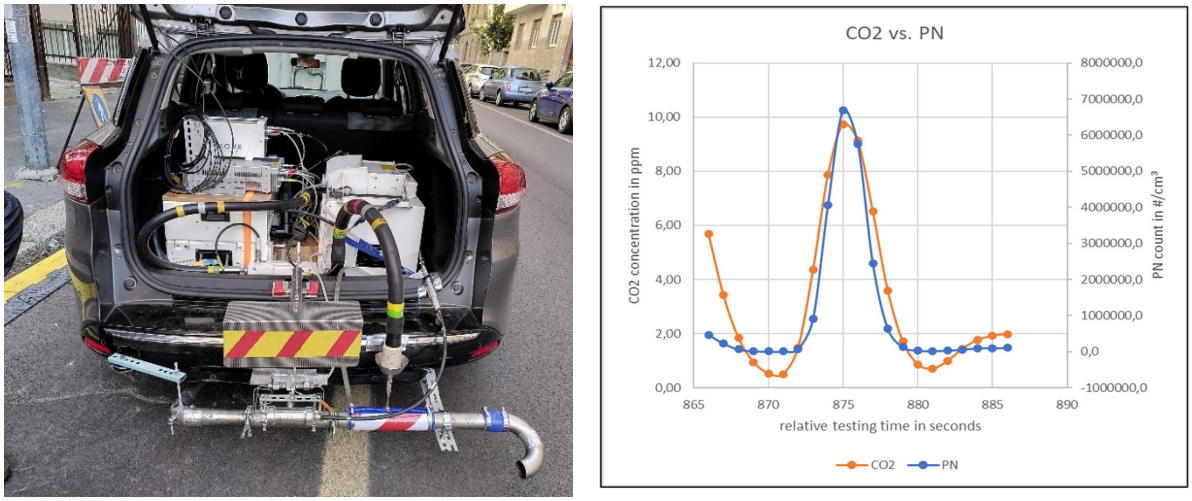

Figure 36. PEMS set-up of the Euro 6b diesel vehicle (on the left, AVL 492 iS GAS PEMS + AVL 496 PN PEMS) and an example of the optimized PEMS time alignment (on the right).

Time alignment 1 – PEMS sensors vs. CO2 signal

For the two diesel vehicles (Golf and Clio Sporter) each pollutant emission trend was aligned to the CO_2 signal via cross-correlation. An example of the aligned PN and CO_2 data is shown in Figure 36.

For the petrol/CNG vehicle (Fiat Panda) the correlation method was not applicable due the more-or-less homogeneous exhaust composition in terms of concentration. Therefore, the delay times were adjusted visually via distinct drive events (e.g.: strong deceleration with fuel cut-offs). Still, this approach was not easy to apply due to very low concentrations and short time windows to analyse.

Time alignment 2 – PEMS to HEAT

The PEMS system logged the data on a 1 Hz basis. This is sufficient for the purpose it was developed for (emission factors for whole drive cycles) but this entails an uncertainty when matching the PEMS and EDAR results. Aiming to optimize the comparison between those measuring systems, the emission values detected were post-processed with an adapted approach, defined GTS (Global Time Shift). The GTS post-processing considered a time range of ±1 seconds compared to the exact passing time of the vehicle, choosing the results with the smallest, absolute differences between EDAR and PEMS concentration-based emission factor (ppm/ppm for gases or PN/moles for PN). This can be interpreted as a "comparison-friendly" approach.

Additionally, a second approach, which selected the PEMS values using the GPS location of the vehicles, was used to compare the emission factors. The same trend was observed compared to the GTS approach with slightly worse results in the case of correlation coefficients.

However, it has been mentioned[12] that a caveat to those approaches is that they assume that what is coming out of the tailpipe at a given time is the same as what is in the entrainment or the entire plume. It was suggested that the mass of pollutants in the on-road vortex has a "memory" of the engine operation, including fuel rate, over a longer time than for 1 Hertz PEMS measurements. Therefore, a high correlation between EDAR and PEMS measurements – other than in particular and ad hoc optimized conditions (e.g., suitable atmospheric conditions, positive slope, positive and constant engine load, and acceleration conditions) – cannot easily be achieved.

Results

The post-processed data of NO, NO_2 and PN measurements is brought into comparison via scatter plots (Figure 37,Figure 38,Figure 39). THC and CH_4 data from the test measurements of the bi-fuel vehicle were not representative enough, as most measurements were in the range of the detection limit of the PEMS measurement system. The PEMS values are presented as a reference on the abscissa and the EDAR values are displayed on the ordinate. To characterise the correlation, we used linear regression, and the corresponding equation is depicted in the top-left area. We added a 1:1 slope to ease the understanding of the sample values' relation to the perfect fit.

For nitrogen oxide (NO) a good agreement (Figure 37, R^2=0.82) was found. Two separate regions can be identified in the plot. The left part with lower emissions ratios portrays the results of the Euro 4 bi-fuel car – the Fiat Panda. When we focus on the higher ratios – representing both diesel cars - an increasing spread for both cars can be seen.

A satisfying relation (Figure 38, R^2=0.58) between the two systems was found for nitrogen dioxide (NO_2). The EDAR system underestimates NO_2 measurements compared to the PEMS system (y = 0.6 x). For NO_2, all shown results come from the two diesel cars as all measured NO_2-results of the bi-fuel car lie below the PEMS's detection limit defined with 5 ppm.

In case particle number (PN) concentration measurements, a rather low positive correlation (Figure 39, R^2=0.35) can be stated. In regard of absolute differences, the EDAR system strongly underestimated PN emissions (y = 0.05x). Like in the NO_2-plot, only results of the two diesel cars are presented since only for these cars a PEMS with PN sensor was used. Correlations were inferior to those previously reported in former studies,[12] which is due to a sub-optimal setup for a comparison with PEMS which would ideally be performed on a consistent uphill slope incompatible with the flatness of the Milan site, the slope of which is -0.5 degrees.

[12] Karl Ropkins et al., "Evaluation of EDAR Vehicle Emissions Remote Sensing Technology," *Science of The Total Environment* 609 (December 2017): 1464–74, https://doi.org/10.1016/j.scitotenv.2017.07.137

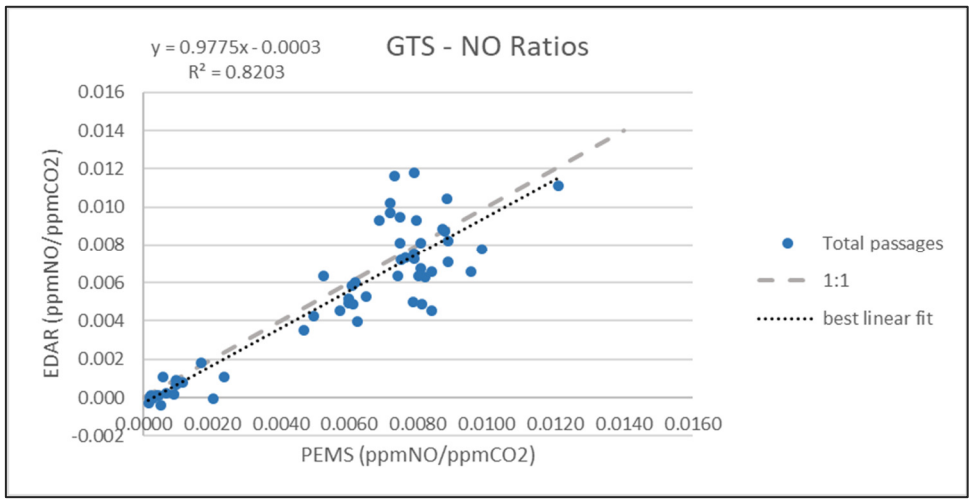

Figure 37. Relation between PEMS and EDAR NO EFs

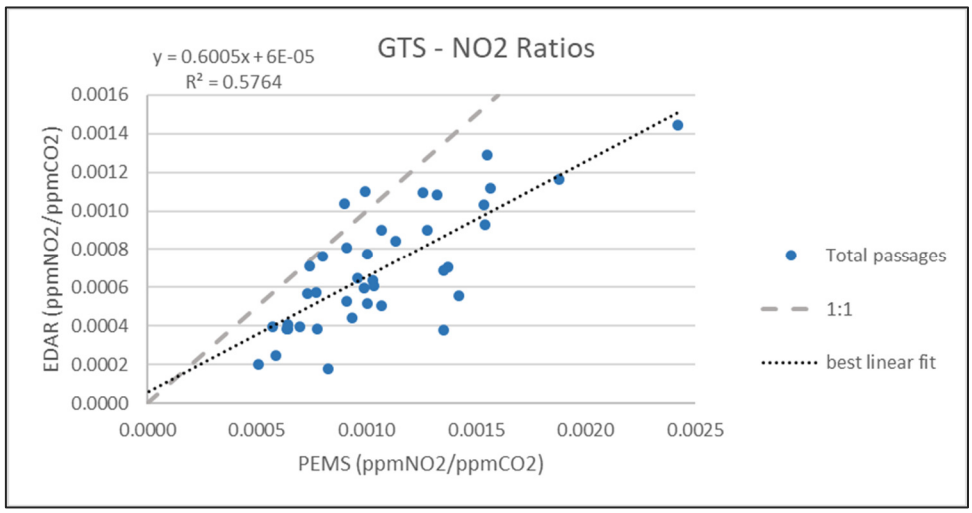

Figure 38. Relation between PEMS and EDAR NO_2 EFs.

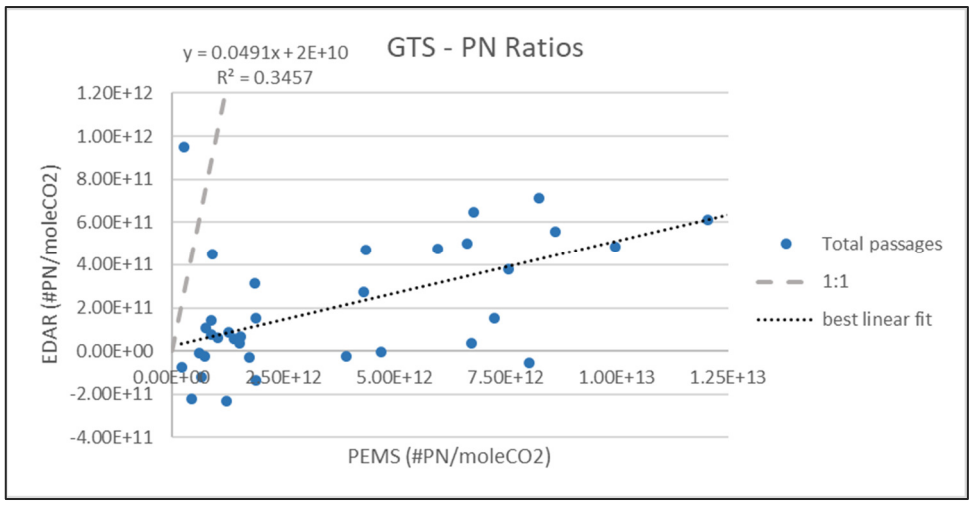

Figure 39. Comparison between PEMS and EDAR PN EFs.

1.4.2. Emission comparison between Point Sampling and PEMS

In addition to the comparison between PEMS and EDAR, we evaluated the PN and NO_x results of the PS system for the test vehicles. This was done based on the calculated fuel-based emission factors.

For the PN evaluation, only measurement data of the test drives of the Renault Clio Sporter (Euro 6b) are included because solid particle number measurements were performed using a catalytic stripper for removal of semi volatile compounds. For the test drives of the VW Golf (Euro 4) the catalytic stripper was not available, and the results are therefore also dependent on the volatile particle fraction which is not measured by PN PEMS instrument. A very good agreement was found between PEMS and PS PN EFs, as shown in the boxplot in Figure 40. Similar mean (PEMS: 10.2e13 particles/kg fuel, PS: 9.0e13 particles/kg fuel) and median (PEMS: 7.5e13 particles/kg fuel, PS: 7.3e13 particles/kg fuel) values were determined for both systems. Overall, also a good agreement was found for the NO_x comparison (Figure 41), which includes data from both diesel vehicles (VW Golf, Renault Clio Sporter). Measurements from PS spread over a larger range compared to the PEMS results. Mean (PEMS: 26.7 g/kg fuel, PS: 25.8 g/kg fuel) and median (PEMS: 26.1 g/kg fuel, PS: 25.2 g/kg fuel) values are in good agreement with a slight underestimation of the PS system compared to the PEMS measurements.

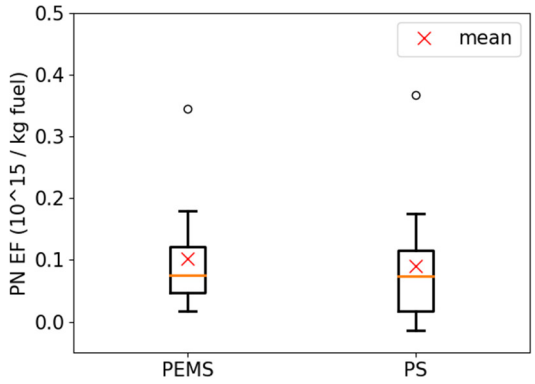

Figure 40. Comparison between calculated PN EFs from PEMS and PS (Renault Clio Euro 6b).

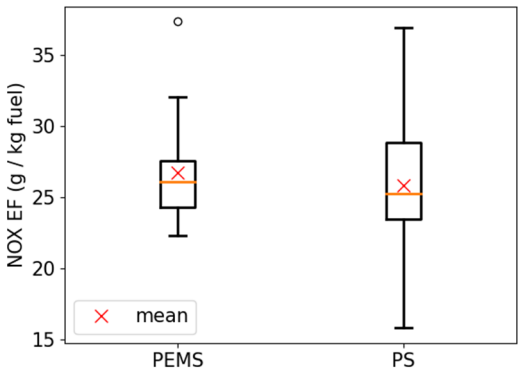

Figure 41. Comparison between calculated NO_x EFs from PEMS and PS.

1.4.3. RES Method Intercomparison - Point Sampling and EDAR

In addition to the PEMS measurements, also comparisons of the measurements of the overall vehicle fleet between the EDAR and the PS system were done during the co-location of the two systems. HEAT PM and PS BC measurements are compared (Figure 42), with 9371 and 6820 vehicle measurements during the co-location, respectively. Generally, it can be said that BC is a subset of PM emissions. Overall mean values of both systems (HEAT: 87.6 mg/kg fuel, PS: 112.5 mg/kg fuel) are in a similar range. Statistically, the distribution of both systems shows large differences. EDAR PM measurements are narrowly distributed around 0, with a median value of 0.4 mg/kg fuel). PS BC results of the overall fleet are distributed over greater range with a median value of 16.4 mg/kg fuel. This results in a factor of about 40 between the two systems in case of median values, where the EDAR system underestimates PM emissions compared to the PS system. A similar trend was shown for the PEMS-EDAR comparison. In case of NO_x measurements, the EDAR system captured 9360 measurements compared to PS with 4562 captured EFs. Statistically, there is a good agreement between the systems for NO_x, both with mean (EDAR: 4.45 g/kg fuel, PS: 4.26 g/kg fuel) and median (EDAR: 0.81 g/kg fuel, PS: 0.80 g/kg fuel) values.

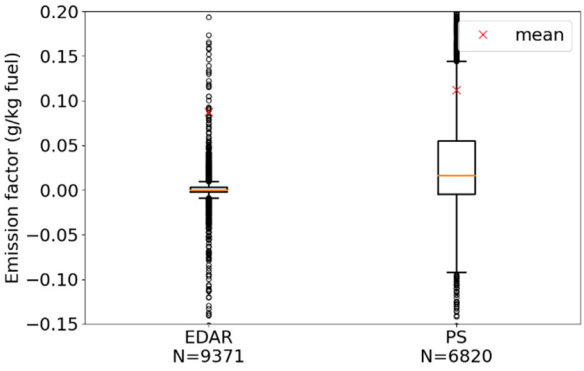

Figure 42. Comparison of PM (HEAT) and BC (PS) in via Madre Cabrini from HEAT and PS.

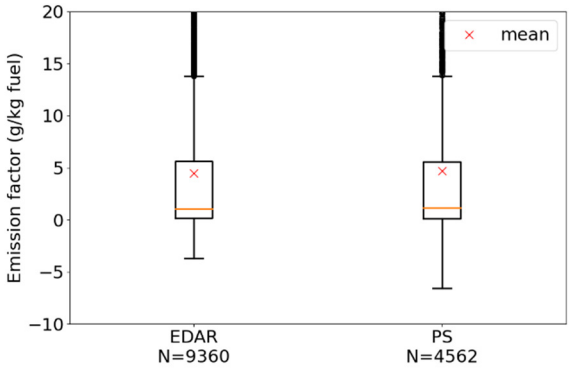

Figure 43. Comparison of NO_x EFs in via Madre Cabrini from HEAT and PS.

1.5. Advanced sensors for air quality monitoring

Sensor technologies have recently become available for Air Quality (AQ) monitoring.[13,14] The city of Milan, through AMAT (a totally owned agency of the Municipality of Milan), is equipped with AQ advanced, i.e., near-reference, sensors.[15] Such technologies seamlessly collect information alongside vulnerable sites to support the implementation of the recently adopted local Air Quality and Climate Plan.

The CARES project provided the unique opportunity to assess a subset of Milan's AQ advanced sensors. In particular, the sensors' capability to detect exposure to vehicular traffic-related emissions, including from high polluting vehicles, was analysed. For that purpose, the data from the experimental Remote Emission Sensing (RES) site of via Madre Cabrini (Milan) was used.

To this end, an AQ compact station with near-reference sensors was deployed in collocation with a relocatable cabin, deployed by Innovhub SSI, equipped with AQ and meteorological reference instruments to verify the sensors' accuracy. Next, the compact AQ station was deployed in combination with the RES measurements in the typical urban street canyon of via Madre Cabrini for eleven days (from 27.09 to 07.10.2021) to detect traffic-related air pollutants (NO_2, NO, CO, CO_2, PM10, PM2.5, PM1 and PN, Black Carbon, etc.).

In the following paragraphs the results from the comparison analysis are presented.

1.5.1. Comparison between advanced sensors and AQ reference instruments

The remote emission sensing campaign was performed in via Madre Cabrini (Milan), involving RES Point sampling, RES commercial, and Portable Emissions Measurement Systems (PEMS). During the campaign, the AQ compact station equipped with advanced (near-reference) sensors, deployed by

[13] European Commission, Joint Research Centre, Borowiak, A., Barbiere, M., Kotsev, A., et al., *Review of sensors for air quality monitoring*, Publications Office, 2019, https://data.europa.eu/doi/10.2760/568261

[14] Ye Kang et al., "Performance Evaluation of Low-Cost Air Quality Sensors: A Review," *Science of The Total Environment* 818 (April 20, 2022): 151769, https://doi.org/10.1016/j.scitotenv.2021.151769.

[15] Silvia Moroni et al., "Near-Reference Air Quality Sensors Can Support Local Planning: A Performance Assessment in Milan, Italy," *Environmental Sciences Proceedings* 19, no. 1 (2022): 36, https://doi.org/10.3390/ecas2022-12814.

AMAT, and a reference air quality relocatable cabin, deployed by Innovhub SSI, were collocated. The collocation enabled simultaneous parallel measurements (Figure 44).

The advanced sensors compact station (Mod. MAS-AF300, Sapiens Env. Technology Co., Ltd) deployed by AMAT is equipped with:

- Electrochemical sensors for detection of gaseous pollutants (NO, NO_2, O_3, CO).
- Photoionization detector for Total Volatile Organic Carbon (TVOC)
- Non-Dispersive Infrared - NDIR detector for CO_2.
- Optical Particle Counter - OPC equipped with 50 channels with length between 0.3 μm and 10.0 μm for PM10, PM2.5, PM1 and Particle Number (PN).
- A 5 wavelength aethalometer, including 880 nm and 375 nm absorption analysis for Black carbon (BC) monitoring. The measurement of BC is referred to the PM2.5 fraction.

Meteorological parameters (ambient temperature, pression, precipitation, wind, and speed direction) can both be monitored with compact sensors integrated in the AQ relocatable station and reference instruments. In the current analysis meteorological reference instruments data were considered.

The reference air quality monitoring station deployed by Innovhub SSI is a relocatable cabin equipped with instruments that measure the following pollutants: Sulfur dioxide (SO_2), Carbon monoxide (CO), Nitrogen oxides (NO_x), Ozone (O_3), Methane and Non-methane hydrocarbons (NMHC), Ammonia (NH_3), Black carbon (BC). The cabin is also equipped with meteorological instruments that monitor the following parameters: wind direction and speed, atmospheric temperature, relative humidity, atmospheric pressure, global solar radiation, rainfall. The SO_2 and CO analyzers are HORIBA model APSA-360 and HORIBA model APMA-360, respectively, while the NO_x analyzer is HORIBA model APNA-360, which uses cross-modulated chemiluminescence. The Ozone analyzer is a HORIBA model APOA-360, utilizing non-dispersive UV absorption with cross-modulated flow. The methane and non-methane hydrocarbons analyzer is a HORIBA model APHA-360, based on flame ionization (FID) with cross-modulated flow. The Ammonia analyzer CNH3S2 relies on the chemiluminescence principle and is equipped with an additional NH_3 to NO converter consisting in a quartz tube filled with quartz wool heated to 980°C. Finally, the Aethalometer® Model AE33 by MAGEE Scientific is the analyzer used for black carbon monitoring.

The instruments used in the reference Innovhub SSI cabin for meteorological parameters detection are produced by MICROS. They are a Relative humidity sensor MICROS model SRHS/C, an Atmospheric Pressure MICROS model SRHS/C SDVD.0/2, an Air temperature MICROS model STEP.0/2V, a Rain gauge MICROS model PLUV, a Total solar radiation sensor (pyranometer) MICROS PIR model, a Wind direction and speed sensor: MICROS model SDVD.0/2. The sensors are fixed on top of an extensible pole by means of a support, consisting of a stainless-steel bar fitted with two collars.

Figure 44. Reference cabin (left) and advanced AQ sensors compact station (right) for monitoring airborne concentrations, and weather conditions in via Madre Cabrini, Milan (Italy).

Via Madre Cabrini is in the centre-southern part of the city, oriented south-west to north-east. It represents a good example of urban street canyons, though with an opening on a lateral side as showed in Figure 45.

Observations were filtered such that data collected were excluded during precipitation events (> 0 mm), windy events (wind intensity > 1.5 m/s) and when wind came through the street canyon opening (wind intensity > 0.2 m/s and direction from 303° to 346°). Data observations before weather-related filtering amount to 25,688. Remaining datapoints after data filtering amount to 22,335 (83%), whereby datapoints excluded are 2,315 (9%) for wind intensity and 1,038 (4%) for rainfall.

Figure 45. Location of the experimentation with air quality monitoring in Via Madre Cabrini, Milan (Italy) along with Remote Emissions Sensing setting.

Collocation results are presented below for NO_2 and BC (Figure 46 and Figure 47). When considering a 1-minute time resolution, very good agreement between AQ advanced sensors and AQ reference instruments can be found, despite the different principles of measure.

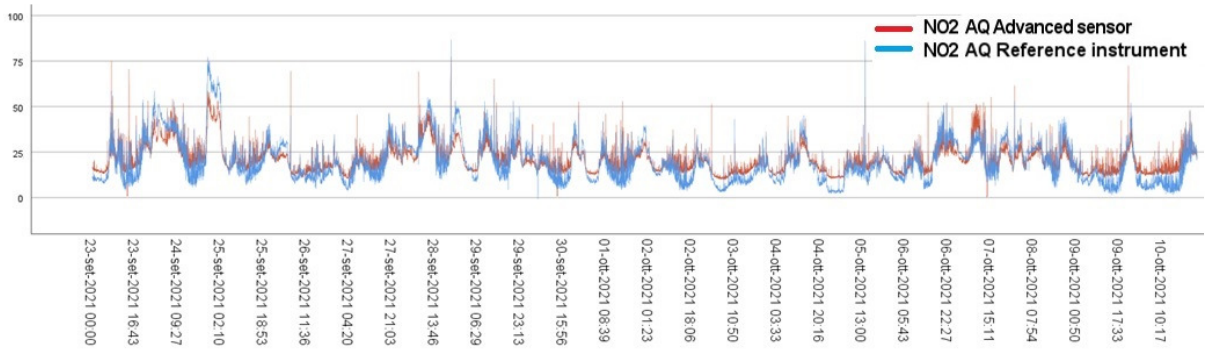

Figure 46. Nitrogen dioxide (NO_2) airborne concentrations [ppb] measured by collocation of the AMAT AQ advanced sensors compact station and the Innovhub SSI reference cabin.

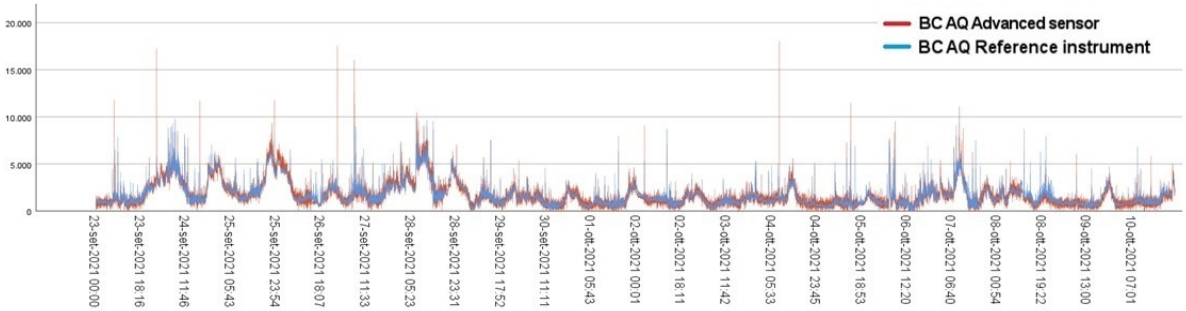

Figure 47. Black Carbon (BC) airborne concentrations [ng/m3] measured by collocation of the AMAT AQ advanced sensors compact station and the Innovhub SSI reference cabin.

The AQ advanced sensors' performance for each pollutant monitored was quantified via the coefficient of determination (R^2) and the regression model, i.e., the slope and y-intercept, in the comparison with the reference Innovhub SSI cabin equipped with the described instruments.

Results (Figure 48 to Figure 50) indicate that the AQ advanced sensors reach good agreement with the reference AQ instruments in detecting airborne traffic tracers such as NO_2 (R^2=0.80), NO (R^2=0.74) and Black Carbon (R^2=0.78) despite the different measuring principle. Also, Ozone (O_3), an important interfering pollutant for airborne NO_2 measurements, presents good agreement between AQ sensors and AQ reference instruments data (R^2=0.80). Carbon monoxide (CO) concentrations feature a lower correlation (R^2=0.40). This is probably due to the very low absolute airborne values near the lower detection limit, which leads to a higher noise variance in the data.

A good agreement is also reached between AQ advanced sensors and the RES Point sampling system data (see section 1.5.2).

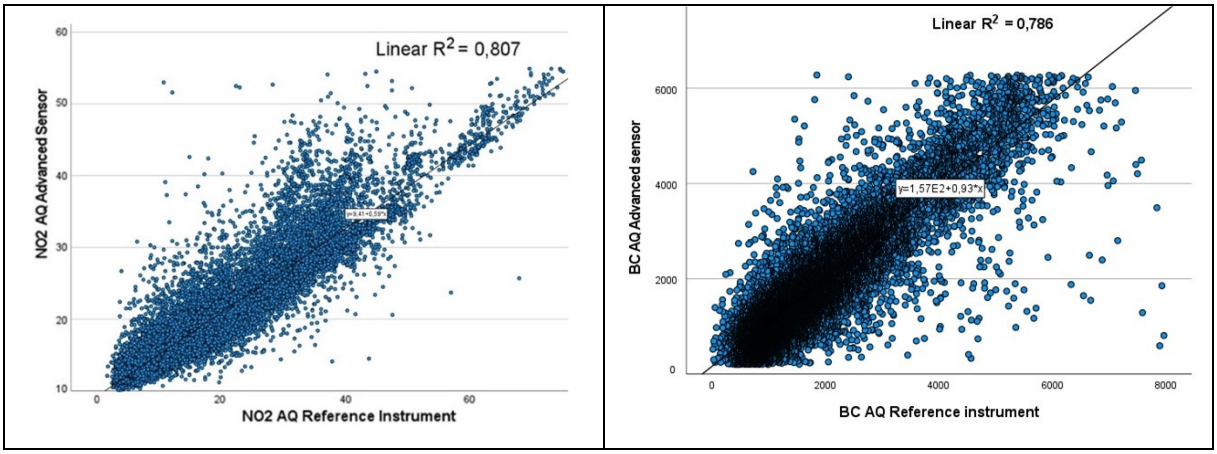

Figure 48. Airborne pollutant concentrations measured by collocation of AMAT advanced sensors compact station and the Innovhub SSI reference cabin: Nitrogen dioxide, NO2 (left) and Black Carbon, BC (right).

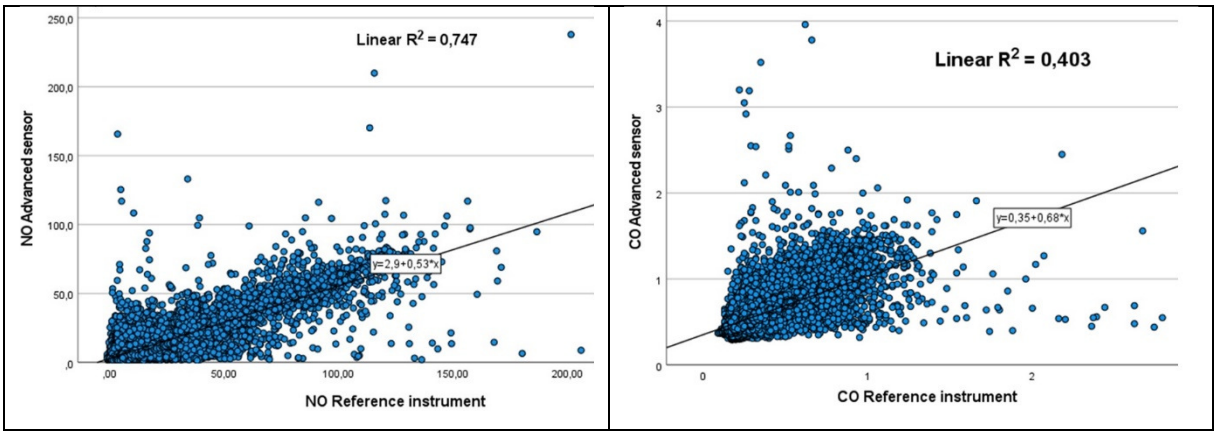

Figure 49. Airborne pollutant concentrations measured by collocation of AMAT advanced sensors compact station and the Innovhub SSI reference cabin: Nitrogen monoxide, NO (left) and Carbon monoxide, CO (right).

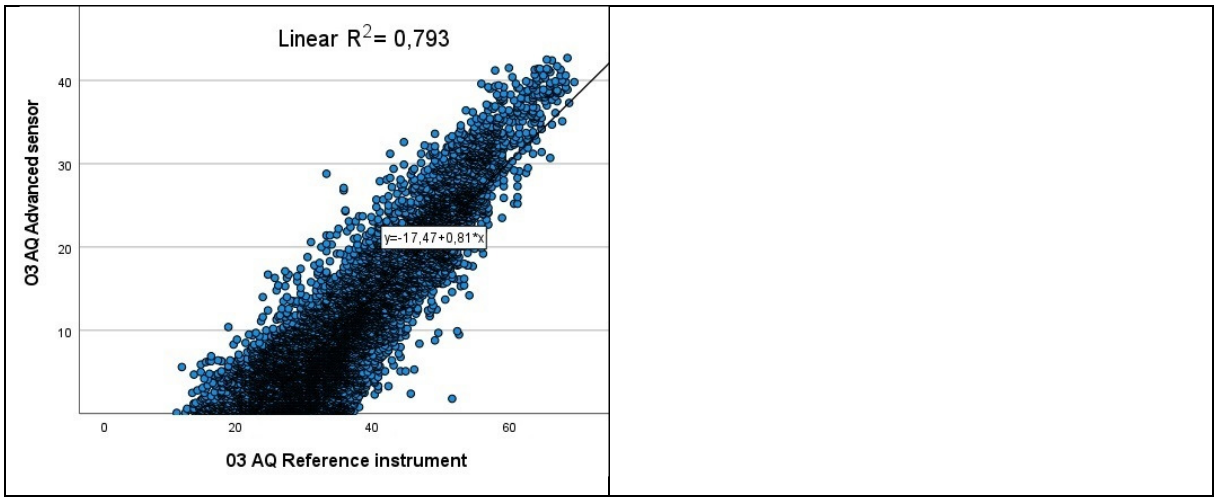

Figure 50. Airborne pollutant concentrations measured by collocation of AMAT advanced sensors compact station and the Innovhub SSI reference cabin: Ozone, O3.

1.5.2. Comparison versus Point Sampling emissions measurements

Air quality data were collected by means of the AQ advanced sensors with a 1-minute resolution and compared with 1-minute resolution measurements from the RES Point sampling system deployed by

TUG and Airyx. Additionally, 5-minute running means were calculated to determine statistical correlation between the two data series.

In observing the related data series, the distance between the RES Point sampling site, monitoring vehicular emissions, and the AQ monitoring site has to be considered. As vehicles pass through via Madre Cabrini, the exhaust plume released by vehicles is first observed by the RES Point sampling at the associated site. Subsequently, the vehicular exhaust plume may travel along the road and reach the AQ advanced sensors, 15 linear meters away. Thus, differences between AQ instruments and AQ advanced sensors' measurements may be due to the time needed by the vehicular exhaust plume to reach the AQ monitoring site from the RES Point sampling site. Additionally, since driving conditions (e.g., vehicle speed and acceleration) could be very different between the two sites, the related vehicular emission factors may also differ.

In Figure 51 and Figure 52, respectively, NO_2 and BC airborne concentrations measured by AQ advanced sensors compact station and vehicular emissions measured by mean of RES Point sampling system are reported.

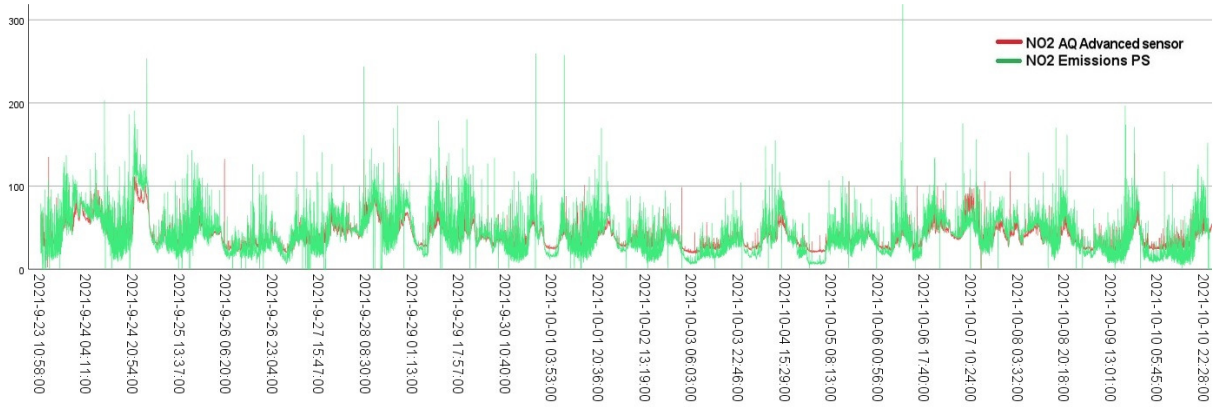

Figure 51. Nitrogen Dioxide (NO_2) concentrations [ppb] measured by collocation of the AQ advanced sensors compact station and NO_2 vehicular emissions measured by mean of RES Point sampling.

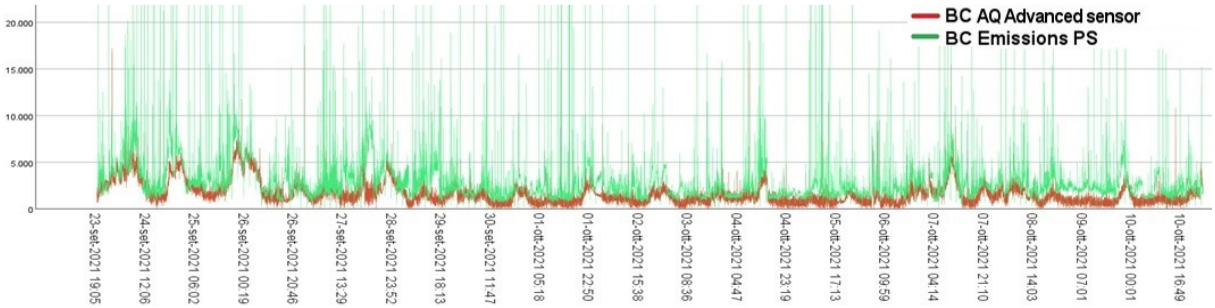

Figure 52. Black Carbon (BC) airborne concentrations [ng/m3] measured by collocation of the AQ advanced sensors compact station and BC vehicular emissions measured by means of RES Point sampling.

A significant positive correlation was observed between the AQ advanced sensors data and the RES Point sampling detections of gaseous traffic-related pollutants such as NO2 (R^2> 0.60) and CO2 (R^2> 0.60). Lower correlation coefficients are found for Black carbon (R^2> 0.30) probably due to the non-gaseous nature of the pollutant (Figure 53).

The coefficient of determination R^2 relative to NO_2 measurements by AQ advanced and by RES Point sampling sensors ranges between 0.6 and 0.8. In particular, the higher R^2 (0.8) is obtained when 5-minute average AQ concentrations are considered, instead of 1-minute ones. This means that:

- the variability of 5-minute NO_2 concentration measurements made by the advanced AQ sensors is 76% explainable by the variability of the measurements performed by emission point sampling sensors with a linear regression model. Specifically, it can be stated that the

same causes due to which measurements of NO_2 vary over time for the emission point sampling sensors are also largely detected by the AQ advanced sensors.
- As the NO_2 emission values observed by the RES Point sampling increase, an average linear increase in the values of NO_2 AQ sensors is observed.
- Graphically, the high R^2 between sensors can be seen in observations concentrated on the regression line.

Moreover, as the level of NO_2 emission increases, as measured by the point sampling sensors, a less than proportional increase in the NO_2 concentration, as measured by the AQ sensors, can be expected. In particular, with the increase of 1 ppb (1,912 µg/m^3) of NO_2 measured by the RES Point sampling sensors, an increase of 0.5-0.6 ppb (0.96-1,15 µg/m^3) is expected on average in the measurements made by the AQ sensors.

The coefficient of determination R^2 relative to BC measurements by AQ advanced and by RES Point sampling sensors ranges between 0.3 and 0.4. In particular, the higher R^2 is obtained when 5-minute average AQ concentrations are considered, instead of 1-minute ones. In addition, conversely to NO_2, as the level of BC emission increases, as measured by the RES Point sampling sensors, a less than proportional increase in the BC concentration, as measured by the AQ sensors, can be expected only when considering a 1-minute concentrations average. This could be attributed to the non-gaseous nature of Black carbon.

The coefficient of determination R^2 relative to CO_2 measurements by AQ advanced and by RES Point sampling sensors ranges between 0.7 and 0.8. In particular, the higher R^2 (0.8) is obtained when 5-minute average AQ concentrations are considered, instead of 1-minute ones. As a result, a clear agreement between the AQ advanced and RES point sampling sensors can be observed.

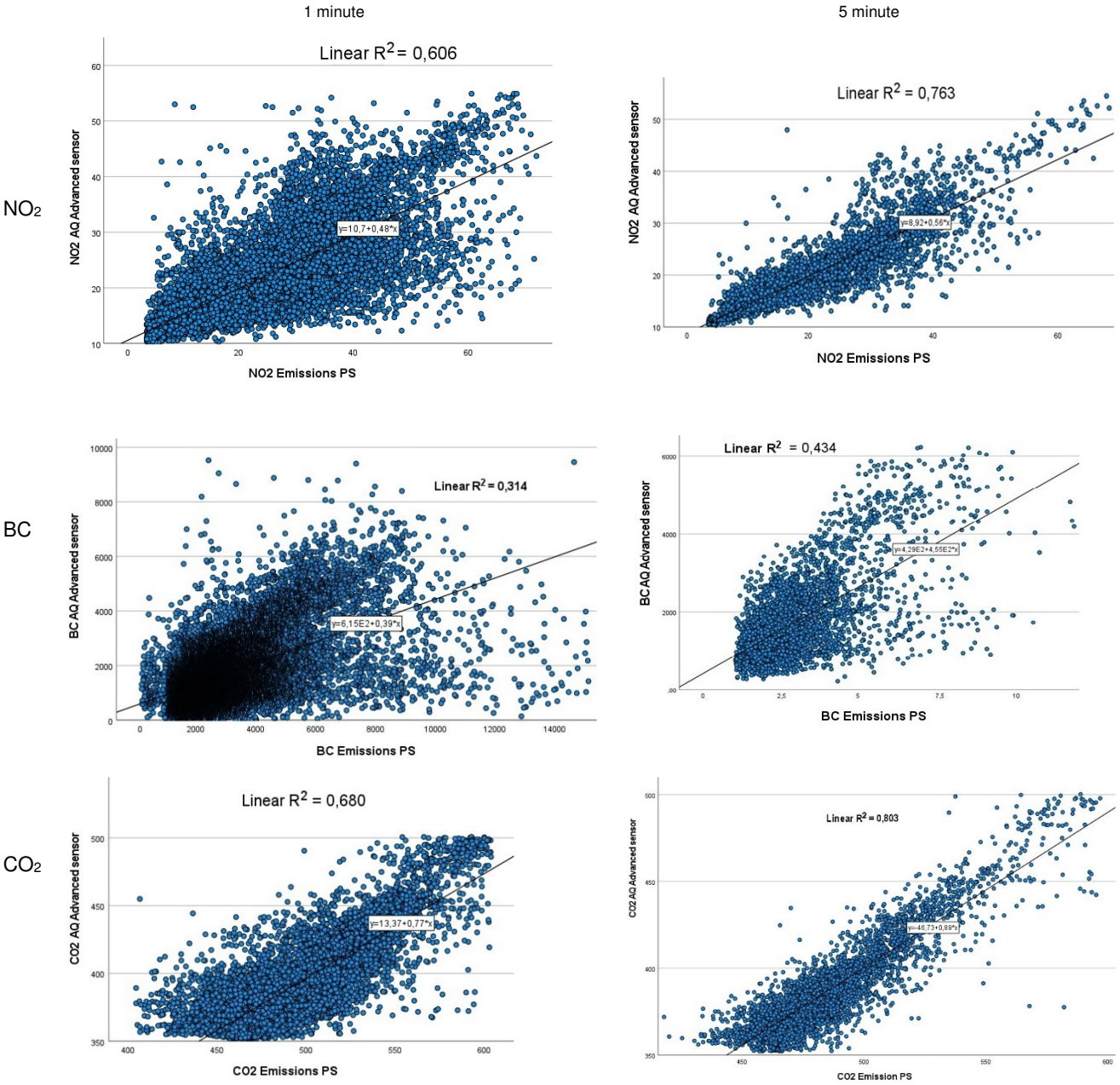

Figure 53. Airborne pollutant concentrations measured by AMAT advanced sensors compact station versus vehicular traffic emissions measured by RES Point Sampling system for Nitrogen dioxide, NO_2 (first row), Black Carbon, BC (second row), Carbon dioxide, CO_2 (third row). Airborne concentrations are considered at 1 Minute level (left) or at 5 Minute level (right).

The effect of the so-called 'high polluters' vehicles circulation on urban air quality has been assessed in Figure 54 and Figure 55. Airborne pollution hotspots were compared to passages of two known highly emitting vehicles equipped with PEMS and deployed for the field campaign by Innovhub SSI (see previous Chapters). The two vehicles are:

- a Renault Clio, Euro 6b, equipped with PEMS,
- a Volkswagen Golf, Euro 4, equipped with PEMS, a tampered Diesel Particulate Filter (DPF).

Both vehicles are equipped with a diesel engine and, while the first revealed itself as a high emitter for NO_x, the second one exhibited a tampered particulate filter.

In the following charts, airborne pollutants concentrations data are referred to the AMAT advanced sensor station co-located with Innovhub SSI reference cabin.

Results demonstrate that: 1) air quality hotspots can be strictly linked due to the passages of high polluters vehicles; 2) the AQ Advanced sensors compact station is capable to capture this phenomenon, except when in unfavorable meteorological conditions (i.e., wind direction, wind speed) or when confronted with particular driving conditions reducing emission factors.

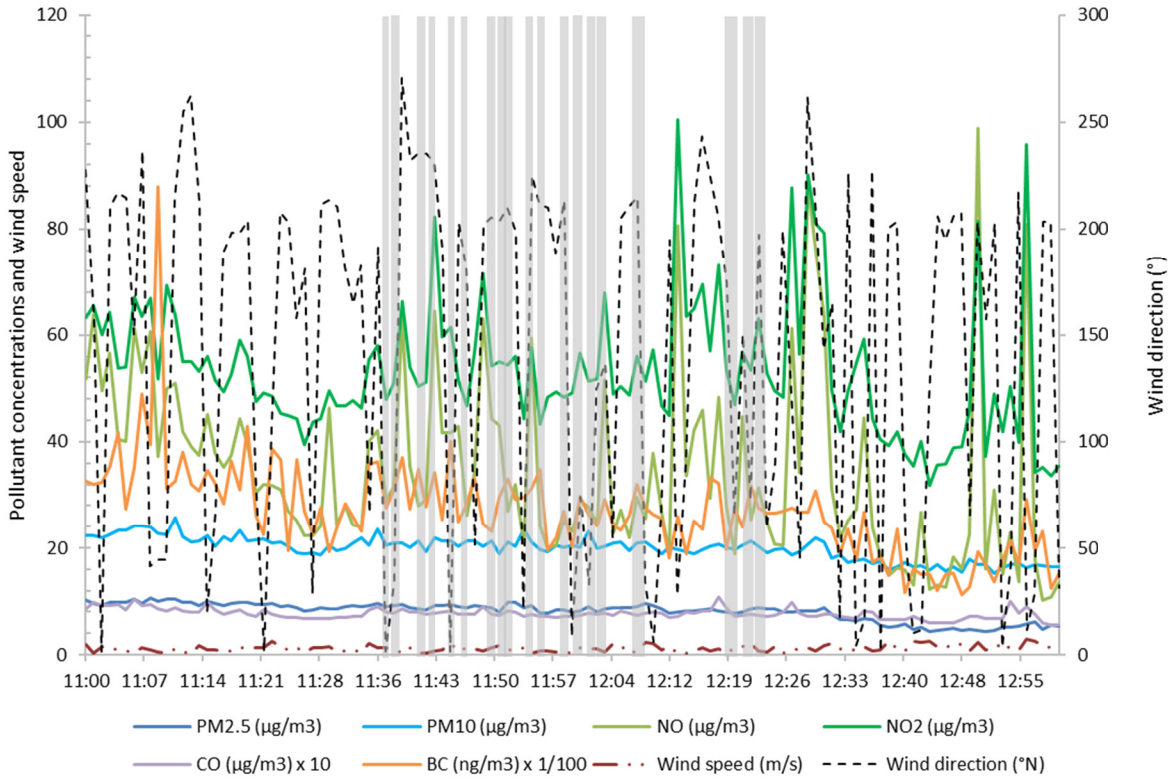

Figure 54. Air quality indicators compared with the high polluting vehicle - a high NO_x emitter (Renault Clio, Euro 6b diesel) passages (grey vertical line). Airborne pollutants concentrations data are referred to the AMAT advanced sensor station co-located with Innovhub SSI reference cabin.

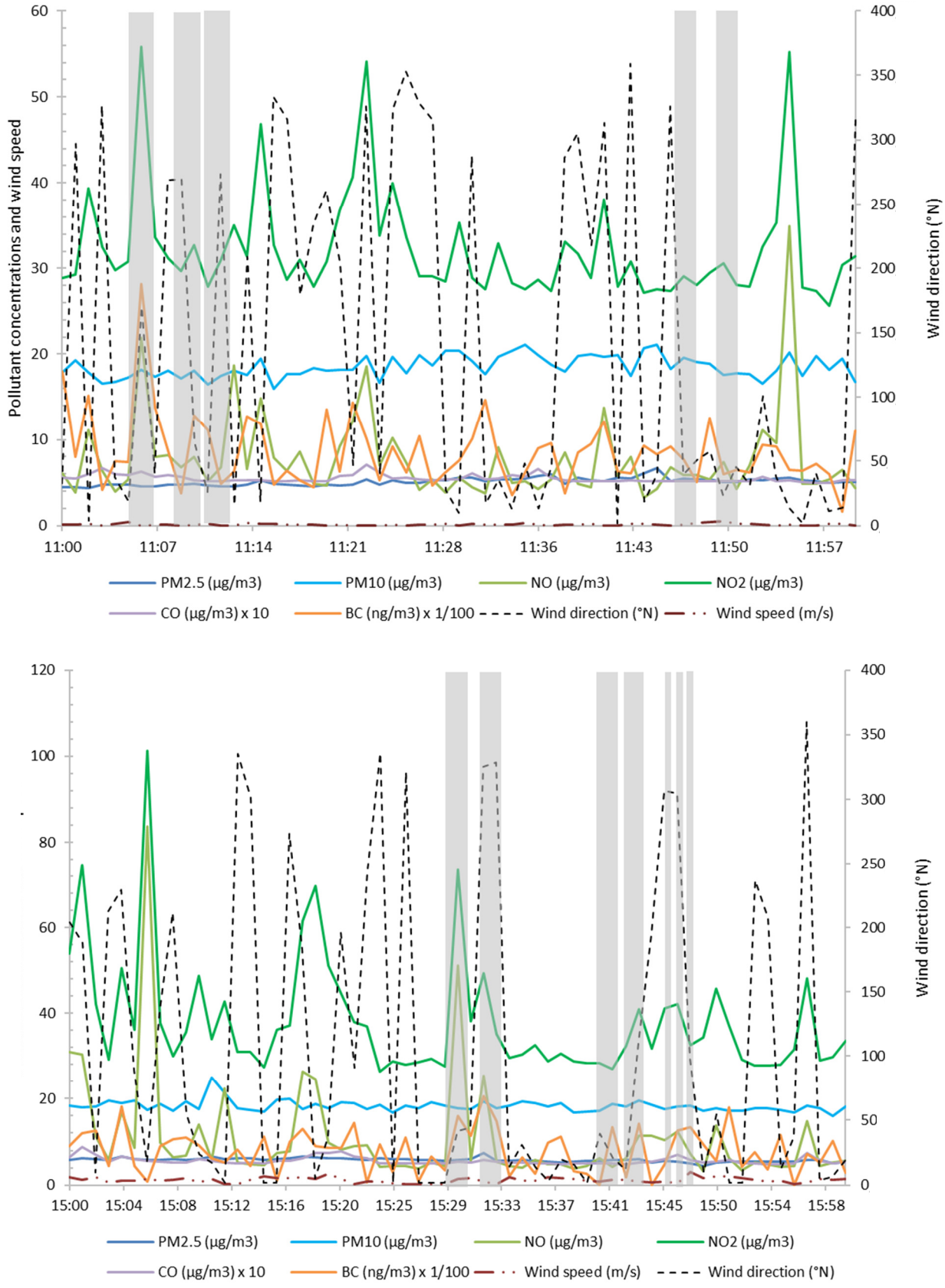

Figure 55. Air quality indicators compared with the high polluting vehicle - DPF tampered (Volkswagen Golf, Euro 4, diesel) passages (grey vertical line). Airborne pollutants concentrations data are referred to the AMAT advanced sensor station co-located with Innovhub SSI reference cabin.

Hourly measurements by the AQ advanced sensors are compared with the SSI AQ reference cabin in Figure 56 to Figure 58. In particular, pollutant concentrations are measured by the AQ advanced sensors, while wind speed and vehicular traffic emissions are measured by the RES Point Sampling system. Results are reported for Nitrogen dioxide (NO_2) in Figure 56, black carbon (BC) in Figure 57, and PM10, PM2.5 in Figure 58. Trends are reported both in normalized and absolute values.

The daily morning and evening peaks, connected with anthropic emissions are well detected in all three plots, as highlighted by the weekly traffic trends. It should be noted that, during the field campaign weeks, there was a clear decrease in NO_2 concentrations due to wind speeds greater than or equal to 1.5 m/s. In Figure 30.a, a good correlation between the RES Point sampling system and AQ reference instrument can be observed, especially from 23/09/2021 to 2/10/2021.

The late evening/night peaks of NO_2 concentrations in the majority of the days of the field campaign not related to vehicular transits monitored in via Madre Cabrini could be attributed to heavy traffic-related emissions produced in the nearby main ring road, higher during weekend days due to recreational activities related vehicular transits.

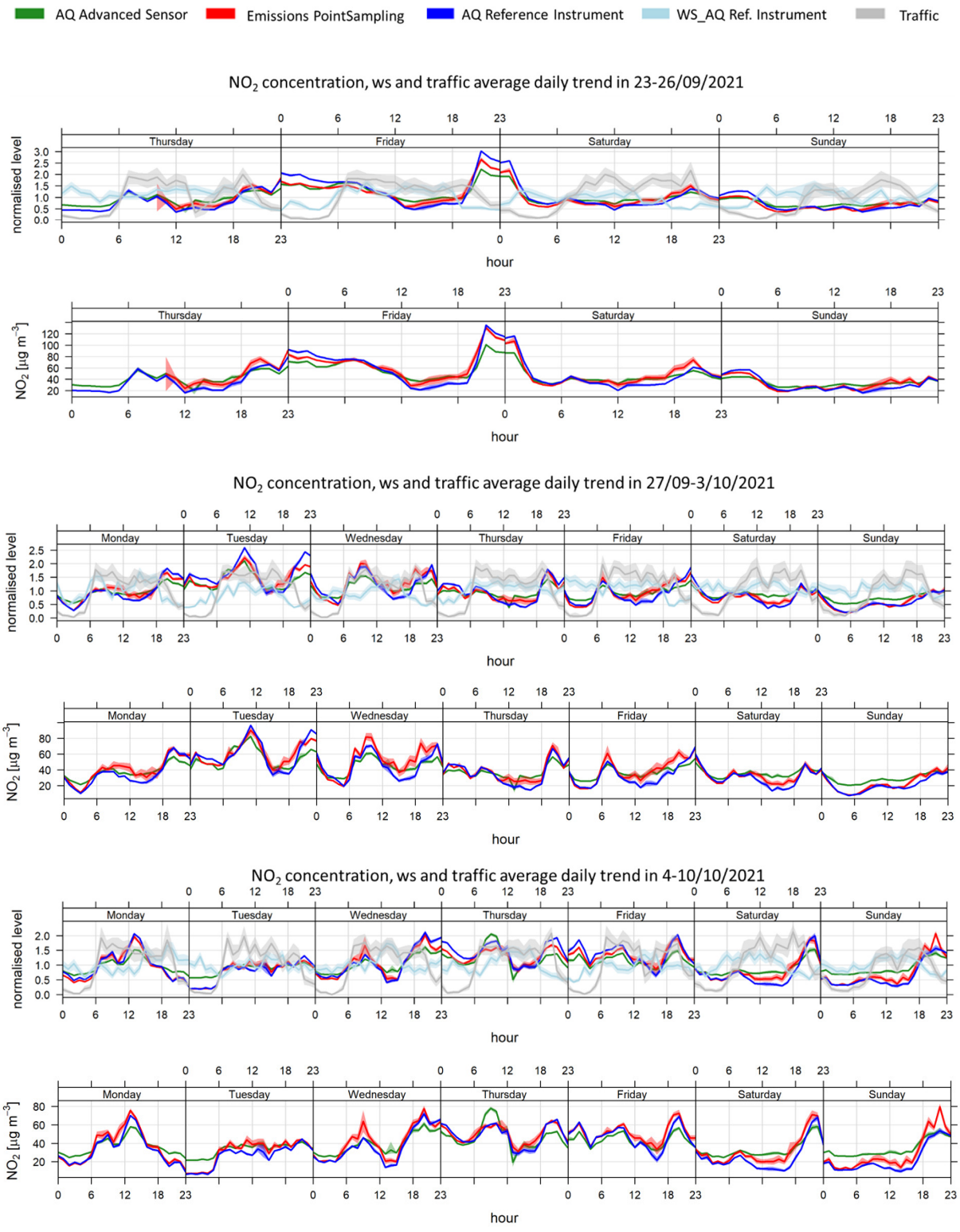

Figure 56. Hourly and weekly airborne pollutant concentrations measured by AMAT advanced sensors compact station versus Reference stations Innovhub SSI, wind speed and vehicular traffic emissions measured by RES Point Sampling system for Nitrogen dioxide, NO_2.

Excellent agreement between the AQ advanced sensor and reference instrument is observed for Black carbon (BC) measurements (Figure 57). Differences between AQ advanced sensors and the RES Point Sampling observations can be attributed to the nanoparticulate nature of BC. Such a nature makes it more difficult for BC, than other gaseous pollutants, to be transported along the 15-meter distance between the two monitoring sites.

NO_2 concentrations are affected by larger-scale phenomena, and the reported measurements could represent local variations. Clear concentration peaks appear in Figure 57 as measured by the RES Point Sampling system on Friday between 12-18 of the first week, between 12-18 on Tuesday of the second week, between 6-12 on Tuesday of the third week, and on Wednesday 12-18 of the second week. These peaks are not followed by the AQ reference instrument and advanced sensor. Differently, at 5 PM on Saturday of the first week, the latter two instruments report a concentration peak. Nevertheless, data for RES Point Sampling are not available within the same temporal range, and therefore it is not possible a comparison to interpret the hotspot data.

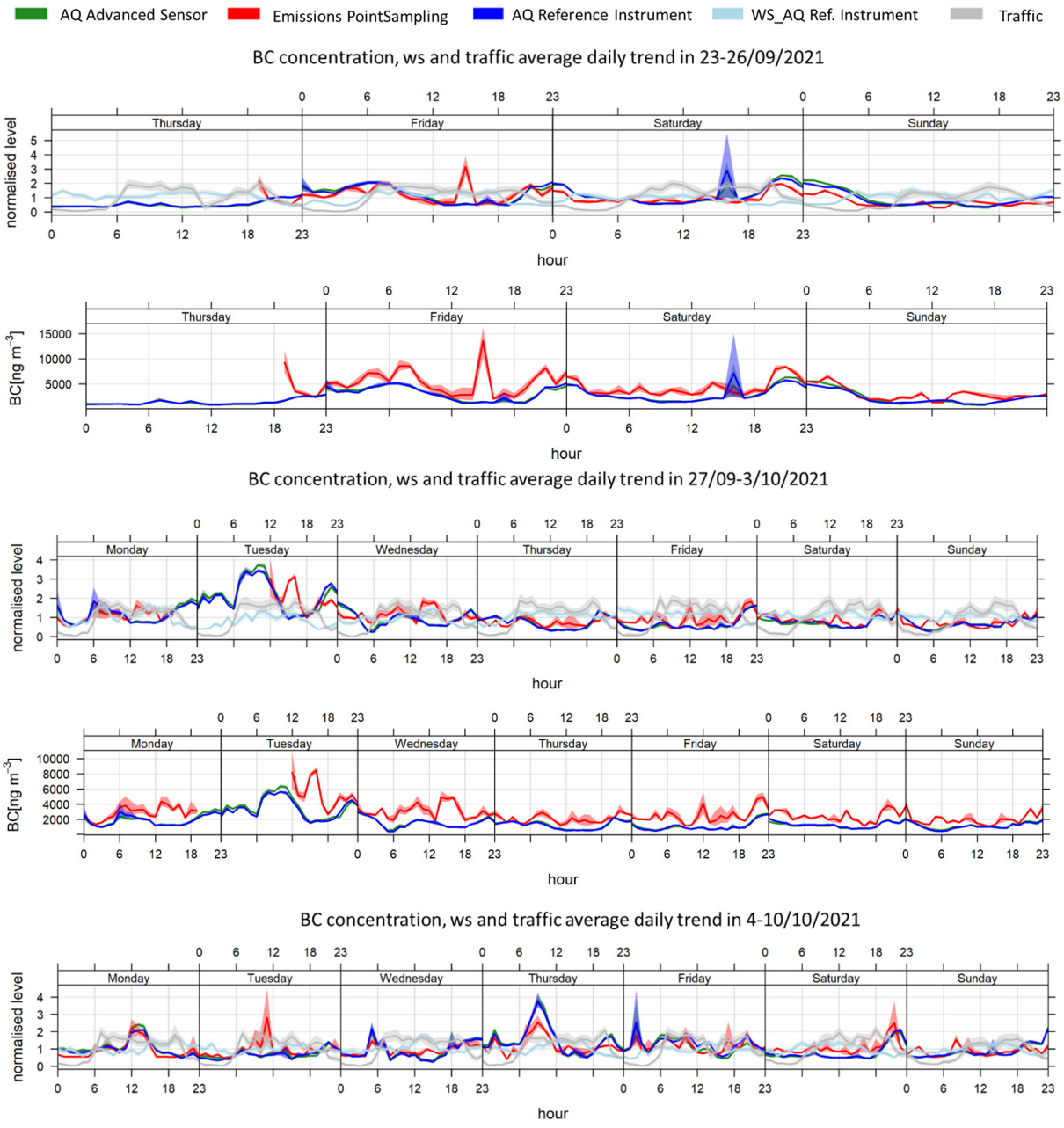

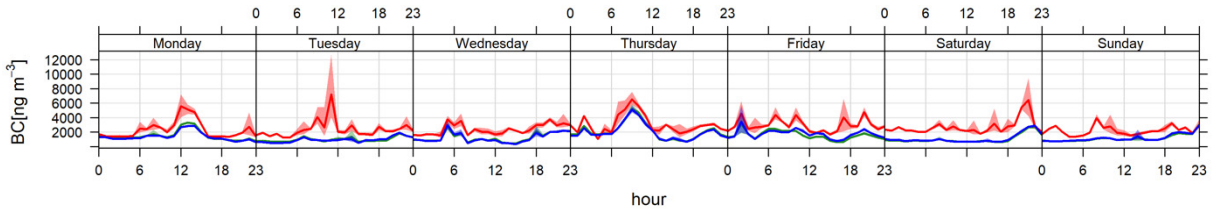

Figure 57. Hourly and weekly airborne pollutant concentrations measured by AMAT advanced sensors compact station versus Reference stations Innovhub SSI, wind speed and vehicular traffic emissions measured by RES Point Sampling system for Black Carbon, BC.

The Spearman correlation confirms a good agreement between the trends of the pollutant levels monitored by RES Point sampling and AQ measures for BC and NO_2 ranging between 0.6 and 0.9.

In Figure 58 hourly and weekly airborne pollutant concentrations measured by AMAT advanced sensors compact station, wind speed and vehicular traffic emissions measured by RES Point Sampling system are reported for PM10 and PM2.5. Trends are reported both in normalized and absolute value forms. It is interesting to note that the PM10 and PM2.5 concentrations daily trends seems to be not related to the vehicular transits.

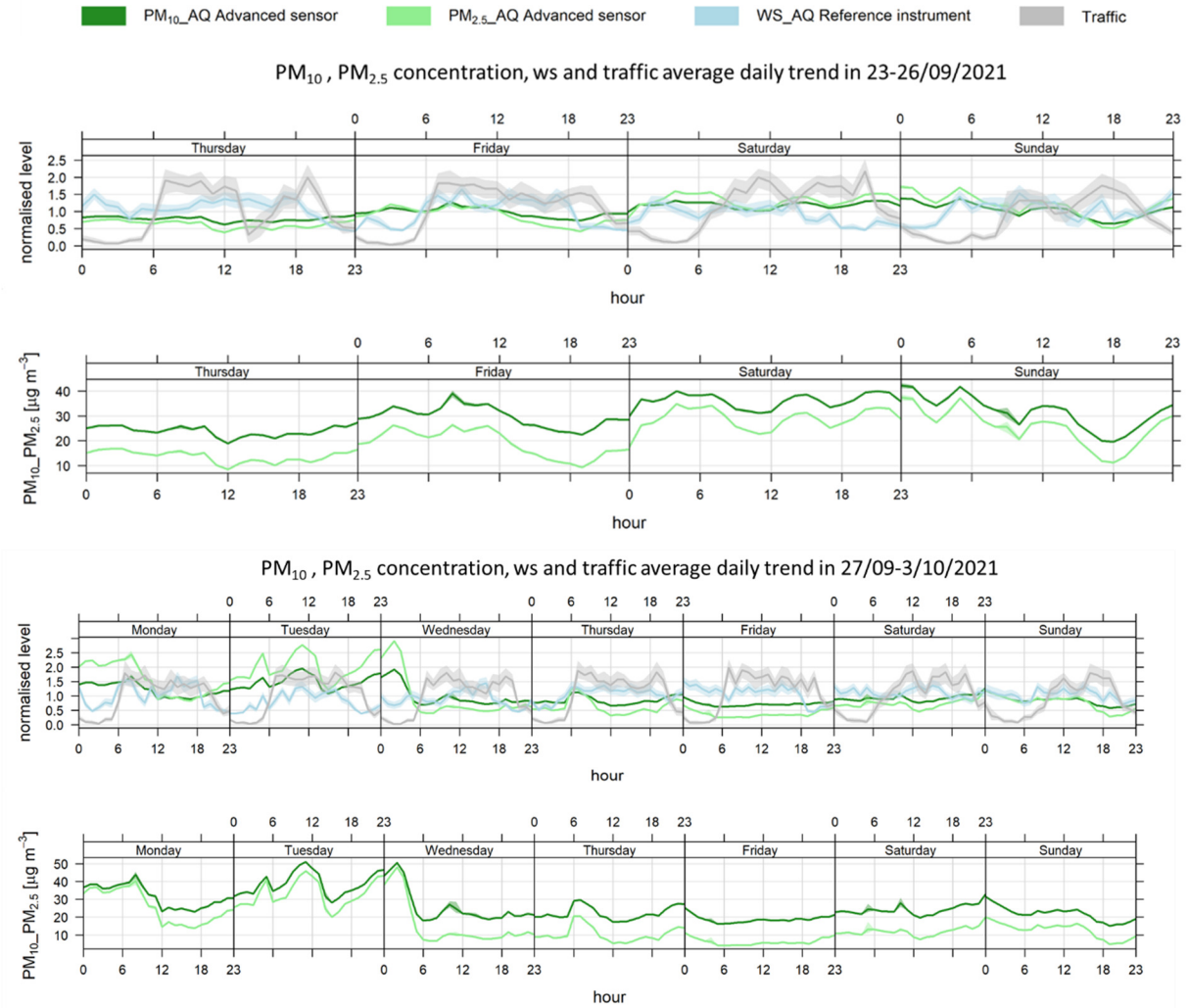

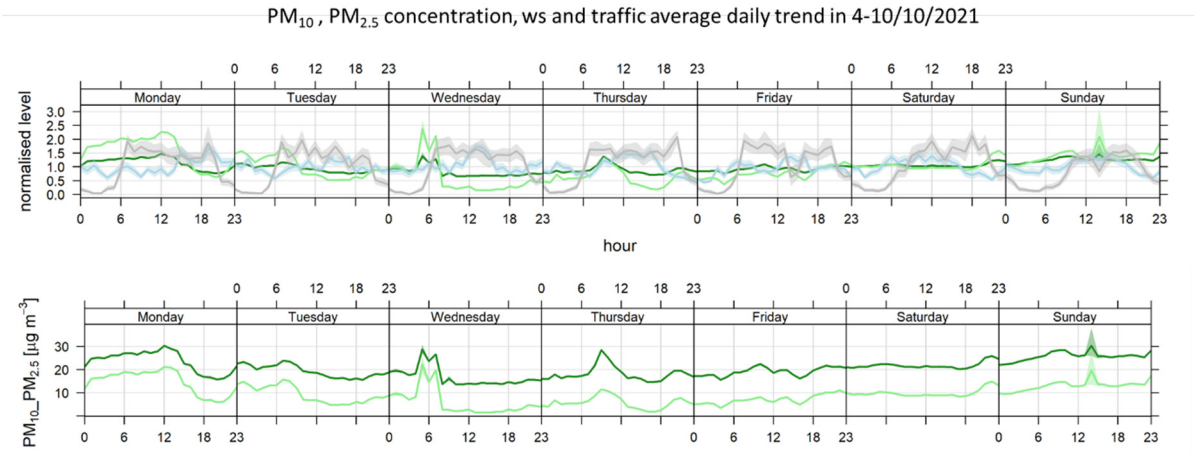

Figure 58. Hourly and weekly airborne pollutant concentrations measured by AMAT advanced sensors compact station, wind speed and vehicular traffic emissions measured by RES Point Sampling system for PM10 and PM2.5.

Particle Number Concentrations (PN) measurement were measured both from AQ advanced sensor compact station and RES Point sampling system. With regard to the instrumentation capabilities, the AQ advanced sensor compact station is able to detect particles' sizes between 0.3 to 10 µm; the RES Point sampling system data detects emissions between 23 nm to 500 nm.

After conducting a Spearman correlation analysis, the dimensional cuts ranging from 0.3 µm to 0.9 µm are selected as those with best hourly correlation between the two instruments (Spearman correlation coefficient around 0.4-0.5). In Figure 59 to Figure 61, hourly data for the three weeks of the campaign are reported in normalized values, being the unit for AQ advanced sensor compact station referred to # particles/m^3, while the one of the RES Point sampling system referred to # particles/cm^3.

The normalised trends indicate that the AQ advanced sensors reach good agreement with the RES Point Sampling system in detecting morning and evening peaks for all the cuts. This is particularly true when considering temporal variation for particles with a diameter of 0.30 µm. In certain episodes also the 0.40 µm cut well follows the RES variations (e.g., morning picks of 6 October 2021).

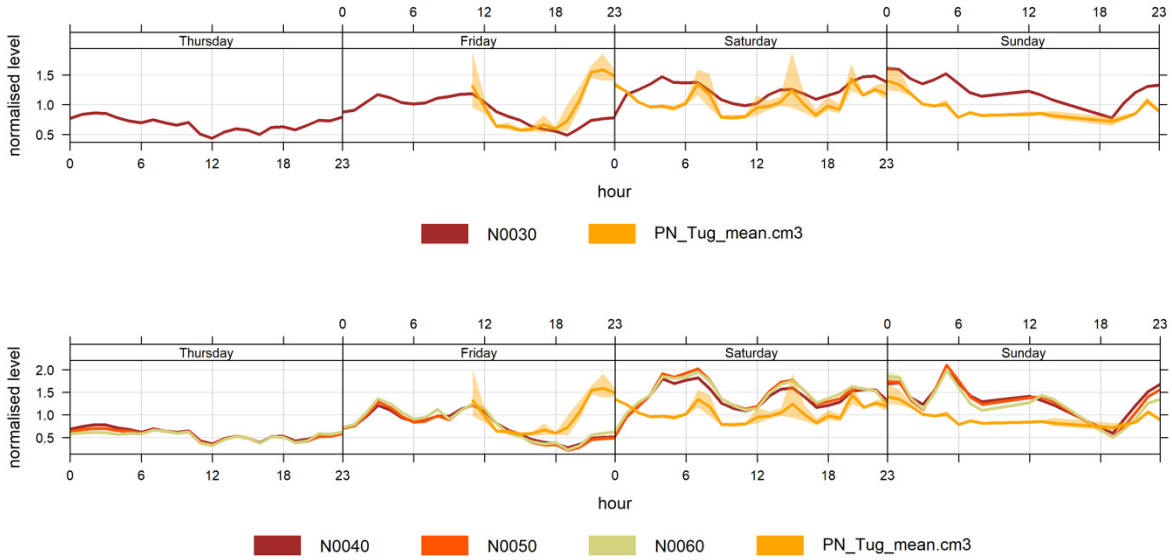

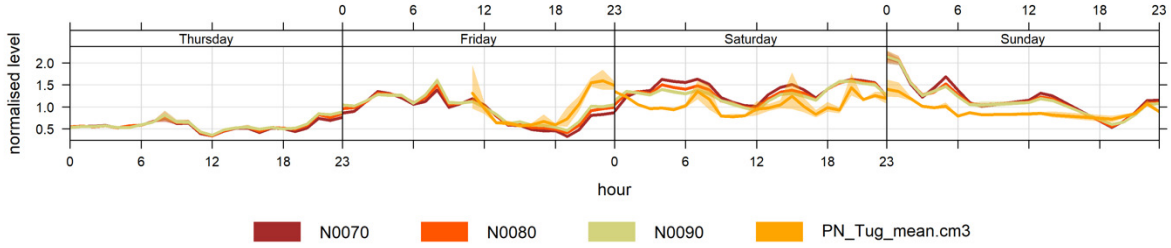

Figure 59. Hourly and weekly airborne particulate concentrations measured by AMAT advanced sensors compact station versus vehicular traffic emissions measured by remote sensing - Point Sampling technique in term of Particulate Number (PN): 0.30 µm (first row), from 0.40 to 0.60 µm (second row), from 0.70 to 0.90 µm (third row). Period: 23 September 2021 -26 September 2021.

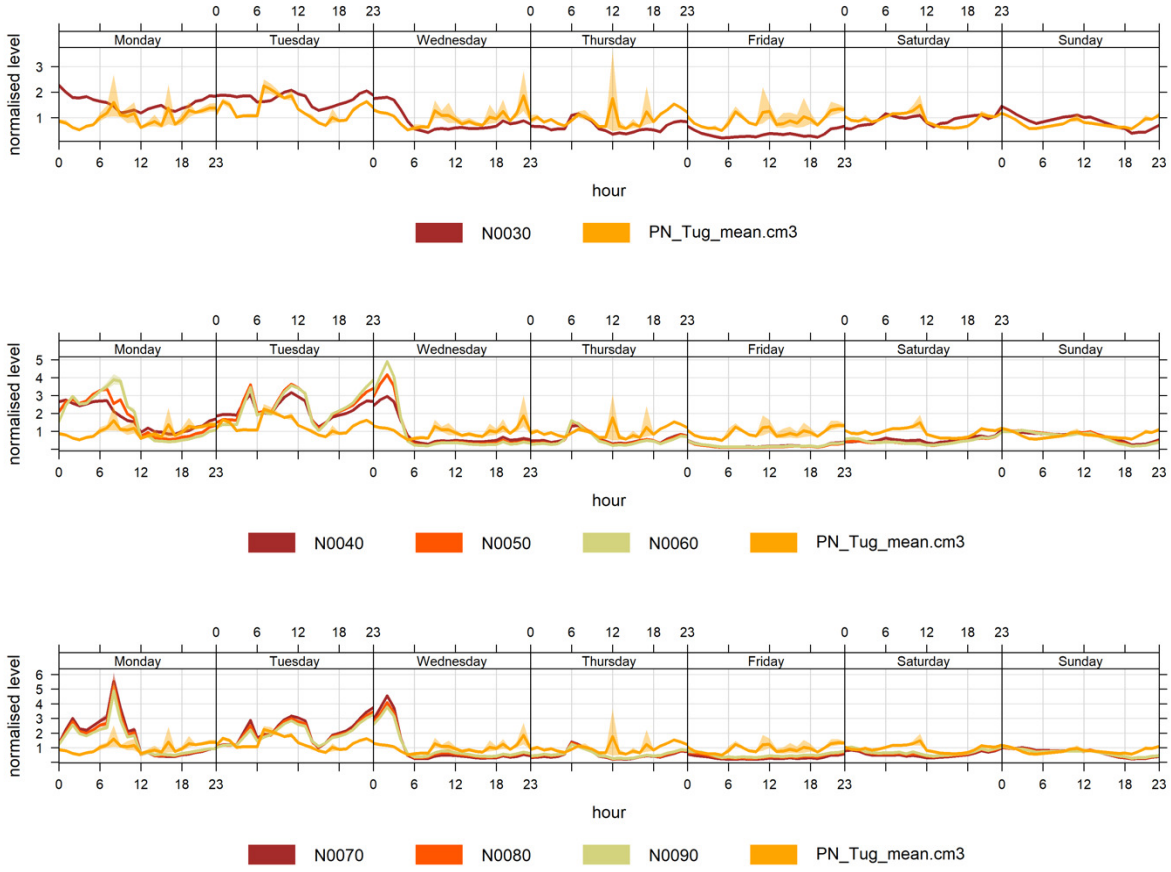

Figure 60. Hourly and weekly airborne particulate concentrations measured by AMAT advanced sensors compact station versus vehicular traffic emissions measured by remote sensing - Point Sampling technique in term of Particulate Number (PN): 0.30 µm (first row), from 0.40 to 0.60 µm (second row), from 0.70 to 0.90 µm (third row). Period: 27 September 2021 - 3 October 2021.

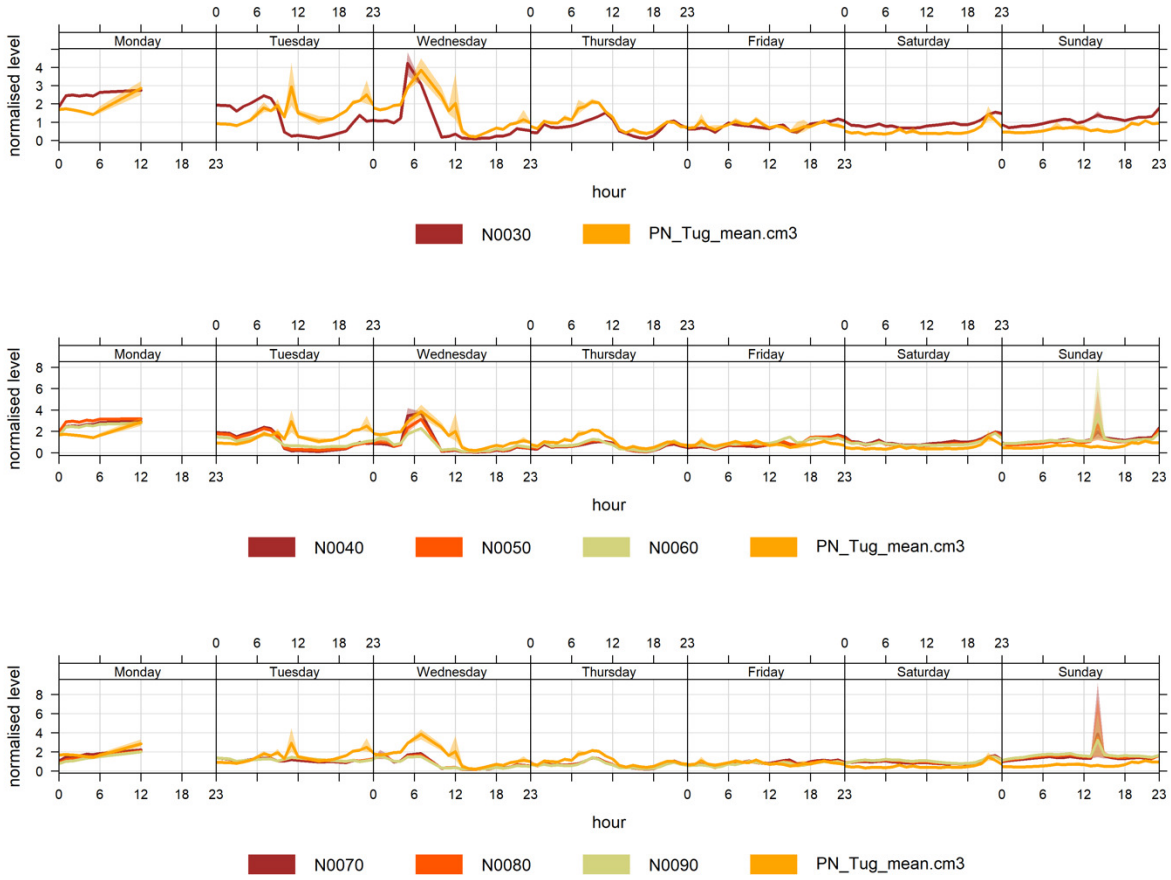

Figure 61. Hourly and weekly airborne particulate concentrations measured by AMAT advanced sensors compact station versus vehicular traffic emissions measured by remote sensing - Point Sampling technique in term of Particulate Number (PN): 0.30 µm (first row), from 0.40 to 0.60 µm (second row), from 0.70 to 0.90 µm (third row). Period: 04 October 2021 - 10 October 2021.

1.5.3. Comparison versus vehicles transit

The analysis of variance (ANOVA) test results shows that AQ advanced sensors are capable to detect each incremental transit of vehicles. To test this hypothesis traffic data was used, categorizing each minute with the number of vehicles that have passed through in that time frame. Next, ANOVA was carried out to test whether the mean value of each AQ advanced sensor pollutant is different among the categories of vehicular transit number. Results are shown in Figure 62 and summarized in Table 4.

The ANOVA test shows good results also with the NO_x emission factor (NO_x/CO_2) monitored by RES Point sampling (right) for each traffic condition (Figure 63).

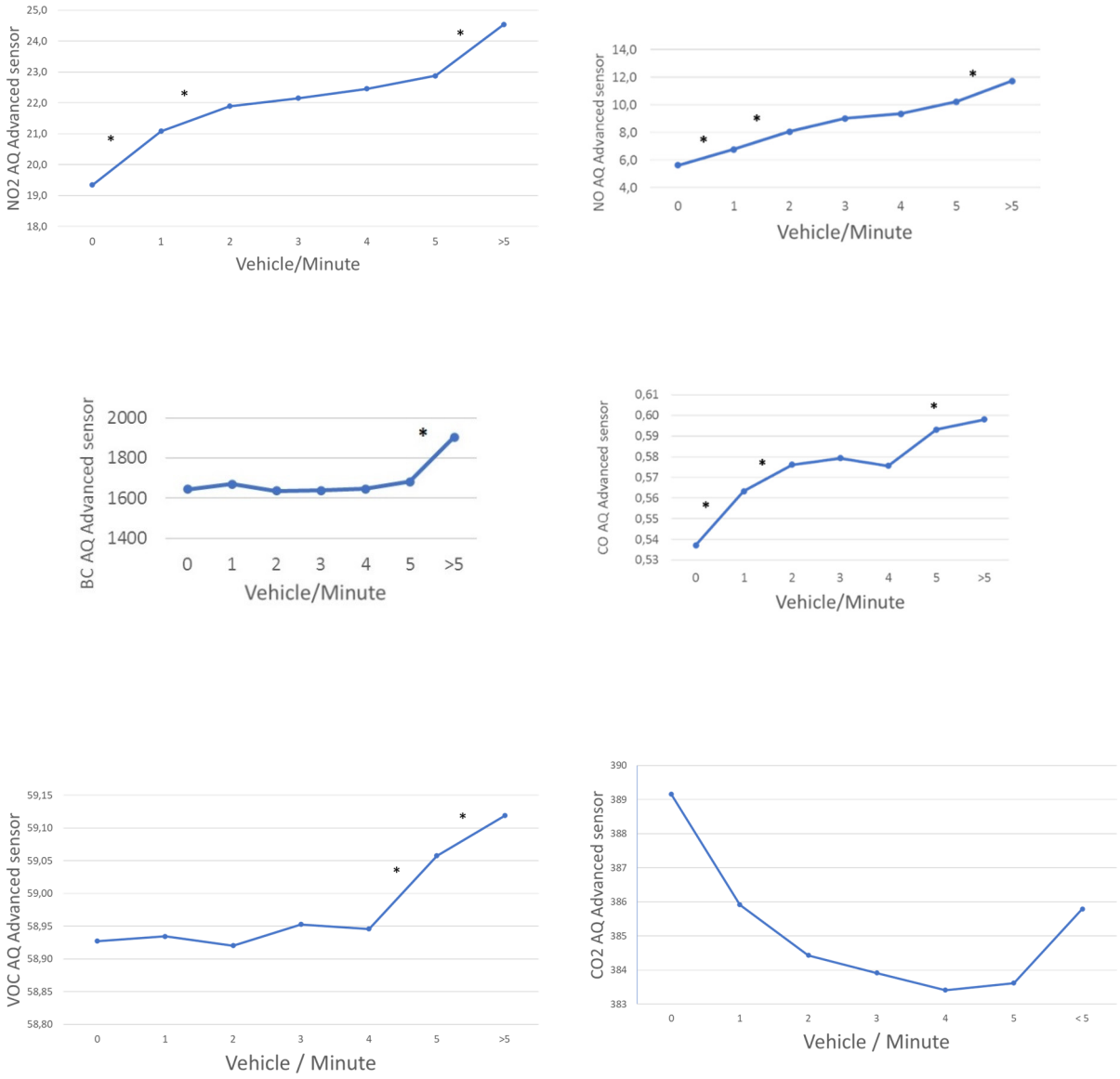

Figure 62. ANOVA results: the mean value of air quality concentrations (monitored by AQ advanced sensors deployed by AMAT of NO_2, NO, BC, CO, VOC, and CO_2 for each traffic condition (number of vehicles transit per minute). Statistically different air quality concentration mean values associated to vehicles/minute classes are marked with *.

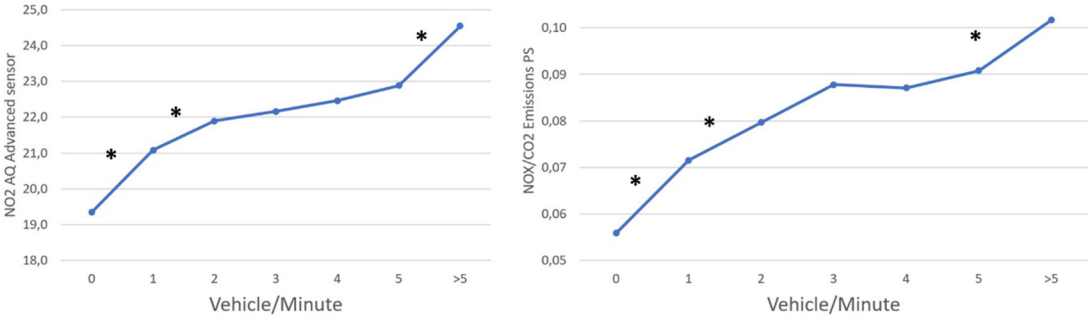

Figure 63. ANOVA results: the mean value of air quality concentrations (monitored by AMAT) of NO_2 (left) and NO_x emission factor (NO_x/CO_2) monitored by Point sampling (right) for each traffic condition (number of vehicles transit per minute). Statistically different air quality concentration mean values associated to vehicles/minute classes are marked with *.

Table 4. ANOVA results: the mean value of air quality concentrations (monitored by AMAT) of NO_2 (left) and NO_x emission factor (NO_x/CO_2) monitored by Point sampling (right) for each traffic condition (number of vehicles transit per minute).

ANOVA

	VEHICLE / MINUTE					
	0 - 1		1 - 2		5 - >5	
AQ Advanced sensor	dif. mean	p. value	dif. mean	p. value	dif. mean	p. value
NO2	1,74	p<0.001	0,81	p<0.001	1,66	p<0.001
NO	1,13	p<0.001	1,29	p<0.001	1,5	p<0.001
O3	2,25	p<0.001	1,44	p<0.001	-1,75	p<0.001
BC					220	p<0.001

	VEHICLE / MINUTE					
	0 - 1		1 - 2		4 - >5	
	dif. mean	p. value	dif. mean	p. value	dif. mean	p. value
AQ Advanced sensor - CC	0,026	p<0.001	0,013	p<0.001	0,022	p<0.001
Emission PS - NOX/CO2	0,015	p<0.001	0,008	p<0.001	0,14	p<0.001

1.6. Airborne Ammonia monitoring

During the same period as the CARES measurements, AMAT and the Municipality of Milan organized a monitoring campaign of ammonia concentrations with the goal to produce a preliminary urban map of the NH_3 distribution over the city.

In 15 urban sites (Figure 64) the ammonia concentrations were measured during one month by means of passive samplers (Passam AG). The monitoring sites were classified into three typologies on the base of the different local emission conditions: background sites, near to ammonia anthropogenic sources (road traffic included) and near to ammonia agricultural sources. As for the road traffic, the ammonia concentrations were monitored at the two EDAR sites (i.e., via Madre Cabrini and via Cilea) and near a motorway. Only in via Madre Cabrini site, the NH_3 measurements were carried out using both passive samplers and a continuous NH_3 monitor device (see above, Paragraph 1.5).

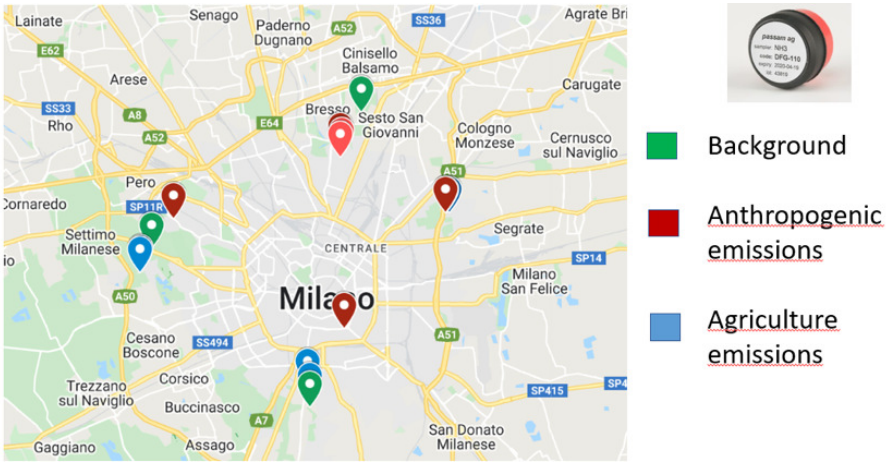

Figure 64. Ammonia concentration measurement sites and a picture of passive sampler.

The measured values confirmed that, over Milan, the ammonia concentrations show a gradient decreasing from South to North (Figure 65).

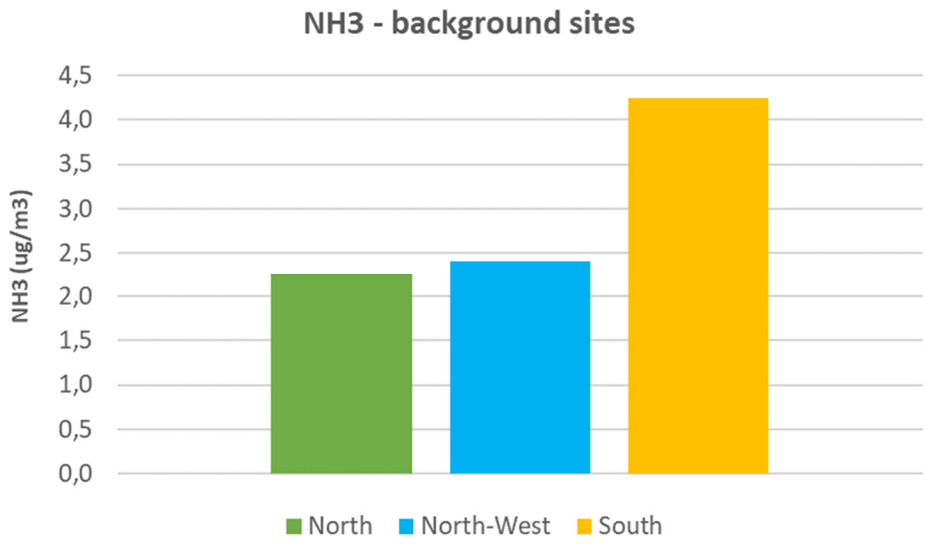

Figure 65. Ammonia concentrations measured at the background sites.

Moreover, these values confirm the importance of local emission sources, because the NH_3 concentrations strongly decrease with the horizontal distance from the source. This aspect is important for the interpretation of the collected data. In fact, the passive samplers in Madre Cabrini were placed just near the lane, whereas the distance of the samplers from the nearest lane was about 5 meters in via Cilea (Figure 66) and about 18 meters in the case of the motorway.

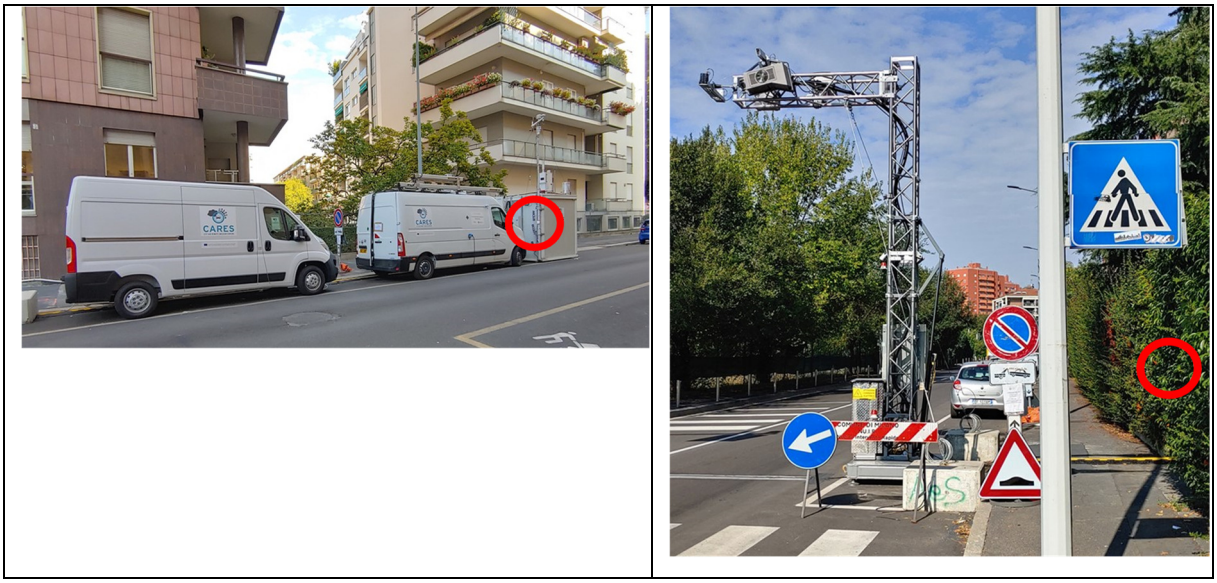

Figure 66. NH_3 samplers' position in Madre Cabrini (left) and Cilea (right).

The obtained results (Figure 67) show that the highest values were measured in via Madre Cabrini. It was confirmed also by the data collected by the continuous analyzer that are in very good agreement with the values measured by the passive samplers (Figure 68), despite the different measurement methods.

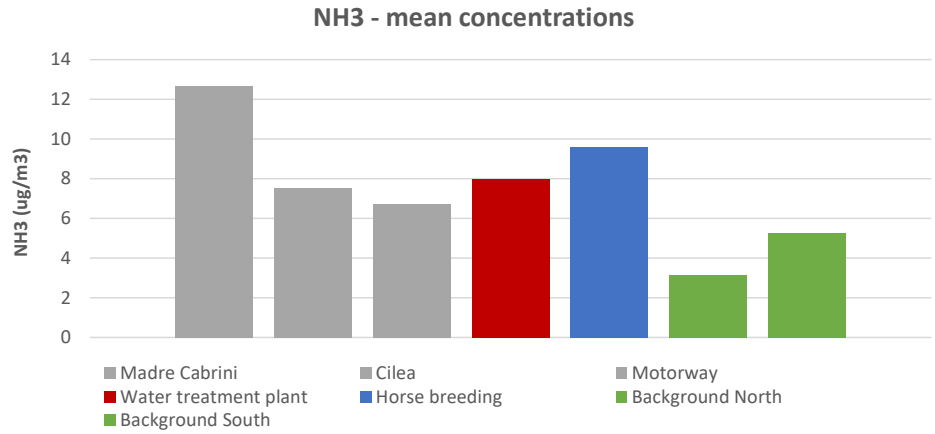

Figure 67. Mean NH_3 measured concentrations.

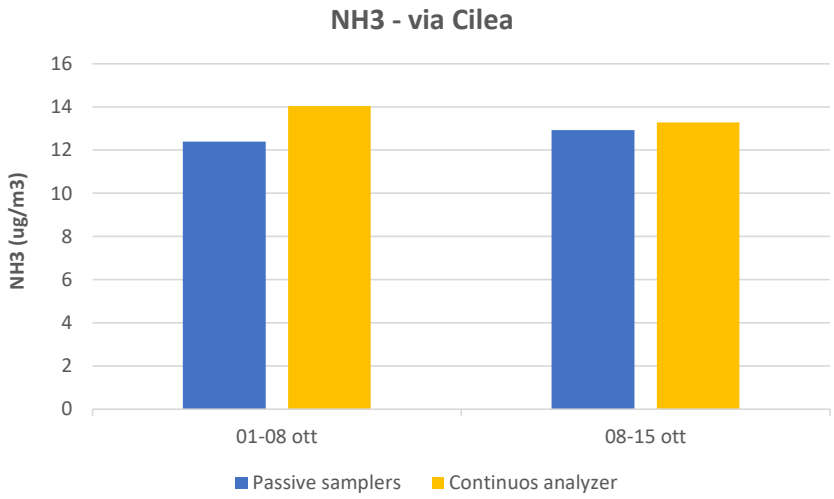

Figure 68. Mean NH3 concentrations measured in via Madre Cabrini.

The relatively higher NH_3 concentrations in via Madre Cabrini could be explained by both the very short distance of the samplers from the emission source (lane) and the geometric characteristics of the monitored roads (Madre Cabrini: buildings at both sides; Cilea: buildings only at one side; motorway: open field).

But the results obtained at the traffic sites compared to the other ones suggest also that the ammonia emissions from road traffic could be higher than usually estimated, according to some recent scientific literature (see for example Farren et al, 2020)[16].

1.7. Road dust Resuspension monitoring

It is well known that the road dust resuspension is an important source of PM in cities and, locally, resuspended particles could heavily affect the measured PM concentration values. In the city of Milan, characterized by low winds, the resuspension is mostly due to the road traffic flows.

For this reason, thanks to the support of the Municipality of Milan and the local street cleaning company (AMSA), a specific activity was carried out in via Madre Cabrini: a dedicated intensive street cleaning was organized during the second part of the measurement campaign Figure 69, left) with the aim to reduce the resuspension contribution to the local PM concentrations and, in this way, to test the performances of some RES and the advanced sensors with a different "primary PM emission" context (indeed, varying the resuspension fraction only).

Moreover, the direct effects of the intensive street cleaning on the resuspended particulate were monitored by means of passive samplers consisting in a set of cylindrical canisters in vertical arrangement (Figure 69, right), installed at the smallest possible distance from the lane and exposed to ambient air for passive collection of deposited PM .[17] The analysis of collected particulate was performed separately before and during the intensive street cleaning (reference periods: September 18 to October 3 and October 4 to October 14 respectively), and at two different sites (Figure 70): via Madre Cabrini (interested by intensive street cleaning) and via Novara (control site, not interested by intensive street cleaning).

[16] Naomi Farren et al., "Underestimated Ammonia Emissions from Road Vehicles," *Environmental Science & Technology* 54 (December 22, 2020): 15689–15697, https://doi.org/10.1021/acs.est.0c05839.

[17] F. Amato et al., "Emission Factors from Road Dust Resuspension in a Mediterranean Freeway," *Atmospheric Environment* 61 (December 1, 2012): 580–87, https://doi.org/10.1016/j.atmosenv.2012.07.065.

The intensive street cleaning consisted of four consecutive passes a day of a sweeping truck, for a total of about 2 litres / day per square meter spilled along the road.

Figure 69. Intensive street cleaning in Madre Cabrini (left) and resuspension passive samplers (right).

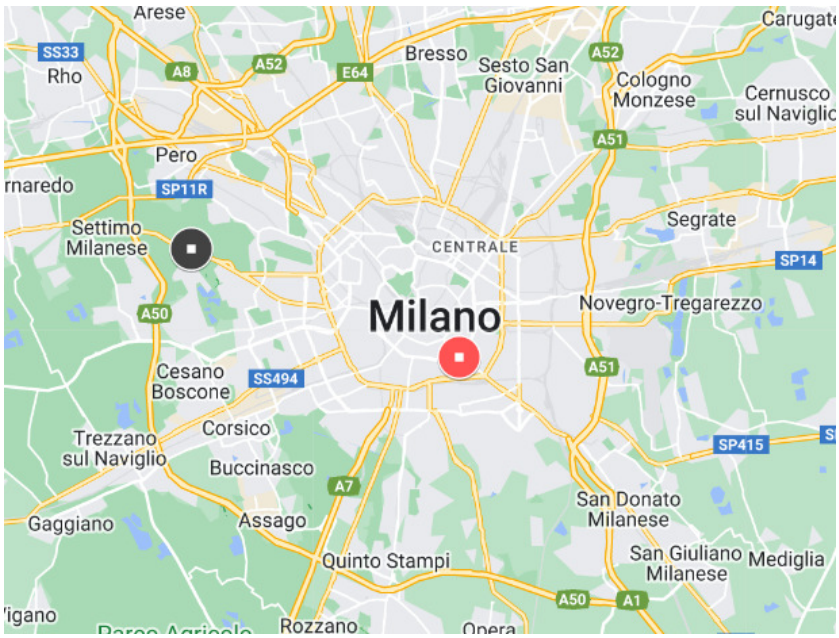

Figure 70. Resuspension measurement sites: via Madre Cabrini (red) and via Novara (black).

The collected data have been analyzed from the point of view of both resuspended particulate matter and measured airborne PM concentrations.

1) Resuspended particulate matter.

Unfortunately, the traffic flows of via Madre Cabrini were too low for the direct quantification of the resuspension Emission Factors. But an accurate laboratory analysis outlined the conclusions reported below.

1a) The particle volume size distributions are shown in Figure 71. Results show, in general, a rather coarse size distribution, typical of mineral dusty materials with mode within 50 mm to 100 mm. As for

the fraction below 10 mm, in the control site (via Novara, black lines in the graph) the percentage amount remains constant over the two measurement periods (4.8% for the first period and 4.7% for the second one). On the contrary, in via Madre Cabrini the particle fraction below 10 mm decreases from 7.3% before the intensive street cleaning (solid red line) to 4.8% during the street cleaning (dashed red line), suggesting that the intensive road washing reduced the PM10 resuspension by about 35%.

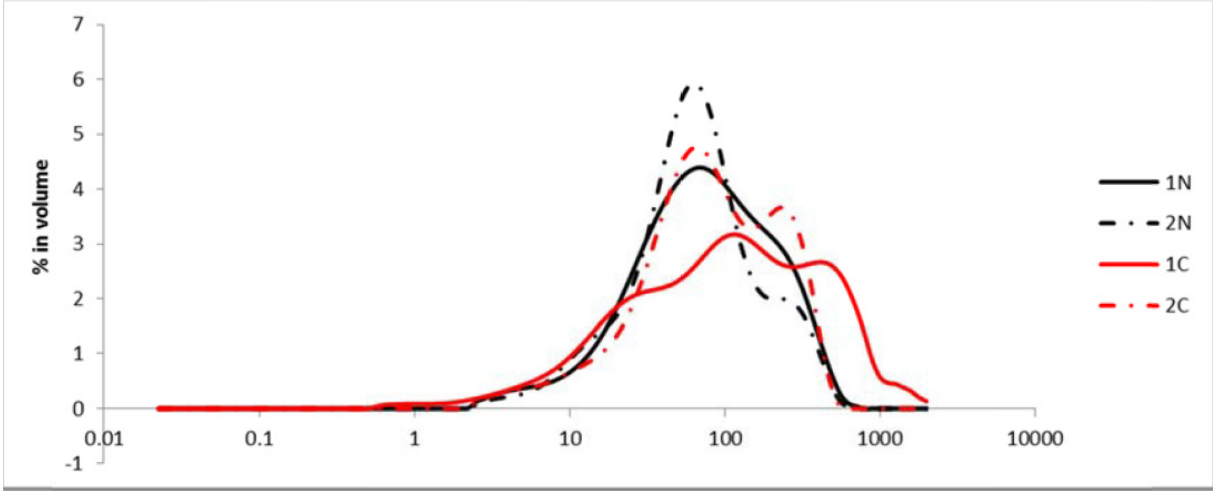

Figure 71. Particle volume size distributions (%) for the measurements in via Madre Cabrini (red) and via Novara (black), during the first period (solid lines) and second period with street cleaning in Madre Cabrini (dashed line).

1b) The resuspended particulate was chemically characterized and analyzed in relation to some specific tracers; in particular, Al, Ca, Ti, and Sr were considered for the road dust resuspension and road wear. The cross analysis of the obtained results at via Madre Cabrini and at the control site suggests a reduction of the road dust / road wear emissions due to the street cleaning ranging from 14% to 40% (mean value: 25%). Considering that the traffic flows did not change significantly in via Madre Cabrini during the two measurement periods, the reduction of the resuspension emission only (without road wear) could be higher. In fact, according to the EMEP/EEA air pollutant emission inventory guidebook 2019, the PM10 road wear emission factor for light vehicles in an urban road could be estimated to around 7 mg/km. Moreover, according to previous resuspension measurements carried out in Milan and the relationship of the resuspension with the traffic speed,[18] the PM10 resuspension emission factor in via Madre Cabrini without intensive street cleaning could be estimated to around 15 mg/km. Thus, the chemical analysis of the resuspended particulate suggests a reduction of the of the road dust emissions only ranging from about 20% to about 60%, with a mean value of 37%, in agreement with the particle distribution size analysis.

2) Air pollutant concentrations.

The temporal behavior of the airborne pollutant concentrations measured in via Madre Cabrini was compared to the values measured by the reference air quality monitoring stations located in the historical center of the city.

2a) The PM10 concentrations measured in via Madre Cabrini and in via Verziere (a reference station located inside the Limited Traffic Area so-called "Area C", as Madre Cabrini, with traffic flows quite similar to those of Madre Cabrini) are shown in Figure 72. Excluding in the analysis the rainy days, the measured data show that the PM10 concentrations at Madre Cabrini and Verziere monitoring stations are quite similar before the intensive street cleaning, whereas during street cleaning the PM10 concentrations in via Madre Cabrini became significantly lower in comparison to those measured in Verziere. In comparison to the values measured at the Verziere station, the PM10 in Madre Cabrini was

[18] Fulvio Amato et al., "Characterization of Road Dust Emissions in Milan: Impact of Vehicle Fleet Speed," *Aerosol and Air Quality Research* 17 (September 1, 2017), https://doi.org/10.4209/aaqr.2017.01.0017.

on average lower by about -7% before the intensive street cleaning and by -31% during the street cleaning, suggesting a reduction of the PM10 concentrations due to the resuspension by about -24%.

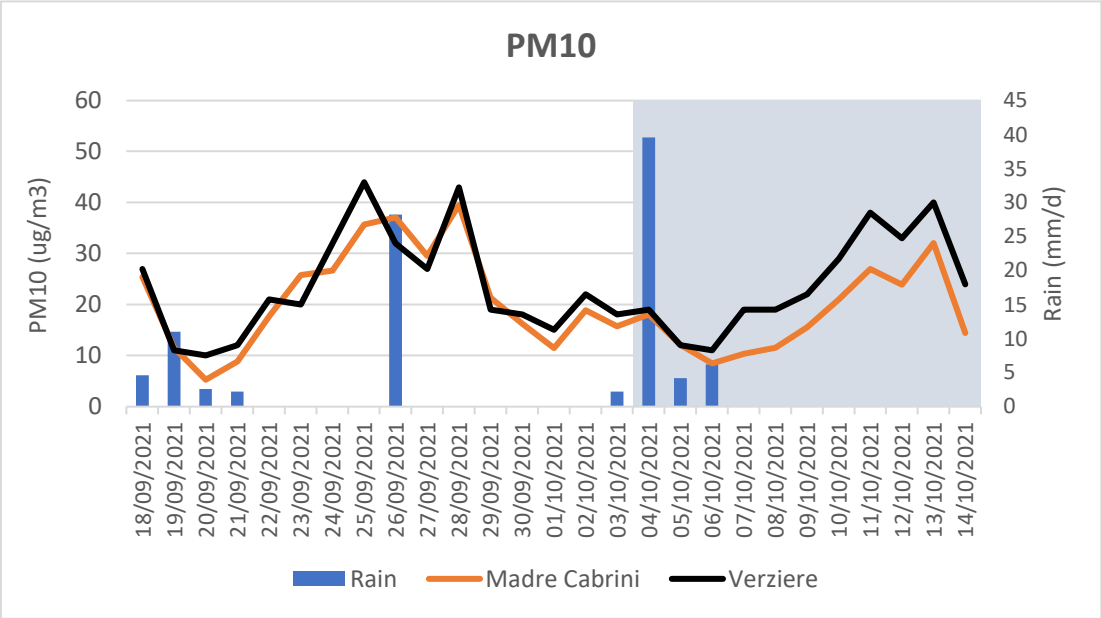

Figure 72. PM10 daily mean concentrations measured in via Madre Cabrini (red) and via Verziere (black). The blue bars show the daily amount of rain. The street cleaning period is highlighted with the light blue background.

2b) The ratios between the concentrations of PM10 and NO_x (the last one not dependent of the street cleaning activities), measured in via Madre Cabrini and in both the reference stations located in "Area C" (i.e. via Verziere, with traffic flows quite similar to those of Madre Cabrini, and via Senato, with very high traffic flows), are shown in Figure 73. The measured data show that the PM10/NO_x ratios are quite well aligned in all considered stations before the intensive street cleaning, whereas after street cleaning the PM10/NO_x ratio in via Madre Cabrini became significantly lower in comparison to those measured in the other stations. It confirms that the PM10 concentrations reduction during the cleaning period is not related to the exhaust emissions nor with the traffic flow intensity. The PM10/NO_x ratio in Madre Cabrini was on average lower than in the other two stations by about -5% before the intensive street cleaning and by -17% during the street cleaning.

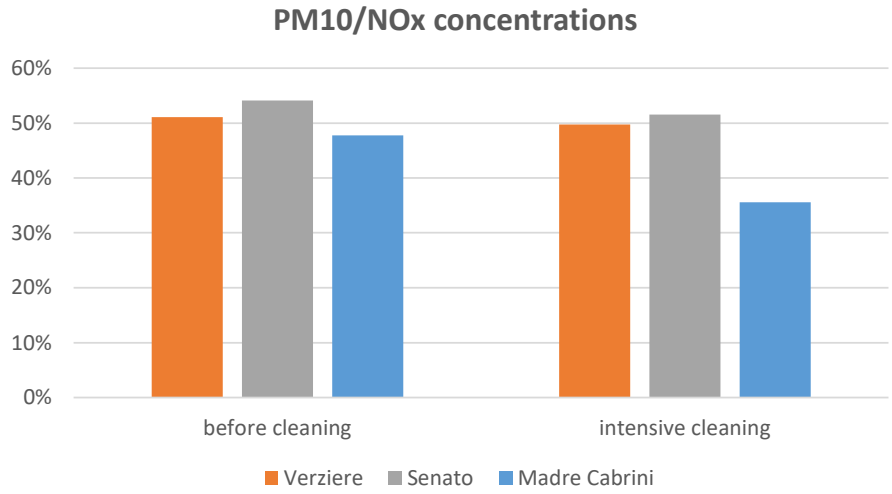

Figure 73. PM10 to NO_x ratio concentrations measured in via Verziere, via Senato and via Madre Cabrini, before and during the intensive street cleaning.

In conclusion, the obtained results have shown that the intensive street cleaning reduced the local PM10 concentrations by about 15% to 25%, with an estimated reduction of PM10 resuspension emissions by about 35% to 40%.

The Institute of Environmental Assessment and Water Research (CSIC – IDAEA) final Report on the quantitative assessment of PM emission factors from road dust resuspension can be found on the CARES website.[19]

[19] https://cares-project.eu/wp-content/uploads/2023/04/Report-CSIC.pdf

2. Krakow campaign

The CARES remote emission sensing campaign in Krakow took place between November and December 2021. The three-week campaign measured various pollutant emissions from more than 100,000 vehicles, while collecting such data as vehicle age and Euro standards to measure the impact specific vehicle groups have on the air quality in the city. Low-cost point sampling instruments were collocated with commercial cross-road remote-sensing systems to evaluate the benefits of combining various remote emission sensing techniques (sites on Figure 74, and colocation on Figure 75). Krakowski Alarm Smogowy and the Krakow Public Transport Authority led the campaign organization, with support from the ICCT and IVL. The testing was carried out by TUG, CTU for point sampling, OPUS RSE with the cross-road technique, and supported by additional instruments from Airyx and TNO.

The measurement objectives were achieved despite covid restrictions and harsh winter weather conditions (Figure 76). Conducting testing in those conditions is not a typical practice and led to key learning such as how the snow, wet roads and dirt may cover plates and might worsen the translucency of the OPUS light-based unit. For the point sampling technique, however, the measurement part is not impacted, but reading the license plates in those conditions remains an issue. Lessons learned from the collocation of instruments in real urban conditions in Milan were successfully applied in Krakow. To match conditions compatible with both point sampling and commercial instruments, it is critical to find locations that match certain testing and traffic criteria (e.g., one lane preferred, no congestion, not more than 400 vehicles per hour). For the first time, point sampling was operated on batteries during the day and sourced electricity from streetlamps during the night. The plates were collected from both remote-sensing techniques and sent to the central registration agency of Poland (CEPiK).

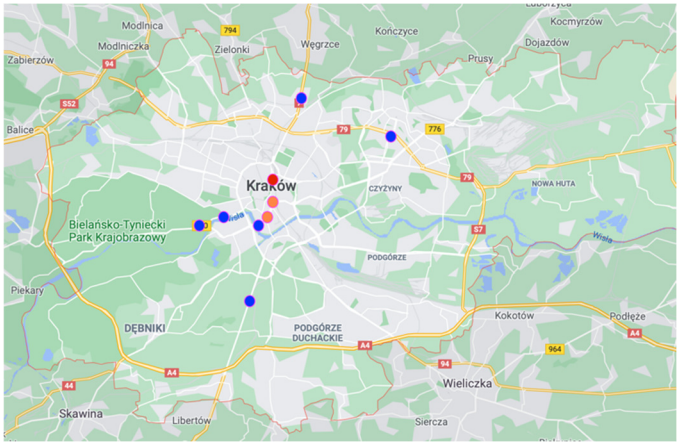

Figure 74. Sampling locations in Krakow. Blue dots indicate cross-road sites, orange point sampling, and red collocation of point sampling and cross-road units.

Figure 75. Collocation of the cross-road remote sensing and point sampling.

Figure 76. Harsh winter conditions encountered during the first testing days.

2.1. Analysis of the OPUS remote-sensing measurements

2.1.1. Composition of the measured fleet

The OPUS remote sensing device in Krakow collected in 128,833 measurements overall where 60,179 were unique vehicle measurements. These measurements were first classified based on vehicle classes as shown in the Figure 77. The measurements were largely predominated by passenger cars (90%) followed by around 7% of light commercial vehicle. Buses made up around 2% and trucks around 1% of the measurements.

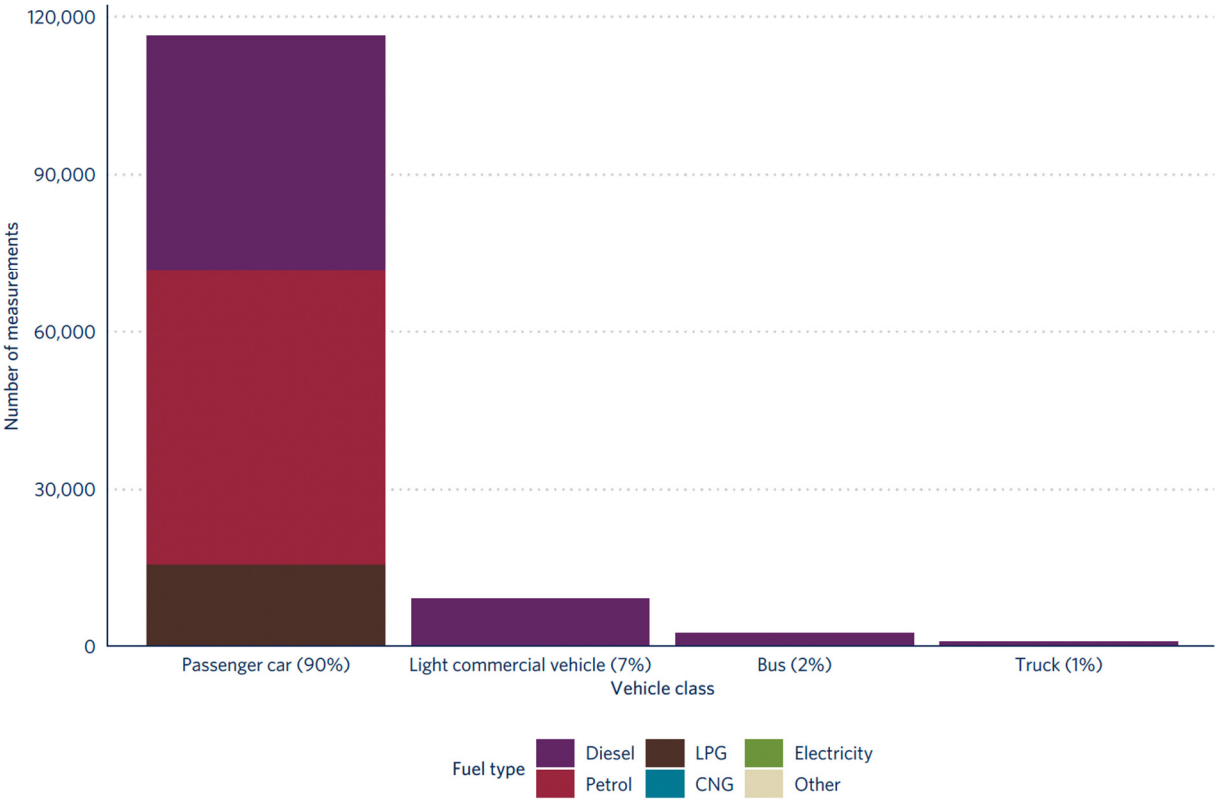

Figure 77. Distribution of vehicle classes and fuel types for all vehicles measured by the OPUS instrument during the Krakow campaign.

The passenger cars were predominantly powered by diesel and petrol fuel type in Krakow. Similarly, there was a significant share of passenger cars which ran on LPG as they were mostly petrol passenger cars which had been retrofitted to run on LPG. This was the first time in Poland that these vehicles are distinguished in the fleet for real-world emission analysis. The light commercial vehicles and heavy-duty vehicles, both buses and trucks ran on diesel fuel.

Looking more detail, 116,361 measurements captured for passenger cars consisted of 54,965 unique passenger car measurements as some vehicles were measured more than once. These passenger cars were mostly powered by petrol comprising 48%, followed by diesel (39%) and LPG (13%) as shown in the Figure 78. Overall, Euro 4 and Euro 6 passenger cars occupy significant shares of the vehicle fleet in Krakow whereas the latest standard Euro 6d and Euro 2 occupy the lowest shares. We see a similar trend as in Milan of decreased popularity of diesel-powered passenger cars with the latest Euro standard cars heavily running on petrol. Diesel vehicles represented 46% of the Euro 5 and 37% of Euro 6 vehicles but this share falls to 26% with Euro 6d-TEMP and 19% with Euro 6d vehicles.

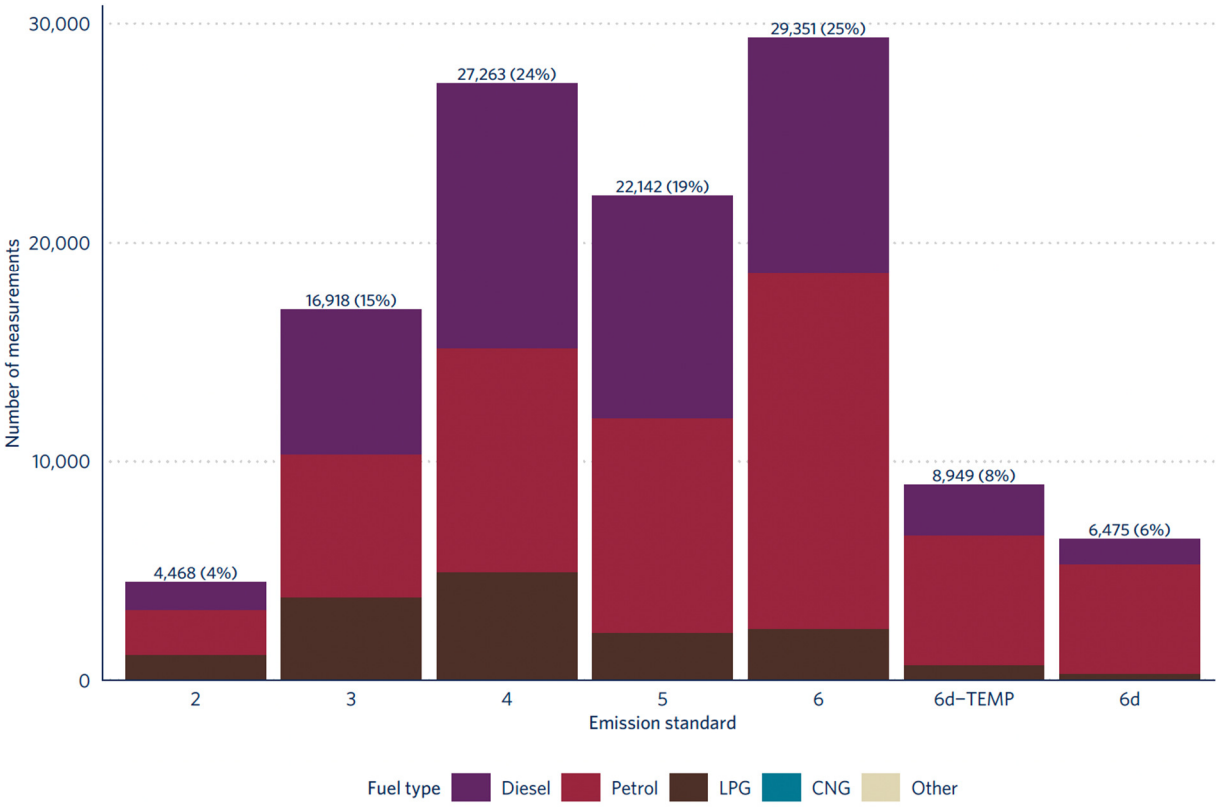

Figure 78. Composition of measured passenger cars in Krakow by fuel type and emission standard.

LPG retrofitted vehicles are highly popular among older passenger cars as they occupy for Euro 2: 26%, Euro 3: 22% and Euro 4: 18%. Their popularity is mainly due to significantly lower fuel price of LPG and price savings in the longer run for retrofitted LPG cars are higher than the cost of retrofitting these vehicles. Significant retrofitted LPG measurements enabled us to compare their emission factors with those of conventional fuel types similar to what was done for Milan.

2.1.2. Vehicle Dynamic Characteristics

As driving conditions parameters have an impact on the emission performance, this section explores them in detail, and are summarized in Table 5. The measurement campaign was conducted in winter season during November and December, and the average ambient temperature measured was 6.1℃ whereas the ambient temperature ranged from -2℃ to 15℃. This harsh winter ambient temperature is later discussed to explain the difference in emission levels among different temperature range.

Table 5. Mean ambient temperature, vehicle specific power (VSP), speed, and acceleration of all vehicle measurements in Krakow.

	Ambient temperature (℃)	VSP (kW/t)	Speed (km/h)	Acceleration (km/h/s)
Average	6.1	9.3	39.8	1.3
Standard deviation	3.7	8.0	12.7	2.4

The distribution of VSP, speed and acceleration for Krakow is shown in Figure 79. Speed and acceleration are used to calculate vehicle specific power in combination with the road slope information. The mean VSP of all measured vehicles in Krakow was 9.4 kW/t.

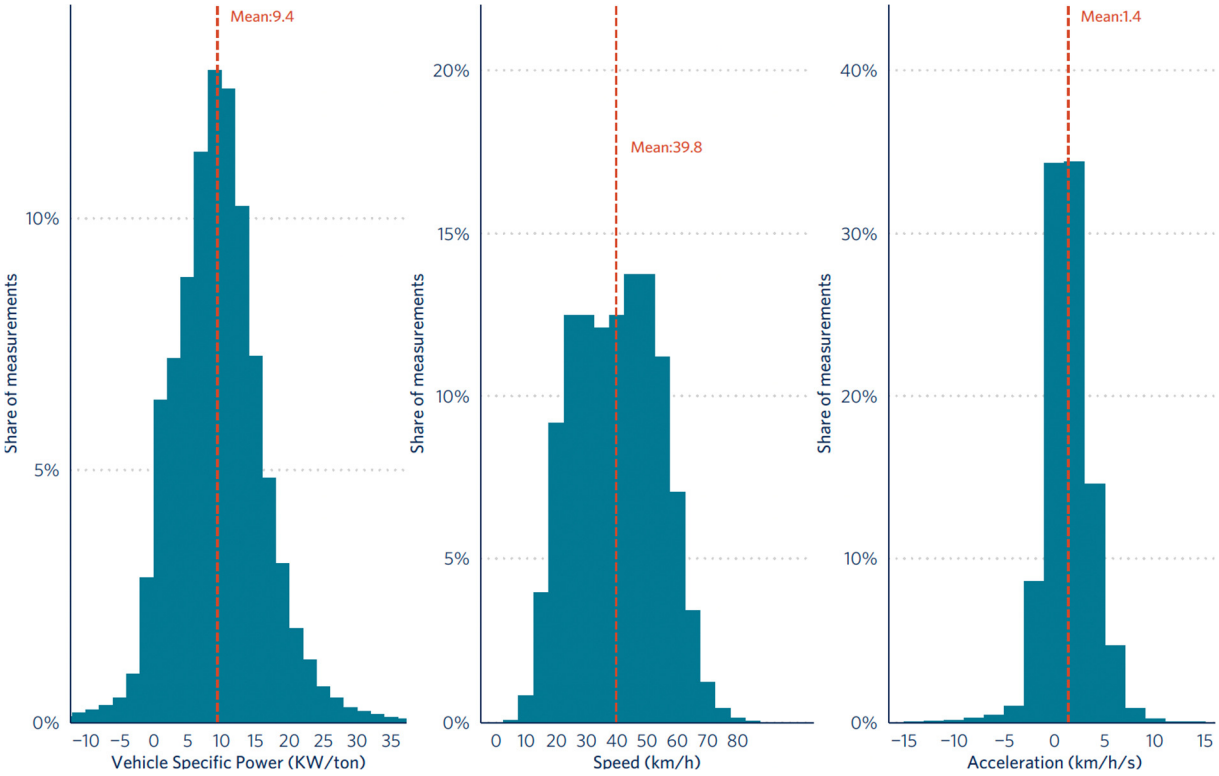

Figure 79. Distributions of vehicle specific power, speed, and acceleration of all measured vehicles in Krakow.

2.1.3. Emissions

This section analyses the pollutant emissions from passenger cars measured in Krakow, as they comprised significant share of measurements. Emissions of all pollutants detectable by the OPUS systems, namely NO_X, PM, CO, and HC were investigated for three fuel types of diesel, petrol and LPG.

Figure 80. Fuel-specific emissions from diesel, petrol and LPG passenger cars measured in Krakow. Only results from 100 or more measurements are presented.

The OPUS measurements for pollutant emissions analysis were filtered out for valid CO_2 status to ensure that only when there are valid CO_2 readings, pollutant emission values will be analysed. The results from the OPUS data as shown in Figure 80 highlighted the clear impact of ambient temperature on PM and HC with abnormally high values of these pollutants below 5℃. As mentioned earlier, the remote sensing campaign was carried out under harsh winter conditions and these values nearly doubled for petrol and LPG cars below 5℃ compared to its counterparts. PM is measured as a fuel-specific opacity using ultraviolet (UV) light, and with these measurements carried out in near zero ambient temperature, there was likelihood of interference between the PM channel with freezing water in the tail pipe exhaust. Plus, there was also likelihood of interference from freezing water with HC, so as per OPUS suggestions and in form of precaution, measurements with ambient temperatures below 5℃ for both PM and HC were filtered out for analysis. Hence, the sample size of PM measurements decreased by around 43% from 95950 to 55119, whereas the sample size of HC decreased by around 39% from 80889 to 49622.

The impact of ambient temperature on HC and PM emissions were further validated by the statistical t-test. Some unresolved questions exist why diesel cars from Euro 5 and onwards which are equipped with Diesel Particulate Filters (DPF) show high PM emissions. It was expected that DPF equipped diesel cars should show no impact on PM under low ambient temperature as DPF's filtration efficiency is independent of the engine and ambient temperature. There is clear room of further research of working of OPUS instrument under near zero ambient temperature conditions. On the other hand, NO_x and CO emission increases slightly looking at ambient temperatures higher than 5℃ compared to lower temperatures. NO_x is known to vary with extreme ambient temperature and humidity.

In Figure 81 where certain readings are filtered out, LPG vehicles show NO_x emissions significantly higher compared to their petrol equivalents. LPG vehicles also show high CO emission levels across Euro standards compared to other fuel types whereas HC emissions are also relatively high compared to the diesel counterparts. In recently announced LEZ in Krakow, LPG is included in the restrictions alongside petrol and the potential benefits of the LEZ restricting old LPG powered vehicles is clearly noticeable due to their significant high pollutant emissions. The latest emission standard vehicles from Euro 6 onwards show lower NO_x, CO and HC emissions compared to previous Euro standards.

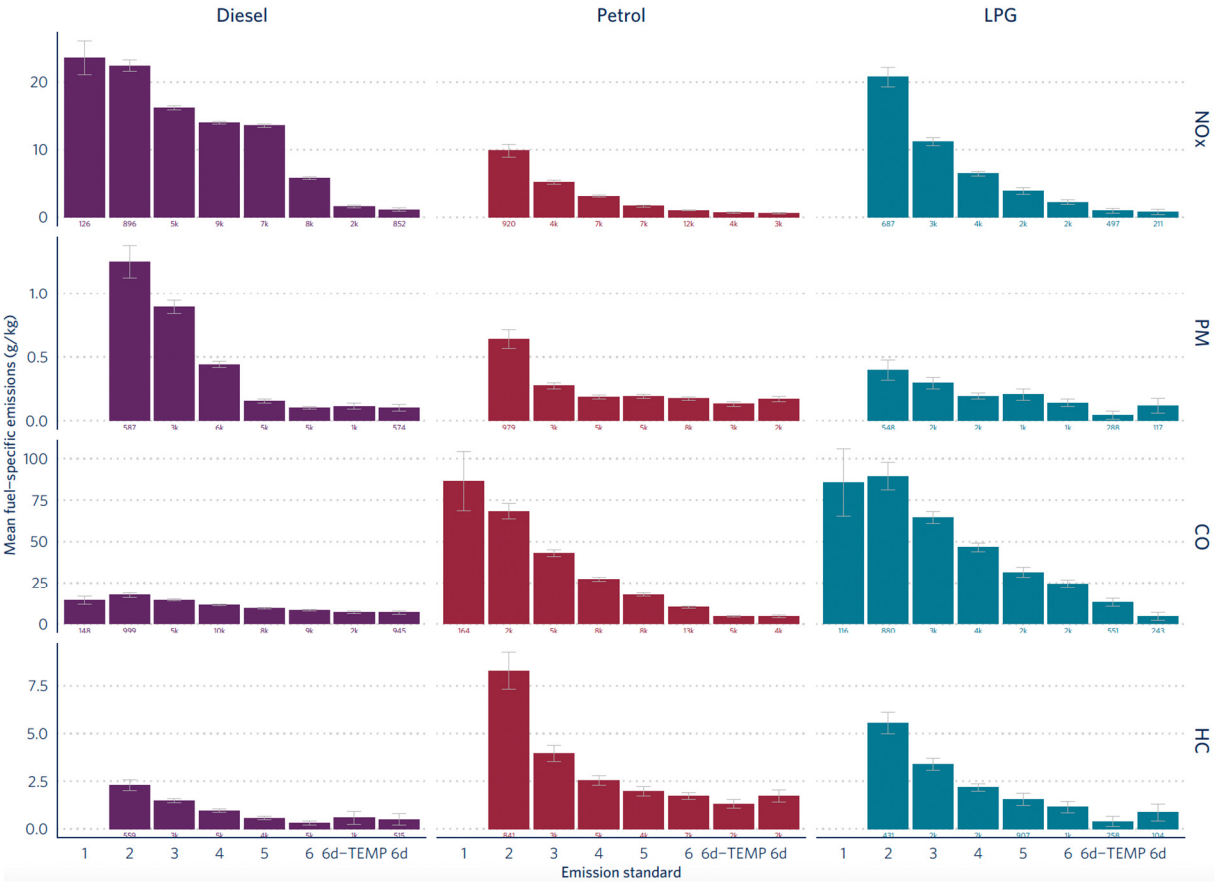

Figure 81. Fuel-specific emissions from diesel, petrol, and LPG passenger cars after filtering out for ambient temperature below 5 ℃ for PM and HC. Only results from 100 or more measurements are presented.

In Figure 82, despite applying the above-mentioned filters, PM emissions for both fuel types in Krakow 2021 are significantly higher than data from the 2019 remote sensing campaign. This discrepancy is likely due to fact that the Krakow 2021 campaign was conducted during winter months (November-December) where average ambient temperature was around 6.1 ℃, and cold starts in engines occurred more frequently, whereas the Krakow 2019 campaign was conducted in summer (June-July).

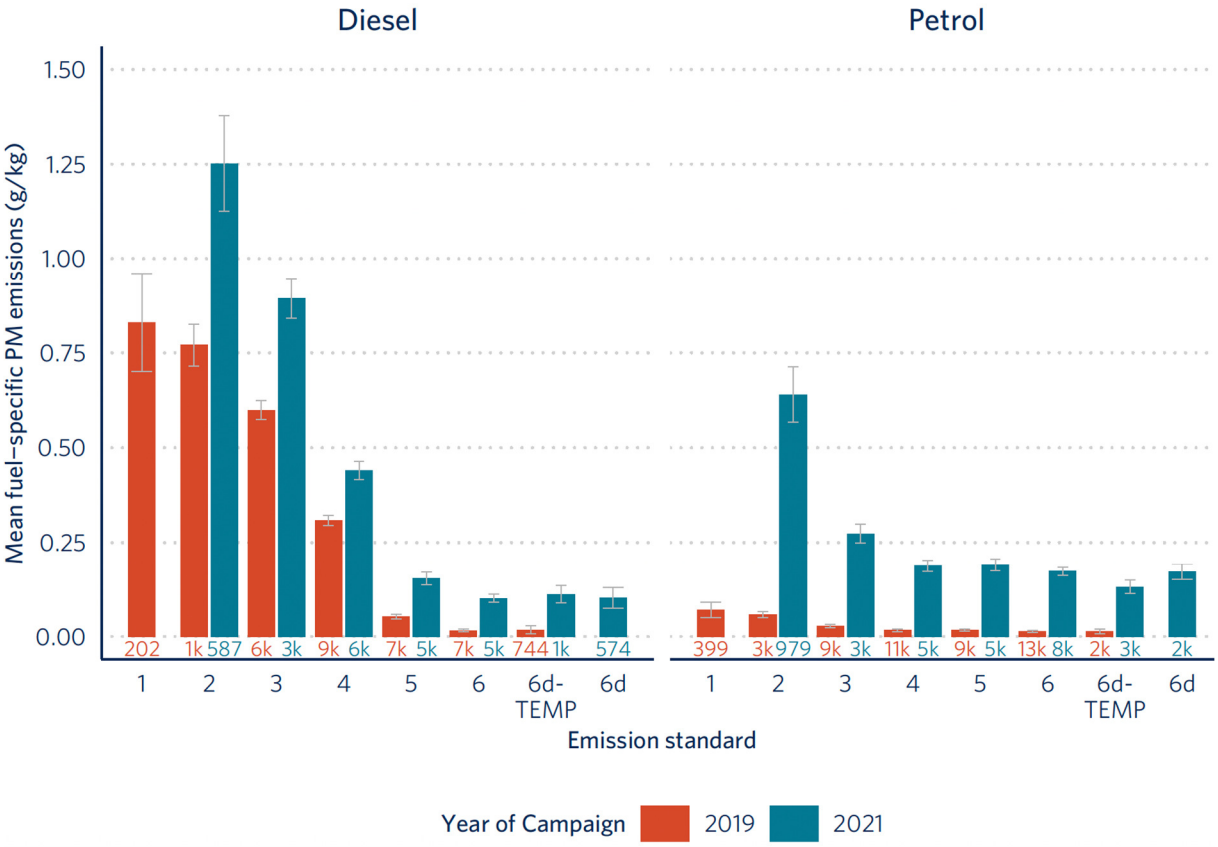

Figure 82. Comparison of fuel-specific PM emissions between Krakow 2019 and 2021 campaign. Only results from 100 or more measurements are presented. PM emissions for year 2021 is filtered out for ambient temperature below 5 ℃.

The fuel-specific NO_x emissions from OPUS data were converted to distance-specific NO_x emission using the same methodology as for Milan which allowed comparing NO_x performance across fuel type. This comparison showed that older retrofitted LPG cars emitted NO_x as high as old diesel cars (Figure 83). These excessively high NO_x emissions for diesel cars persist till Euro 6 standards in alignment with Milan's campaign results. With the introduction of Euro 6d-TEMP, NO_x emissions reduce significantly by 75% compared to its preceding standard, Euro 6, and lie within the regulatory limit as well as on the on-road limit. Over time with newer emission standards, petrol cars show a steady decrease in NO_x emission in line with the Milan result and perform better compared to their LPG and diesel counterparts.

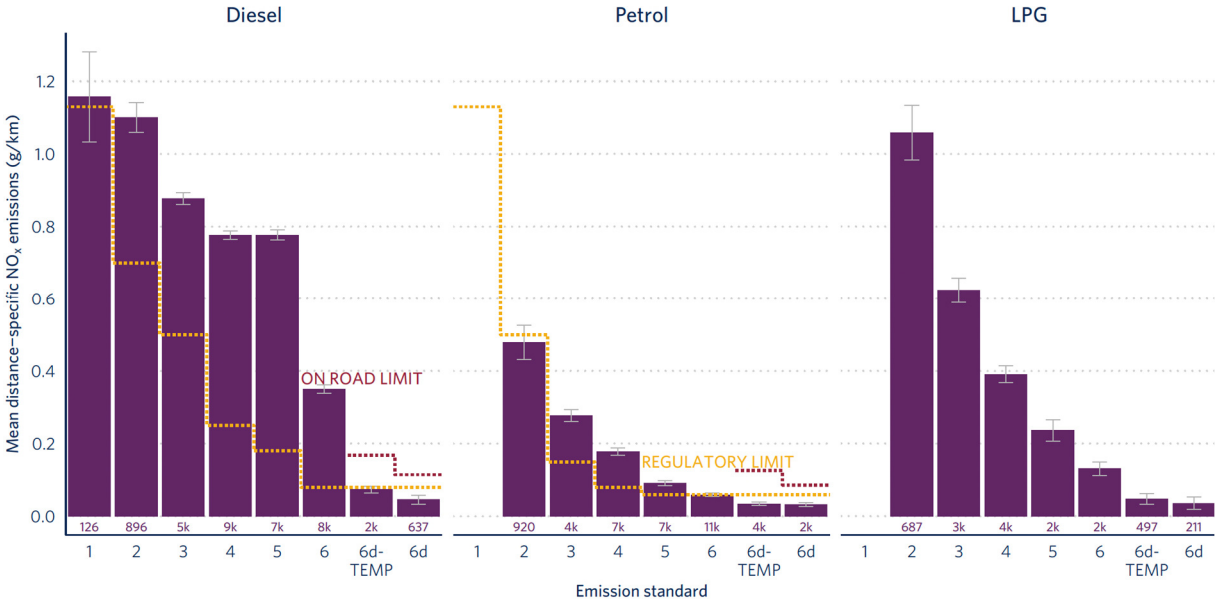

Figure 83. Distance-specific NO_x emissions from passenger cars for fuel types of diesel, petrol, and LPG. Only results from 100 or more measurements are presented.

When compared with the OPUS remote sensing campaign data collected in June 2019, NO_x emissions for petrol vehicles are quite comparable in both campaigns as shown in Figure 84. NO_x emissions in the 2021 campaign are higher compared to 2019 for older diesel vehicles (older than Euro 5 standards). The difference in NO_x emissions between these two campaigns seems to be lower from diesel Euro 6 vehicles onwards.

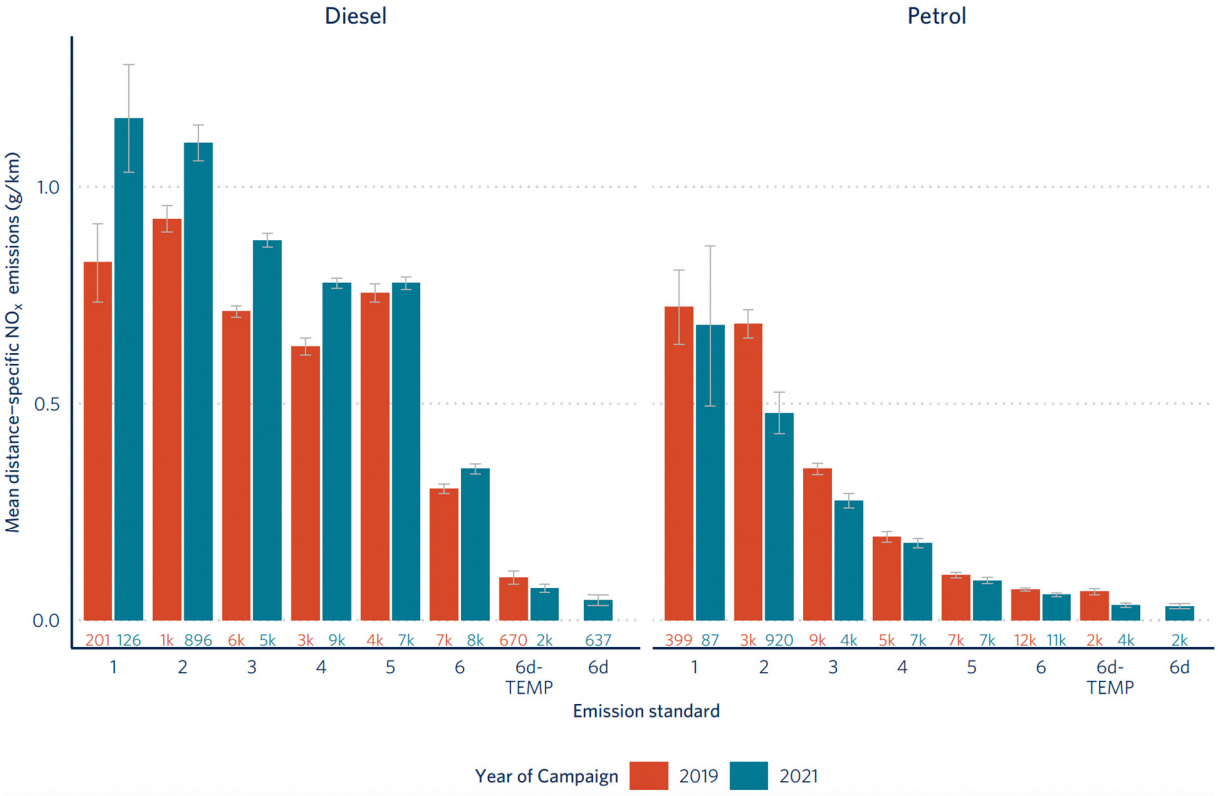

Figure 84. Comparison of distance-specific NO_x emissions between 2019 and 2021 Remote Sensing Campaign. Only results from 100 or more measurements are presented.

As shown in Figure 85, the data collected on PM emissions in Krakow in align with our previous findings from Milan, show significant emissions for diesel pre-Euro 5 vehicles that are not equipped with DPF. Although PM emission from pre-Euro 5 diesel seem in line with the emission standard limit, these vehicles emit way more than their petrol or LPG equivalent. Mean PM emissions for DPF equipped Euro 5 diesel cars is higher than emission limits and this is likely related to some malfunctions in these vehicles.

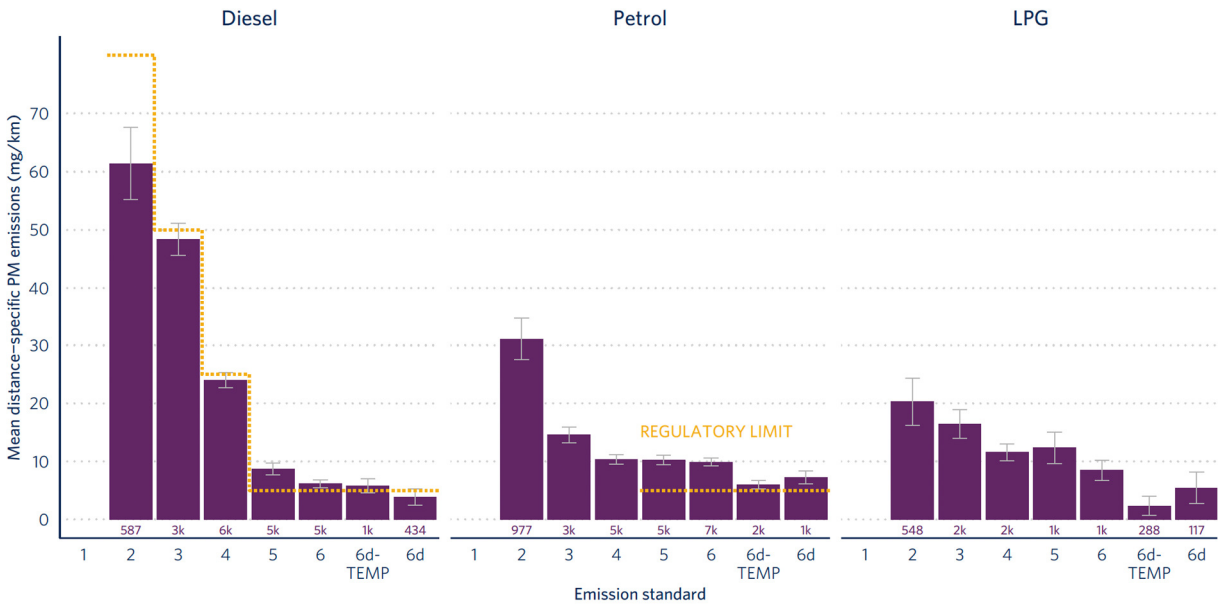

Figure 85. Distance-specific PM emissions from passenger cars for fuel types of diesel, petrol, and LPG. Only results from 100 or more measurements are presented.

With the introduction of newer emission standards for diesel cars, PM emissions undergo significant reductions from Euro 6 onwards which is in line with the regulatory threshold limit. On the contrary, PM readings for the latest Euro standard petrol cars are higher than the threshold limit but this might be due to low ambient temperature. In cold temperatures, gasoline cars may produce more carbonaceous particulate matter than modern filter-equipped diesel cars.[20] The results from point sampling from section 2.2 point towards the same tendency of PM emissions from petrol vehicles in winter conditions.

Evaluation of emission shares of Krakow passenger cars

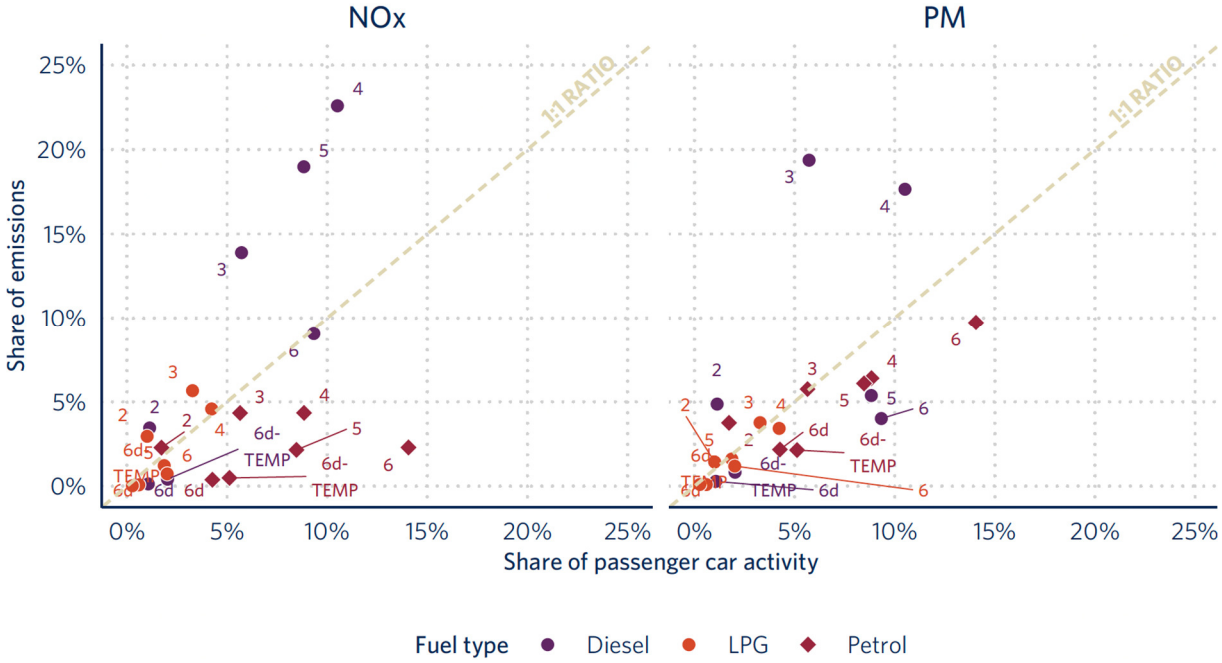

Figure 86. Passenger car activity shares and its estimated share of NO_x and PM emissions in Krakow by fuel type and emission standards. Only groups with 100 or more measurements are presented.

[20] S. M. Platt et al., "Gasoline Cars Produce More Carbonaceous Particulate Matter than Modern Filter-Equipped Diesel Cars," *Scientific Reports* 7, no. 1 (July 13, 2017): 4926, https://doi.org/10.1038/s41598-017-03714-9.

The emissions produced by passenger cars differ depending on their fuel type and emission standard. Since each of these cars has a different representation in Krakow's vehicle fleet, they contribute to emissions at varying rates. In this section, we utilize the proportion of measured passenger cars as an approximation of passenger car activity, and we calculate the share of emissions by applying distance-specific emission estimates for each passenger car's fuel type and emission standard. The data presented in Figure 86 can be useful in shaping policies for the upcoming low-emission zone in Krakow. It indicates that older diesel cars have a significant impact on NO_x and PM emissions. Even though Euro 4 and below diesel cars constitute only 17% of passenger car activity in Krakow, they contribute to 40% of the total passenger car NO_x emissions and 45% of the total passenger car PM emissions. Therefore, aligning with the current Krakow LEZ plans can result in significant reductions in passenger car NO_x and PM emissions. However, further improvements can be made by banning Euro 5 diesel cars, which are currently not included in the announced LEZ in Krakow. Euro 5 diesel cars account for approximately 8% of passenger car activity but contribute to 19% of NO_x emissions, highlighting the potential benefits of phasing them out.

Light Commercial Vehicles (LCVs)

As part of the Krakow CARES Campaign, we obtained 9143 valid measurements for Light Commercial Vehicles (LCVs) primarily powered by diesel fuel. To conduct a thorough analysis of their pollutant emissions, we grouped the LCVs into three categories based on their curb weight, all of which fell under the N1 type approval category, indicating a mass of less than 3.5 tonnes. These categories were Class I (curb weight less than or equal to 1305 kg), Class II (curb weight greater than 1305 kg and less than or equal to 1760 kg), and Class III (curb weight greater than 1760 kg). Using the same ICCT methodology as before, we calculated the distance-specific NO_x emissions based on the fuel-specific values collected during the campaign. Overall, we found that higher class LCVs had higher NO_x emissions as shown in Figure 87.

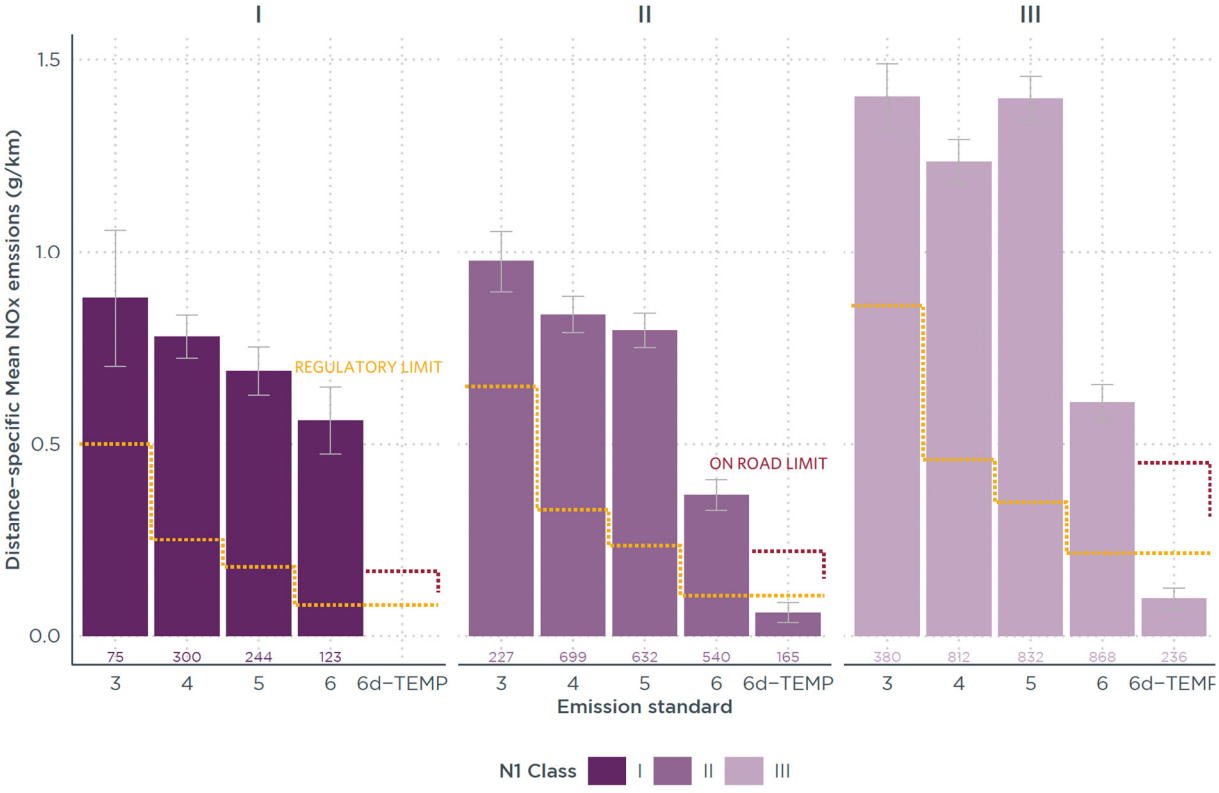

Figure 87. Distance-specific NO_x emissions from Light Commercial Vehicles (LCVs) for all classes of N1 diesel fuel type. Only results from 50 or more measurements are presented.

We observed that older diesel LCVs emitted NO_x at levels more than two times higher than the regulatory limit, but this improved after the introduction of Euro 6d-TEMP, which enabled NO_x emissions to meet not only the on-road limit but also the regulatory limit. These findings highlight the emission benefits of Euro 6d-TEMP LCVs across all LCV classes compared to pre-Euro 6d-TEMP LCVs.

Heavy Duty Vehicles (HDVs)

OPUS gathered 859 valid measurements for trucks and 2,453 valid measurements for buses in Krakow. To compare the remote sensing emission measurements with the established regulatory limits across Euro standards for buses and trucks, the fuel-specific metrics were converted to energy-specific metrics using the previously adopted ICCT methodology.[21] The average real-world NO_x emission for all trucks and buses was found to be higher than 1.5 g/kWh, except for Euro VI-D trucks, as depicted in Figure 88. The average NO_x emissions for Euro VI buses exceeded the allowed threshold by almost two times, while for trucks, it was higher by around 4 times. The variation in observed emissions concerning laboratory regulatory limits could be attributed to different driving conditions in the real world, such as the start-stop drive cycle and cold start, faulty emission control system, malfunctions, and tampering.

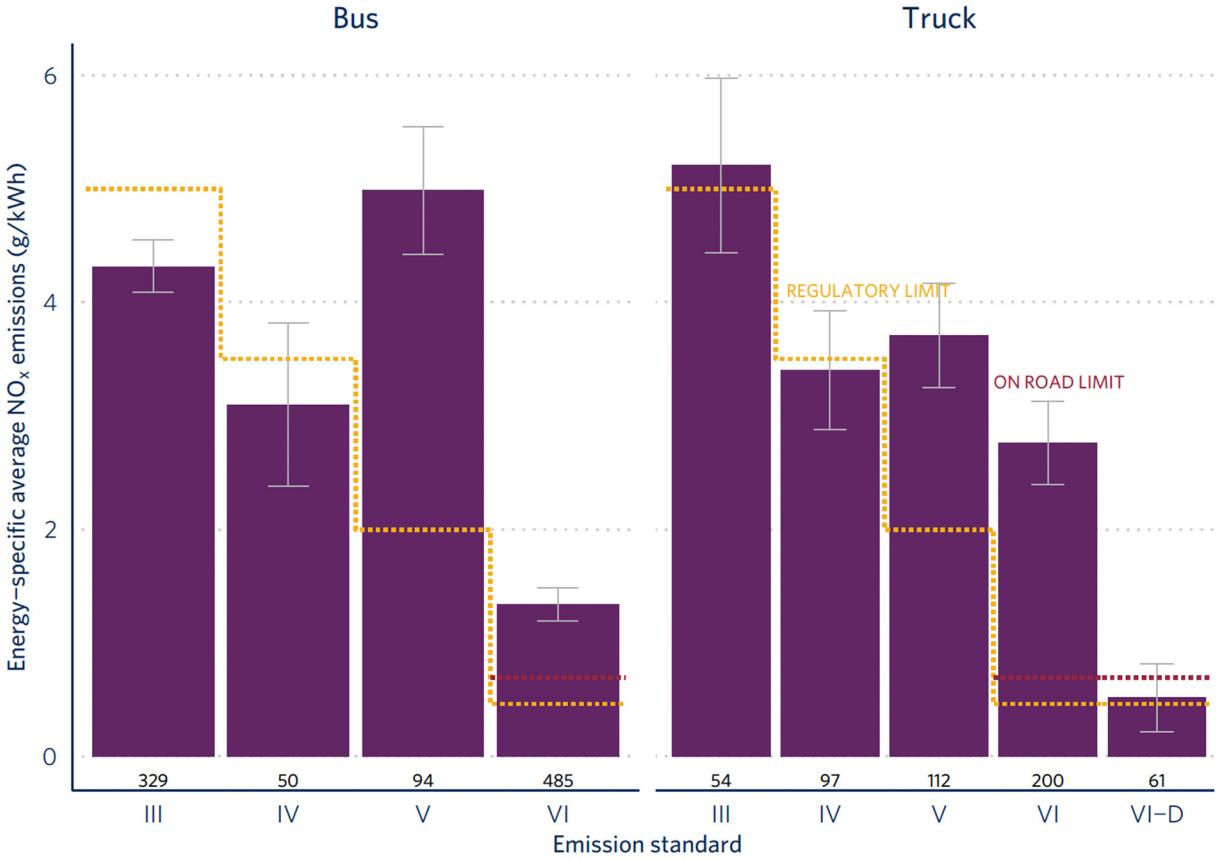

Figure 88. Energy-specific NO_x emissions for Bus and Truck. Only results from 30 or more measurements are presented.

2.2. Point Sampling

For the Krakow campaign, the same PS setup as described in section 1.3.1 was deployed. PN (SPN) measurements were conducted with a catalytic stripper for volatile particle removal during the whole campaign.

Captured Vehicle Fleet:

The captured vehicle fleet was similarly distributed compared to the Milan city campaign measurements. In case of measured vehicle types (Figure 90), passenger cars were predominantly measured (84 %) followed by light commercial vehicles (9.2 %). A significant amount of city buses (6 %) was captured, due to the bus stop next to the measurement location. Due to the winter term measurements, virtually no two or three wheelers were captured. Reviewing the fuel type of the captured vehicles (Figure 89),

[21] Sina Kazemi Bakhshmand et al., "Remote Sensing of Heavy-Duty Vehicle Emissions in Europe" (Washington, D.C.: International Council on Clean Transportation, August 29, 2022), https://theicct.org/publication/remote-sensing-of-heavy-duty-vehicle-emissions-in-europe/.

almost exclusively diesel and petrol vehicles were measured. The following emission results focus on passenger cars (vehicle category: M1).

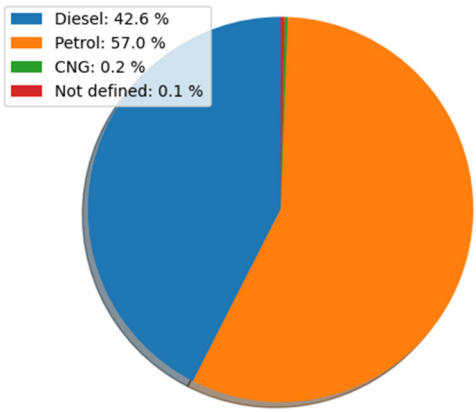

Figure 89. Krakow - Captured vehicles according to fuel type.

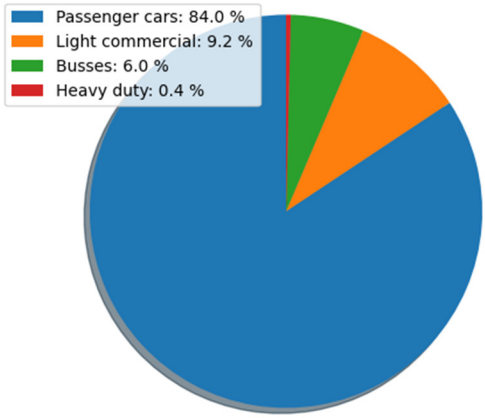

Figure 90. Krakow - Captured vehicles according to vehicle type.

Emission measurement results:

The BC emissions in the Krakow campaign are in the same range as the Milan values (Figure 91). The diesel cars show the same monotonic decrease from Euro 3 up to Euro 6. Emissions from Euro 3, 4 passenger cars are lower compared to the Milan campaign, in contrast to Euro 6 cars, which show higher BC emissions. The petrol cars (Figure 92), on the other hand, have a steady trend as in the Milan campaign but the mean values and the variance are significantly higher. This could come from a greater temperature dependence at low temperatures of petrol vehicles, which was previously reported by Platt et al. (2017). PN measurements are well related to the BC results. The diesel results from Euro 3 to Euro 6 decrease steadily and the absolute values are comparable to the Milan results. PN results of the petrol passenger cars show a similar picture as the BC results. Higher emissions were measured compared to the Milan campaign, which could be related to a larger impact at low temperatures. In case of NO_x measurements for diesel passenger cars, a similar reduction from Euro 5 to Euro 6 compared to Milan can be stated (Figure 95). Overall, NO_x emission factors for diesel cars are lower compared to the Milan campaign. Similarly, NO_x emissions of Euro 6d-TEMP (and median values of Euro 6 in contrast to Milan) were below the Euro limit. In contrast to that, NO_x emission factors of petrol passenger were higher.

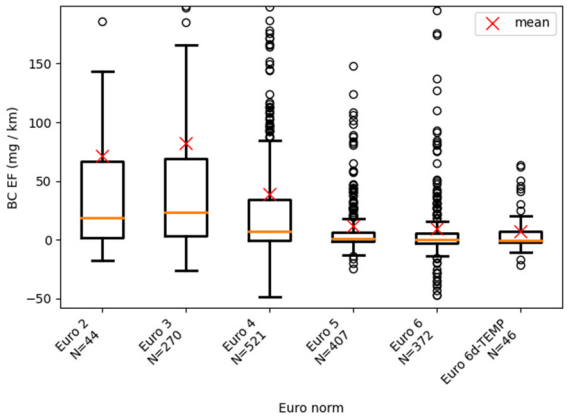

Figure 91. Krakow - BC emissions of diesel passenger cars for different Euro norms.

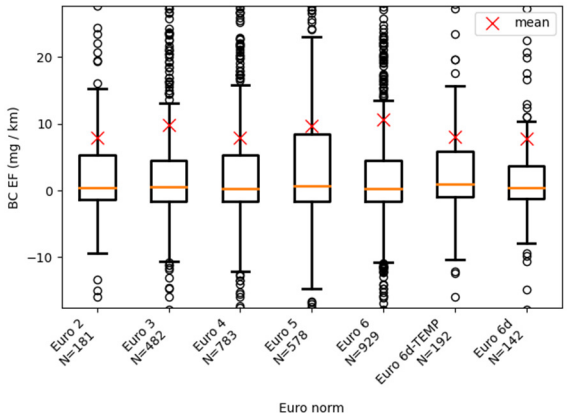

Figure 92. Krakow - BC emission of petrol passenger cars for different Euro norms.

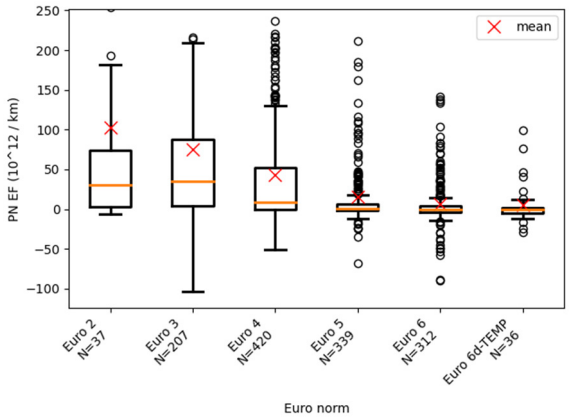

Figure 93. Krakow - SPN emissions of diesel passenger cars for different Euro norms

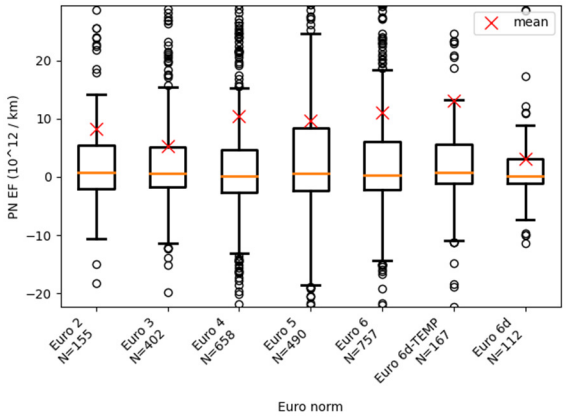

Figure 94. Krakow - SPN emissions of petrol passenger cars for different Euro norms

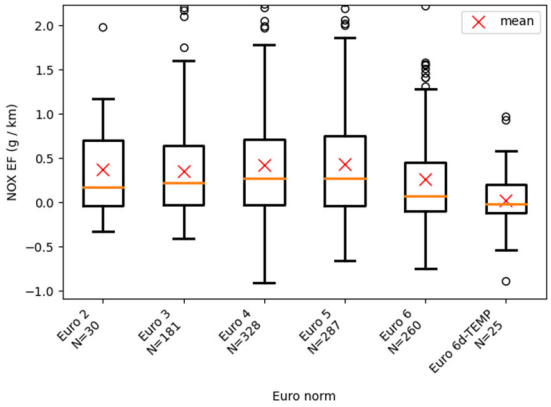

Figure 95. Krakow - NO_x emissions of diesel passenger cars for different Euro norms

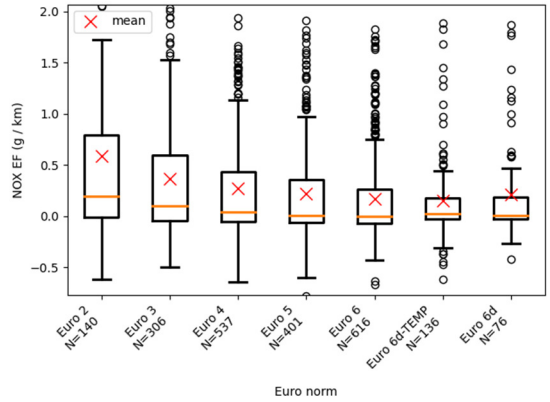

Figure 96. Krakow - NO_x emissions of petrol passenger cars for different Euro norms

3. Prague campaign

Initially planned as the first campaign, the CARES testing in Czech Republic was the last and took place between September 5th and September 22nd, 2022. The focus of the campaign was the identification of high emitters. Cross-road instruments from OPUS was used associated with point sampling from TUG and plume chasing from Airyx set up in a car and in TNO's van developed as part of WP1. The initial target to collect 100,000 measurements was achieved. In addition to Prague, the testing was carried out in the city of Brno. The sections below present the results for the cross-road OPUS, point sampling and plume chasing techniques.

3.1. Analysis of the OPUS remote sensing instruments

3.1.1. Composition of the measured fleet

The data was collected in two cities, Prague and Brno, using the OPUS remote sensing device, which collected a total of 120,611 valid measurements, out of which 71,825 were unique vehicle measurements. Prague contributed to approximately 102,500 valid measurements, while Brno contributed to around 18,100 valid measurements. These measurements were initially categorized based on vehicle classes, as shown in Figure 97. Passenger cars accounted for most measurements at 73%, followed by approximately 11% of light commercial vehicle measurements. Trucks accounted for around 1% of the measurements, while bus measurements were negligible. About 14% of the measurements had a missing vehicle class.

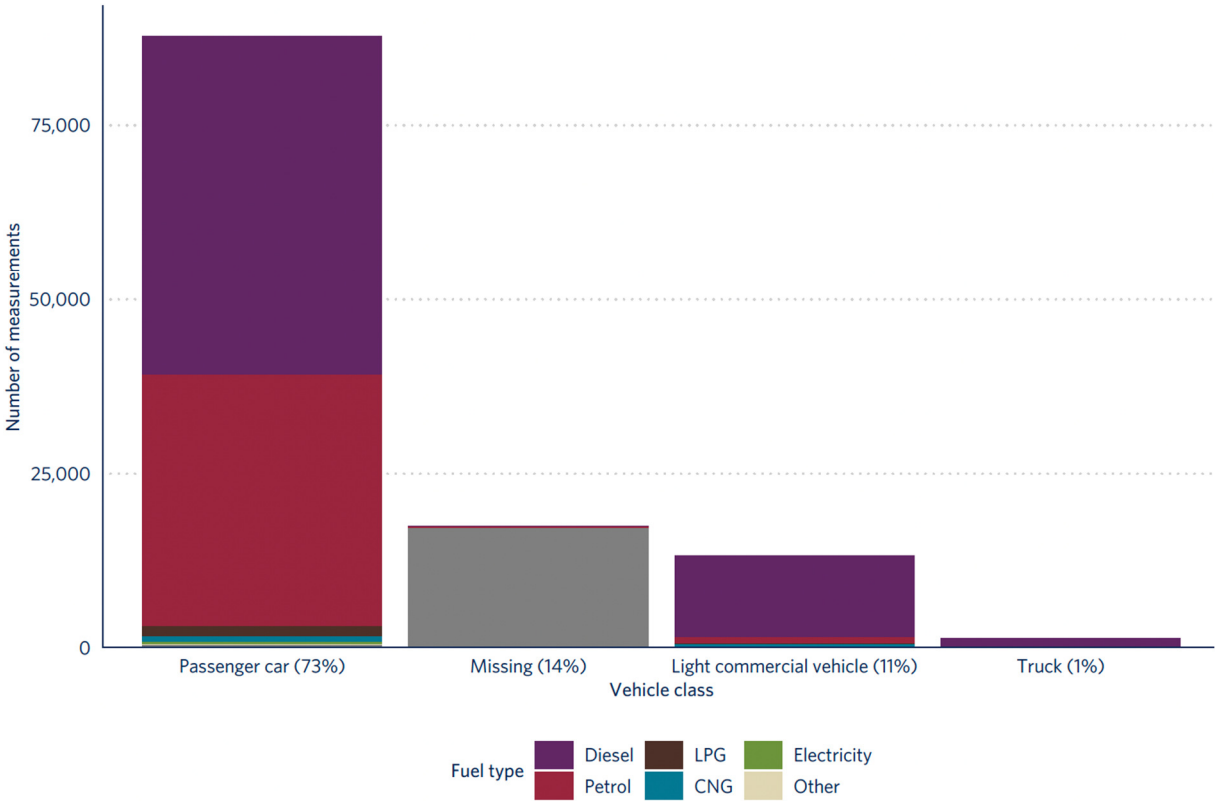

Figure 97. Distribution of vehicle classes and fuel types for all vehicles measured by the OPUS instrument during the Prague and Brno campaign.

In Prague and Brno, the high share of passenger cars that were measured by the OPUS device were powered by diesel, accounting for approximately 55% of the collected measurements. The proportion of passenger cars powered by LPG and CNG was low, with only 822 CNG passenger cars and 1,464 LPG passenger cars identified. The number of electric passenger cars was only 393. LPG and CNG fuel types combined represented less than 3% of the overall fuel share. As for light commercial vehicles and heavy-duty vehicles, including buses and trucks, they all ran on diesel fuel. There were more measurements with missing vehicle classes in Brno (32%) compared to Prague (11%) as shown in the Figure 98.

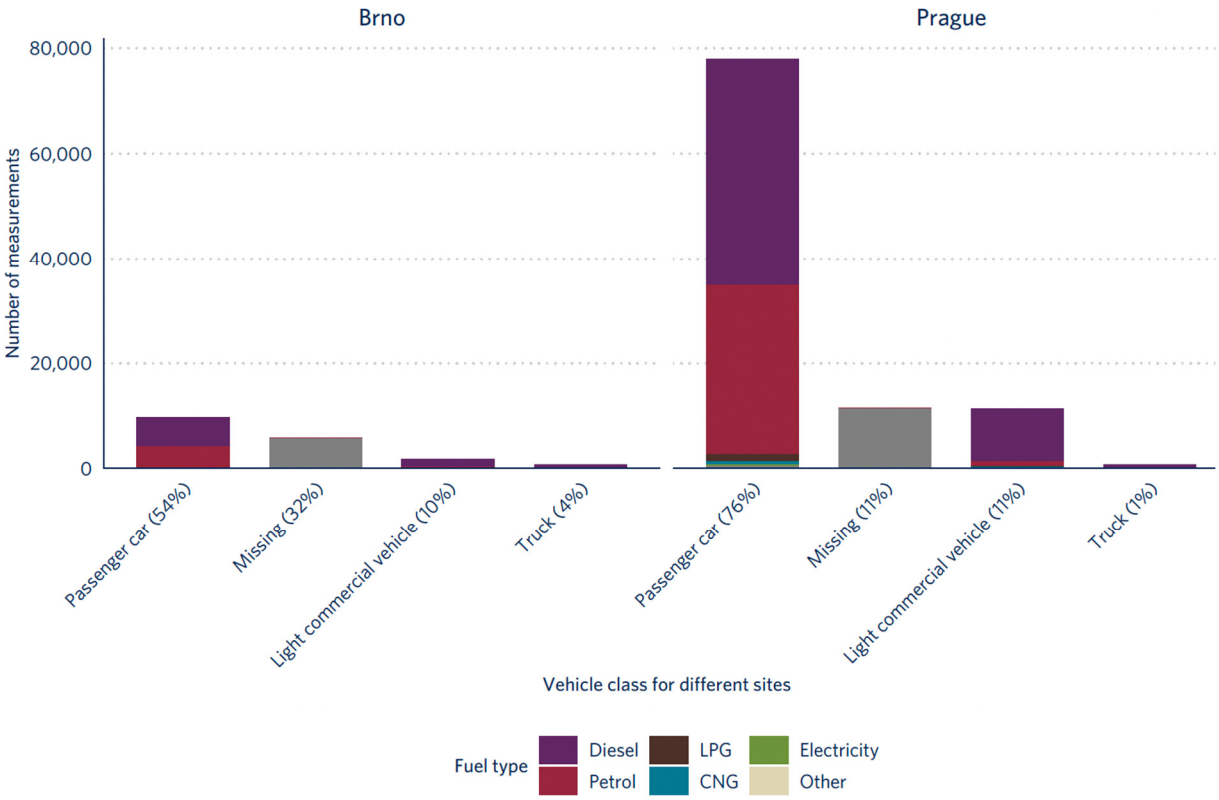

Figure 98. Distribution of vehicle classes and fuel types for all vehicles measured by the OPUS instrument by site in Czech Republic

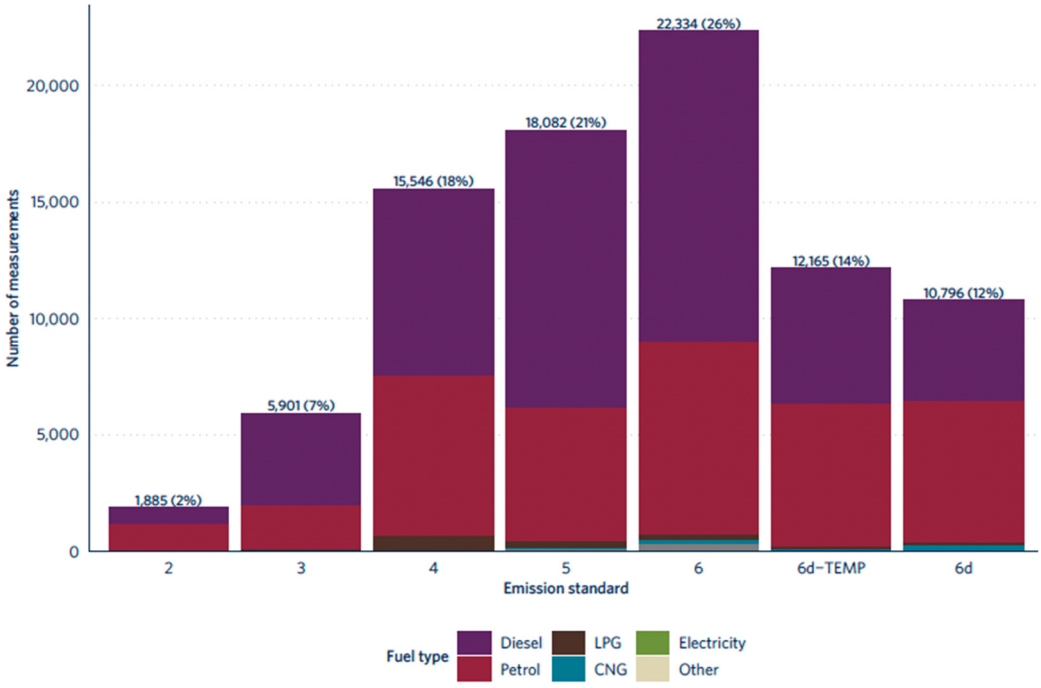

Figure 99. Composition of measured passenger cars in Prague and Brno by fuel type and emission standard.

Figure 99 illustrates that recent passenger cars follow a similar trend to Milan and Krakow during the CARES campaign. These passenger cars are primarily fueled by petrol, with petrol accounting for 50% of the share in Euro 6d-TEMP and 56% in Euro 6d models. On the other hand, older passenger cars that comply with previous emission standards are mainly powered by diesel, with diesel fuel occupying 67% share in Euro 3, 52% share in Euro 4, 67% share in Euro 5 and 60% share in Euro 6. For Euro 2 standard vehicles, petrol-powered cars make up the majority at 57%, while diesel cars constitute only 40%.

3.1.2. Vehicle dynamic characteristics

This section delves into the impact that driving conditions have on emission performance and presents a summary of these parameters for Prague and Brno in Table 6. During the Prague 2022 campaign, new temperature probes used by the OPUS RSE malfunctioned, resulting in temperature readings of 0℃. To address this issue, weather data from the National Oceanic and Atmospheric Administration (NOAA) were utilized for the entire duration of the Prague campaign via the Worldmet[22] R package. Since the measurement campaign took place in September 2022 during the autumn season, the average ambient temperature recorded was 9.4℃ in Brno and 15.1℃ in Prague. The values were derived from NOAA weather stations situated near the airport in Prague and Brno. Upon comparison with previously collected ambient temperature readings from OPUS and HEAT in Milan and Krakow respectively, differences were observed. Those may be due to the variation in land cover and elevation between the airport and the city. The weather station in the airport is located in an open area and records relatively lower temperatures in contrast to the city, which is exposed to a denser urban settlement. Moreover, there is a possibility of differences in instrumentation. To address this, a linear regression was used to calculate the offset for the Krakow campaign conducted by OPUS, which was then used to adjust the ambient temperature for Prague and Brno. The offset value calculated was 4.7 ℃ and the new adjusted values are 14℃ in Brno and 19.8℃ in Prague, as shown in Figure 100. Prague in average had warmer ambient temperature compared to Brno.

Table 6. Mean corrected ambient temperature, vehicle specific power (VSP), speed, and acceleration of all vehicle measurements in Prague and Brno.

		Ambient temp (℃)	VSP (kW/t)	Speed (km/h)	Acceleration (km/h/s)
All measurements (Brno + Prague)	Average	19.0	10.4	30.0	2.2
	Standard deviation	4.2	6.8	6.7	2.2
Brno	Average	14.0	4.1	20.9	1.1
	Standard deviation	3.5	5.7	7.1	2.6
Prague	Average	19.8	11.4	31.5	2.3
	Standard deviation	3.7	6.4	5.4	2.1

[22] David Carslaw, "Worldmet: Import Surface Meteorological Data from NOAA Integrated Surface Database (ISD)," February 6, 2023, https://CRAN.R-project.org/package=worldmet.

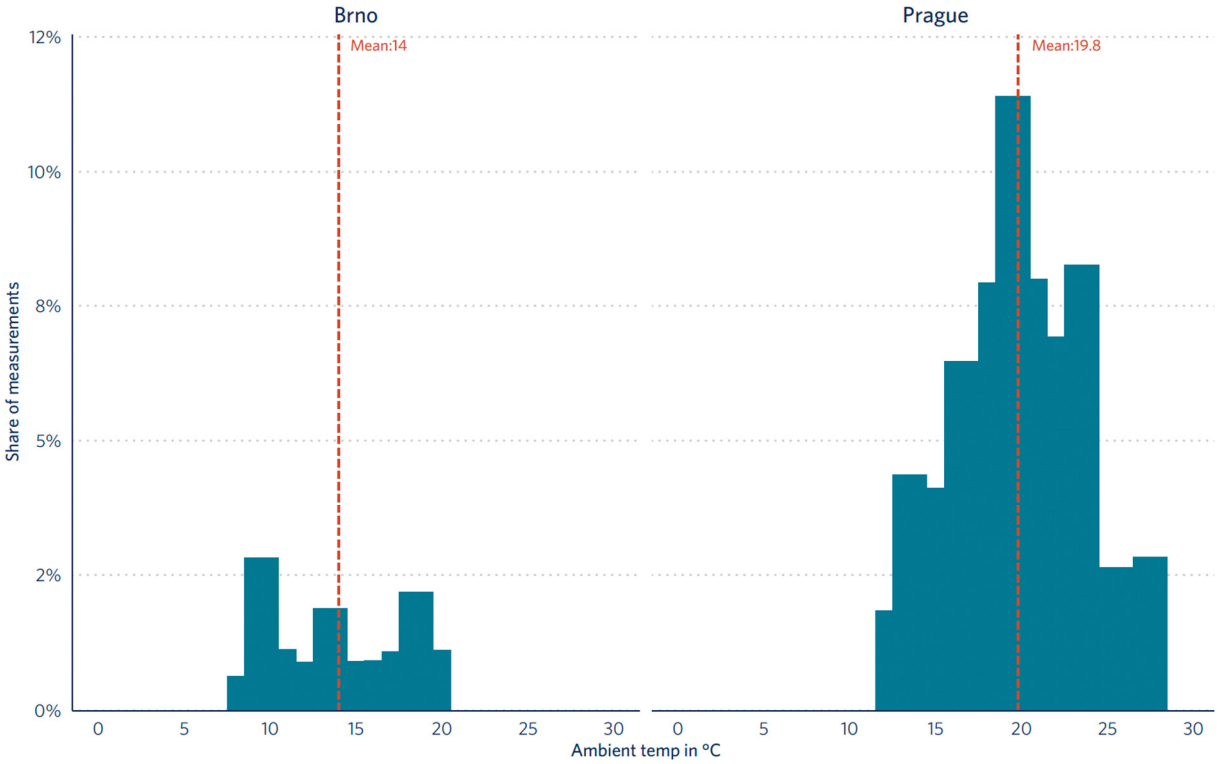

Figure 100. Distributions of ambient temperature of all measured vehicles by site.

Figure 101 illustrates the distribution of VSP, speed, and acceleration in Prague and Brno. Vehicle specific power is calculated by utilizing speed, acceleration, and road slope information. The average VSP of all vehicles surveyed in Prague and Brno was 10.8 kW/t, while the average speed and acceleration were 30.6 km/h and 2.2 km/h/s, respectively.

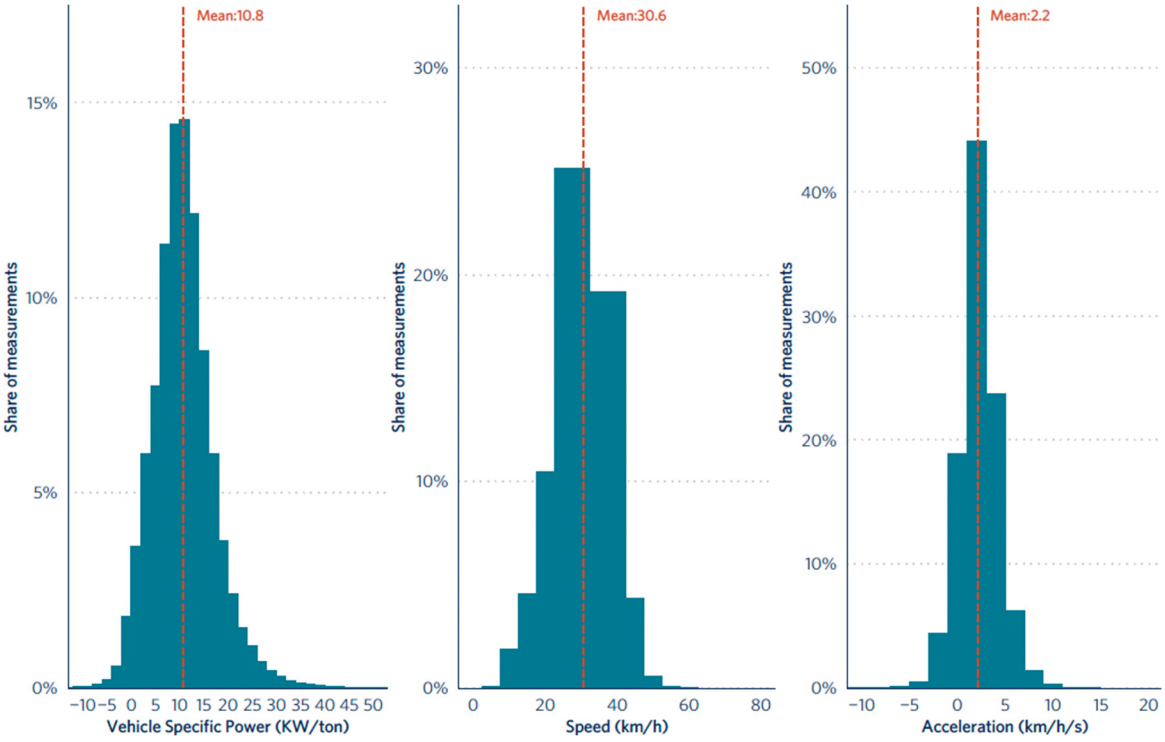

Figure 101. Distributions of vehicle specific power, speed, and acceleration of all measured vehicles in Prague and Brno.

3.1.3. Emissions

This segment examines the pollutant emissions from passenger cars in Prague and Brno, which constituted a significant portion of the measurements. The OPUS systems detected emissions of all detectable pollutants, including NO_x, PM, CO, and HC, for diesel and petrol fuel types. LPG and CNG are not a significant fuel type in our measurements. The average fuel-specific emissions of pollutants were studied, and Figure 102 reveals that older diesel cars, Euro 5 and earlier, emit considerably more NO_x and PM pollutants than their petrol counterparts. We observed a significant decrease in PM emissions from Euro 5 when diesel cars were fitted with DPF. Compared to diesel vehicles, petrol passenger cars emit higher average CO and HC emissions.

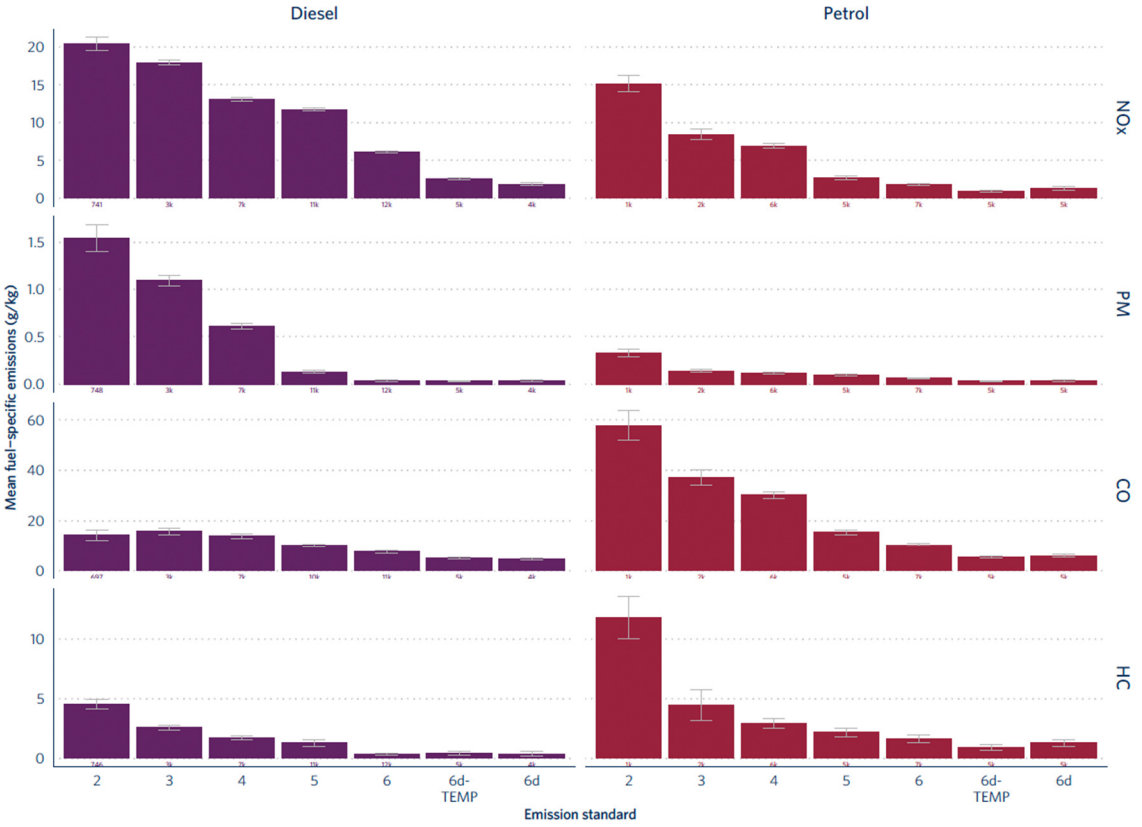

Figure 102. Fuel-specific emissions from diesel and petrol passenger cars in Prague and Brno. Only results from 100 or more measurements are presented.

Upon analysing the distance-specific average NO_x emissions observed during the Prague and Brno campaign, it was found that the average NO_x emissions were higher in older diesel cars, as demonstrated in Figure 103 is consistent with the findings in Milan and Krakow. Although newer emission standards for diesel cars have led to a decrease in average NO_x emissions, the emissions are still over two times higher than the threshold limit until Euro 6. The Euro 6d-TEMP diesel fails to meet the regulatory limit for NO_x emissions but satisfies the on-road limit. The average NO_x emissions from newer petrol passenger cars significantly decrease from Euro 6 onwards.

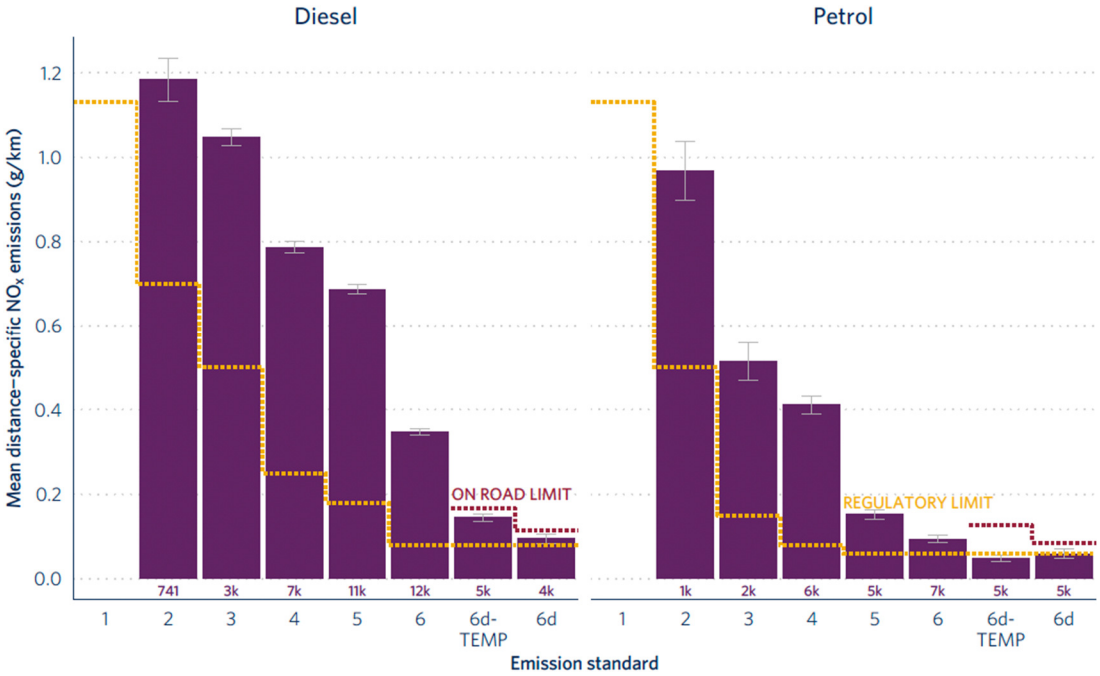

Figure 103. Distance-specific NO_x emissions from passenger cars for fuel types of diesel and petrol. Only results from 100 or more measurements are presented.

However, the average NO_x emissions of Euro 5 and older petrol cars are remarkably high compared to levels seen in Milan and Krakow, which is a cause for concern. To further investigate, the top 10% of high emitters of NO_x for older petrol vehicles of Euro 5 and below were compared with the remaining NO_x emitters. Fuel-specific values for pollutants were used as the metric for the comparison. The aim was to determine if NO_x high emitters for petrol also exhibited high emissions of HC and CO. With modern gasoline vehicles equipped with a three-way catalytic converter as part of the exhaust system, NO_x emissions should not be as high since the converter controls three pollutants: CO, HC, and NO_x. However, the Figure 104 shows that higher average NO_x emissions correspond with higher average CO and HC values, which could indicate three-way catalyst malfunctions rather than deliberate lean operation or unintentional one due to faulty oxygen sensors.

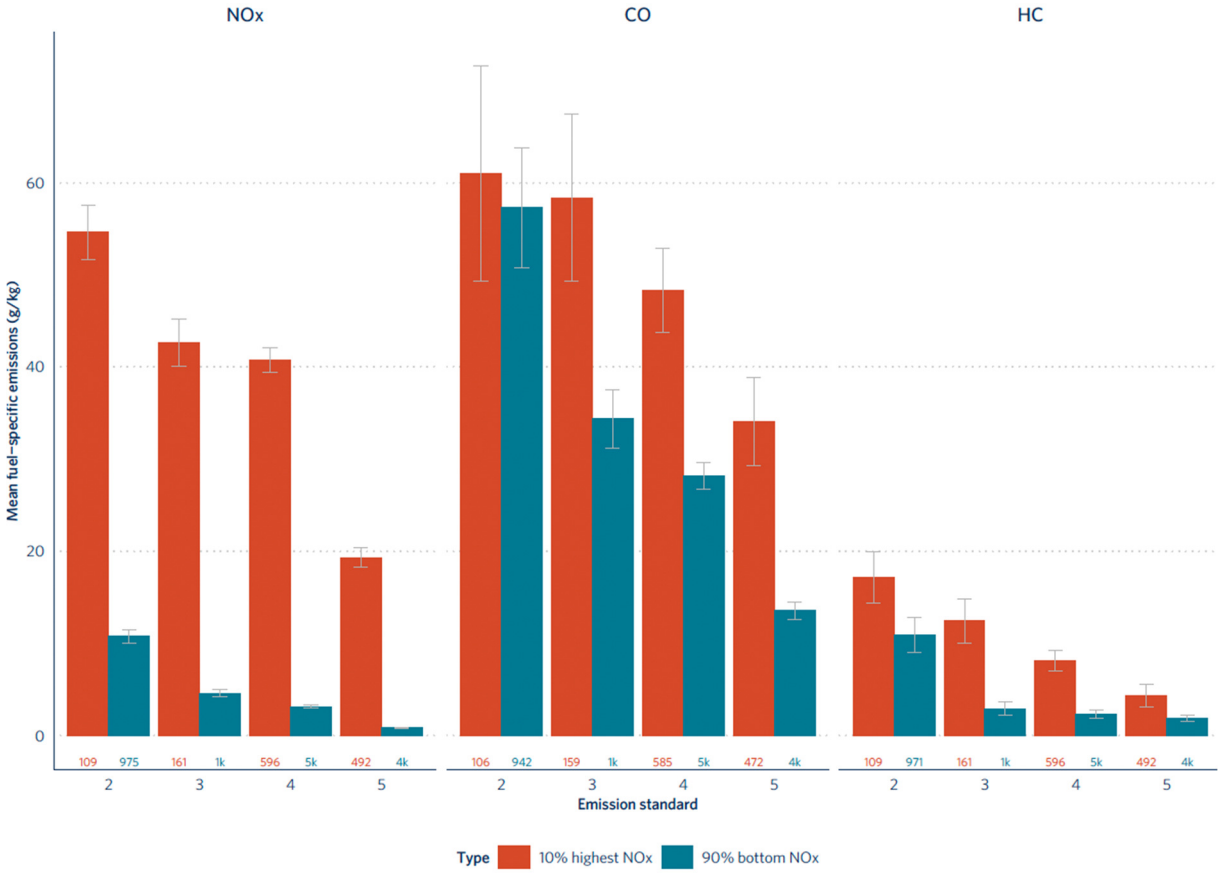

Figure 104. Comparison of trends of Fuel-specific NO_x, HC, and CO emissions from the 10% highest NO_x emitters against the 90% remaining NO_x emitters.

The average real-world PM emissions improve significantly from Euro 6 diesel onwards with the introduction of DPF and lies within the regulatory limit in Prague and Brno OPUS measurements. For Euro 5 and older diesel passenger cars, average PM emissions are higher than threshold limit as shown in Figure 105.

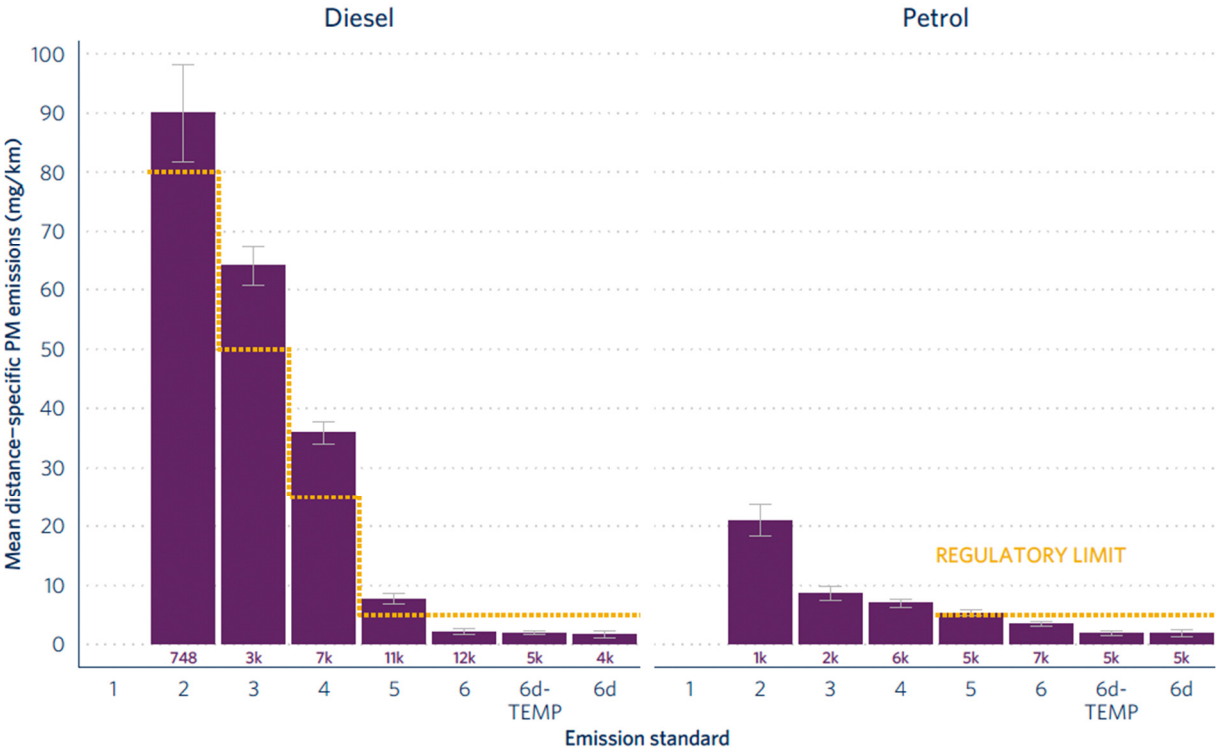

Figure 105. Distance-specific PM emissions from passenger cars for fuel types of diesel and petrol. Only results from 100 or more measurements are presented.

Share of emissions vs share of passenger car activity

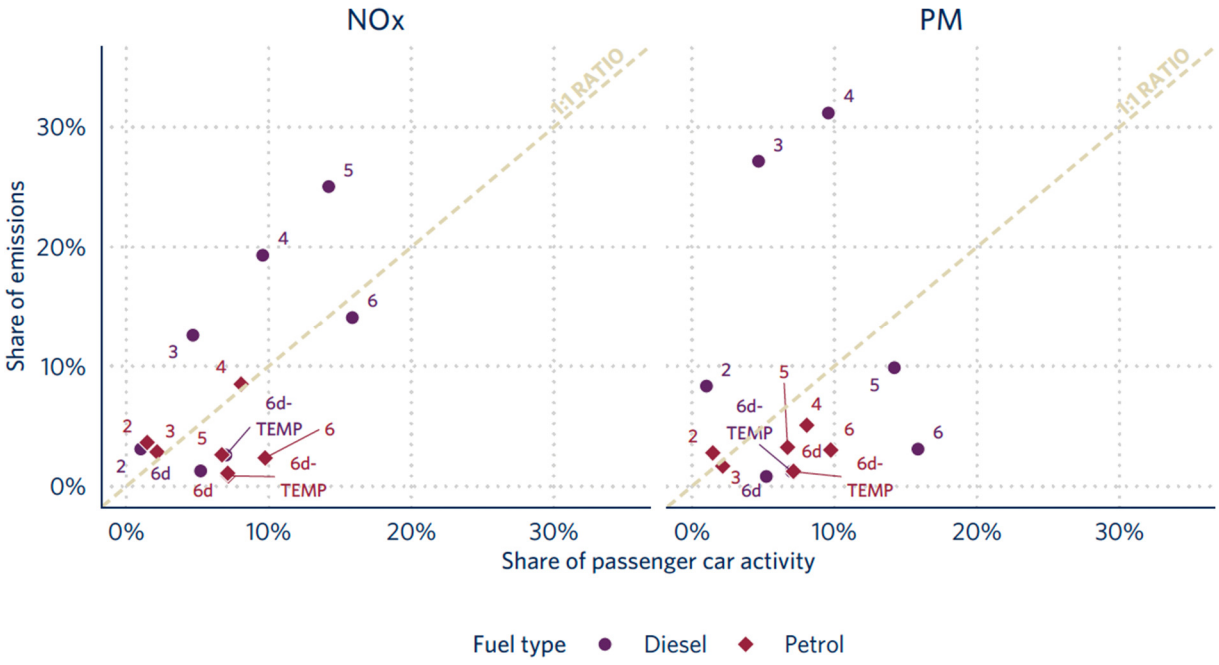

Figure 106. Passenger car activity shares and its estimated share of NO_x and PM emissions in Prague and Brno by fuel type and emission standards. Only groups with 100 or more measurements are presented.

Upon analyzing the data presented in Figure 106, we find that older diesel passenger cars produce higher share of NO_x and PM emissions compared to their share of passenger car activity. Despite making up only 30% of passenger car activity in Prague and Brno, diesel cars certified to Euro 5 earlier contribute to 60% of the total passenger car NO_x emissions. Similarly, diesel cars certified to Euro 4 and below are responsible for around 67% of total passenger car PM emissions, while accounting for approximately 15% of passenger car activity.

High PM emitters

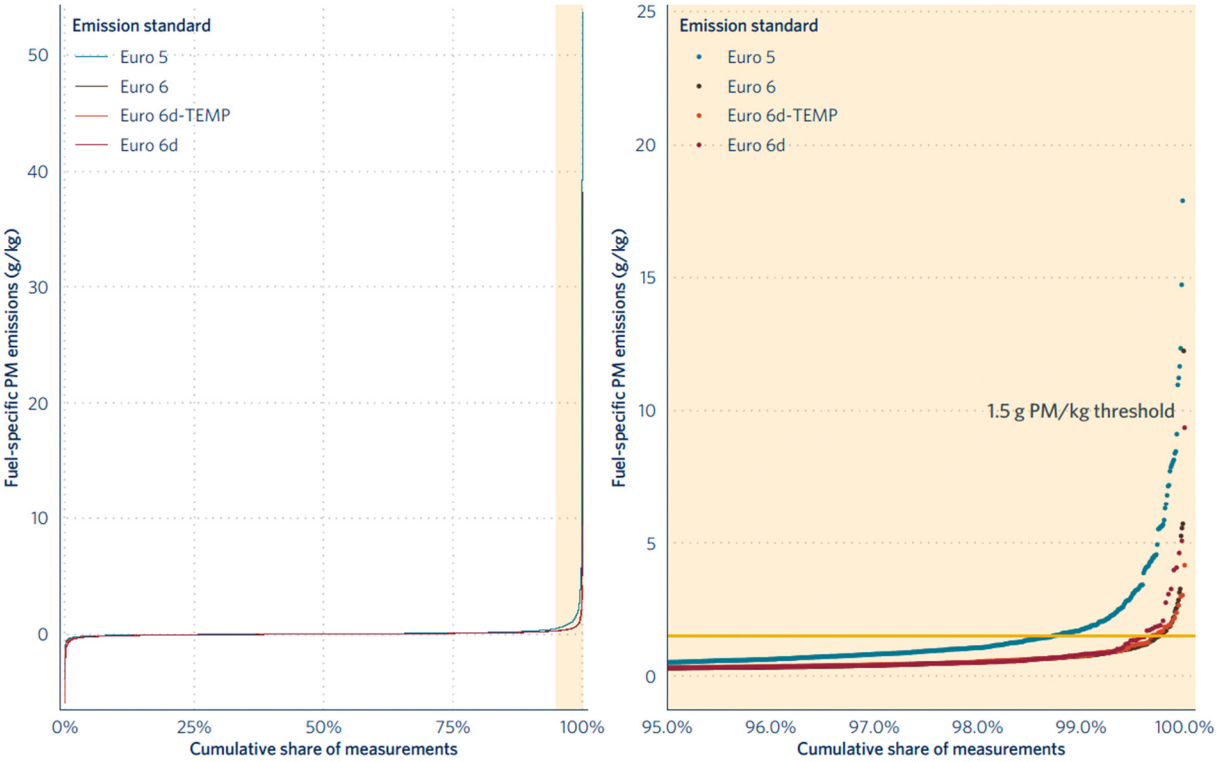

Figure 107. Cumulative distribution of diesel passenger cars and fuel-specific PM emissions by emission standard for vehicles certified to Euro 5 or above in Prague and Brno. Left panel shows the full range and the right panel shows a close-up of the 95th – 100th percentile range.

In Prague and Brno, Figure 107 indicates that only a small proportion of diesel vehicles equipped with DPF exceed 1.5g/kg PM emission, a threshold above which DPF malfunctions is considered probable.[23] As shown in the right panel, only around 1.28% of diesel vehicles certified to Euro 5, 0.246% of those certified to Euro 6, 0.31% of those certified to Euro 6d-TEMP, and 0.37% of those certified to Euro 6d were over the 1.5g/kg fuel threshold. Yet, these vehicles accounted for 42%, 26%, 21% and 38% of the total PM emissions within their respective emission standard groups Euro 5, Euro 6, Euro 6d-TEMP and Euro 6, respectively. This clearly highlights the importance of rigorous monitoring and inspection of passenger vehicles to detect these individual high emitting vehicles.

LCVs

As a part of the Prague CARES Campaign, we gathered 13,162 valid measurements for Light Commercial Vehicles (LCVs) that were mostly powered by diesel fuel. Employing the same analysis technique as the one used for Krakow, we computed the mean distance specific NO_x emissions based on the fuel-specific NO_x emissions gathered during the campaign. The results indicated that LCVs in higher classes exhibited greater NO_x emissions, as illustrated in Figure 108. The most recent Euro standards for light commercial vehicles, including Euro 6d-TEMP and Euro 6d, conform to both the on-road limit and regulatory threshold limit for emissions in line with results seen in Krakow.

[23] Mridul Gautam and Donald Stedman, "Correlation of the Real-Time Particulate Matter Emissions Measurements of an ESP Remote Sensing Device (RSD) and a Dekati Electronic Tailpipe Sensor (ETaPS) with Gravimetrically Measured PM from a Total Exhaust Dilution Tunnel System," n.d., 61.

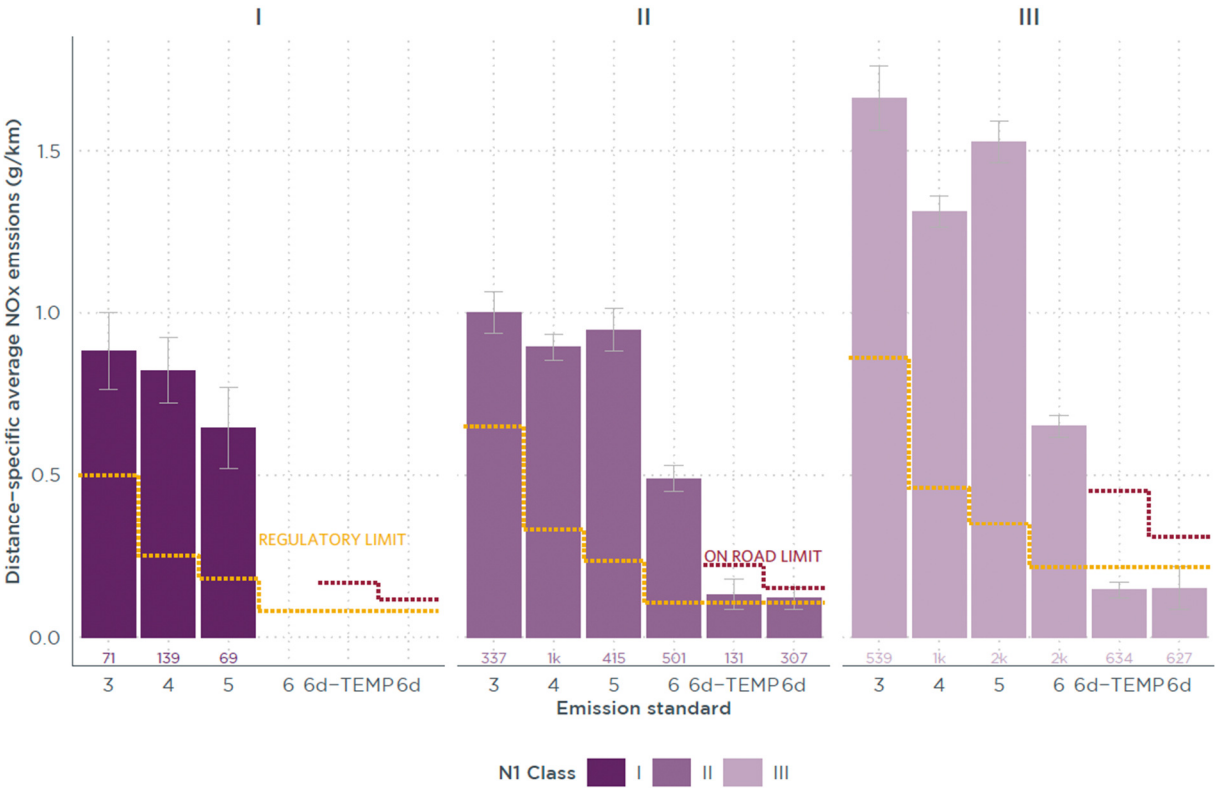

Figure 108. Distance-specific NO_x emissions from Light Commercial Vehicles (LCVs) for all classes of N1 diesel fuel type. Only results from 50 or more measurements are presented.

OPUS collected a total of approximately 1378 measurements for trucks, with 713 measurements obtained in Prague and 665 measurements obtained in Brno. We utilized the same analysis technique employed in Krakow to convert fuel-specific NO_x emissions into energy-specific levels. To reach a critical number of measurements, Euro VI-D and Euro VI-E trucks were combined under the emission standard Euro VI-D/E trucks. As shown in Figure 109, on average the NO_x emissions from Euro VI trucks exceeded the on-road threshold by nearly a factor of two, while the average NO_x emissions from Euro VI-D/E trucks were approaching the Euro VI on-road limit.

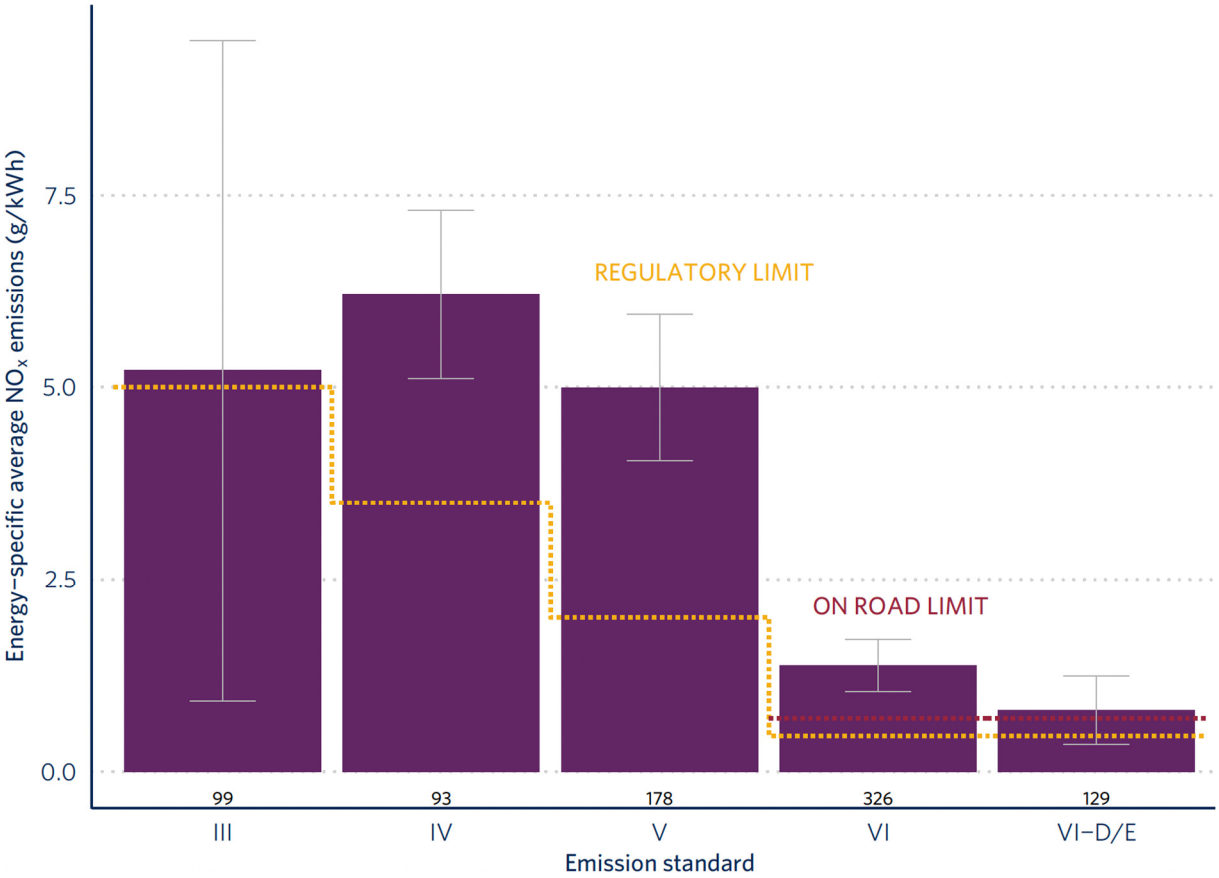

Figure 109. Energy-specific NO_x emissions for Truck in Prague and Brno. Only results from 30 or more measurements are presented.

3.2. Point Sampling

For the Prague campaign, the same PS setup as described in section 1.3.1 was deployed. PN (SPN) measurements were conducted with a catalytic stripper for volatile particle removal during the whole campaign.

Captured Vehicle Fleet:

Taking a look at the measured vehicle fleet at the four measurement spots in Prague and Brno, mainly passenger vehicles (81.7 %, Figure 111) were measured followed by light commercial vehicles (9.4 %). Also, a non-negligible number of busses (2.1 %) and heavy-duty vehicles (1.1 %) were captured. In case of fuel type (Figure 110), diesel vehicles (53.3 %) make up the largest share. For a significant number of vehicles (9.3 %), the fuel type was not defined in the vehicle technical information.

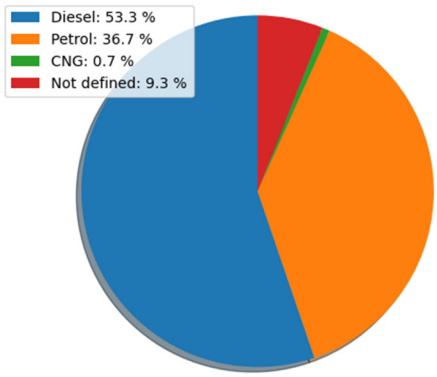

Figure 110. Prague - Captured vehicles according to fuel type.

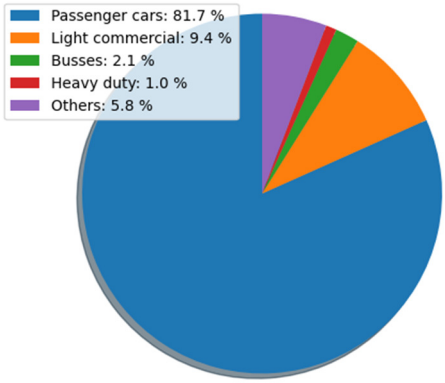

Figure 111. Prague - Captured vehicles according to vehicle type.

Emission measurement results:

Compared to the diesel passenger car BC results of the other two campaigns the Prague measurements show the highest absolute values for Euro 2-4 classes (Figure 112). BC emissions of petrol vehicles (Figure 113) are similar for the different Euro classes, with mean values around or slightly below 10 mg/km (median values < 1 mg/km). Compared to diesel passenger car emissions, the petrol BC emissions are somewhere between the emissions of the diesel Euro 5 and Euro 6 passenger cars. Compared to the other campaigns, BC emissions of petrol passenger cars were higher compared to the Milan campaign and were partly in the same range as for the Krakow measurements. Ambient temperatures were especially during the first days of the campaign rather low (< 10 °C). PN measurements show for both diesel and petrol vehicles the same trends as described for BC (Figure 114 and Figure 115). In case of measured NO_x emission data (Figure 116 and Figure 117), a strong decrease for Euro 6 vehicles can be stated, similarly to the other campaigns. Results are quite similarly distributed compared to the Milan campaign for both diesel and petrol vehicles. NO_x emissions of petrol vehicles are steadily decreasing with increasing Euro norm.

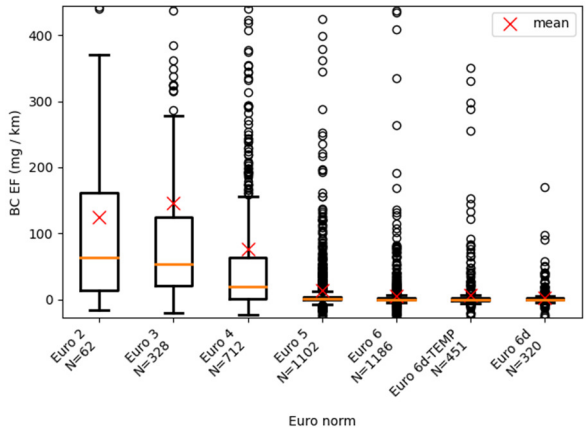

Figure 112. Prague - BC emissions of diesel passenger cars for different Euro norms.

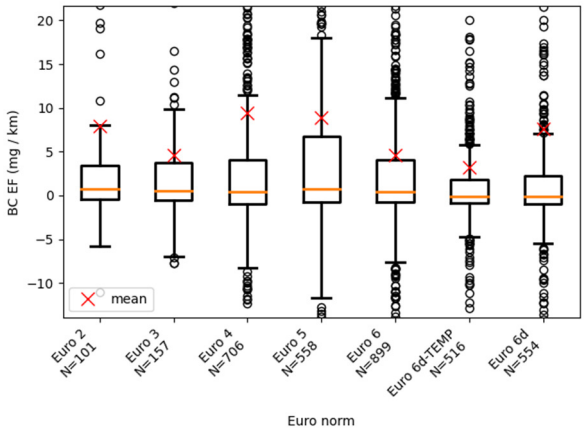

Figure 113. Prague - BC emissions of petrol passenger cars for different Euro norms.

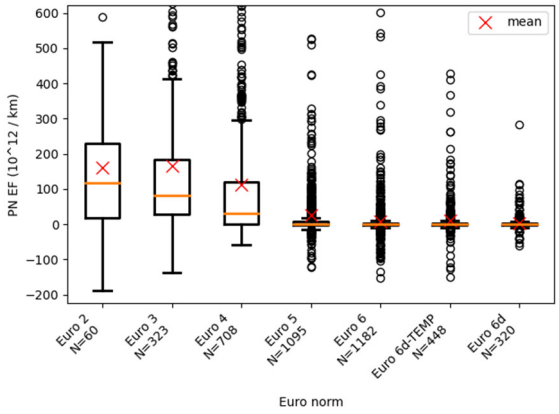

Figure 114. Prague - SPN emissions of diesel passenger cars for different Euro norms

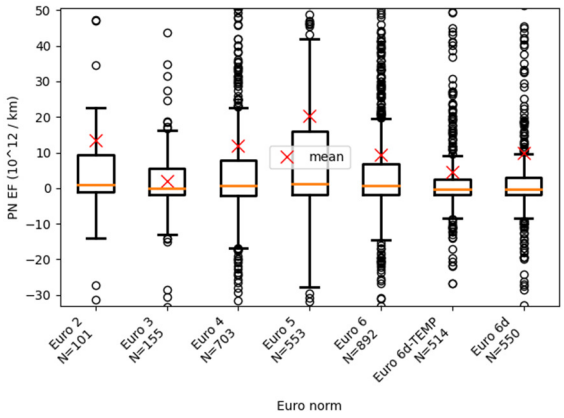

Figure 115. Prague - SPN emissions of petrol passenger cars for different Euro norms

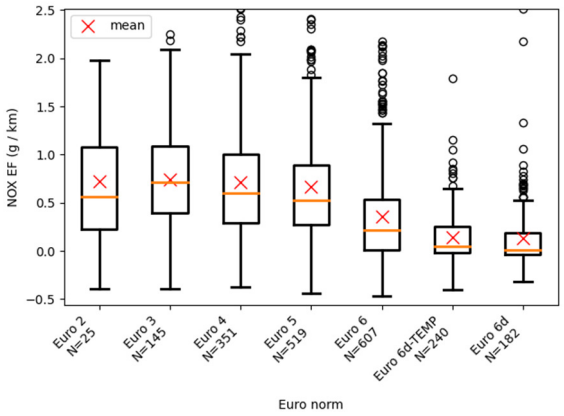

Figure 116. Prague - NO_x emissions of diesel passenger cars for different Euro norms

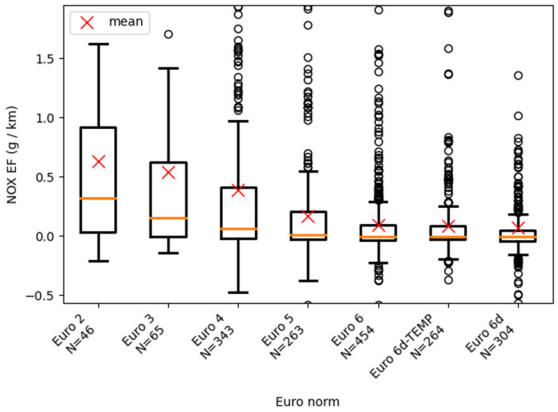

Figure 117. Prague - NO_x emissions of petrol passenger cars for different Euro norms

3.3. Plume chasing

3.3.1. Measurement Setup

During the measurement campaign in Prague a total of 2,000 valid vehicle chases were conducted using the Plume Chasing measurement technique. Out of these, over 900 were heavy-duty vehicles (HDVs), a main focus of the campaign. Two different setups were used during the campaign. The first setup was a scientific measurement setup (shown on the left in Figure 118118, which had different instruments for particle and gas measurements installed in a measurement van from TNO (see Table 7). The goal was to compare different particle instruments and find a suitable instrumentation for screening high particle

Figure 118118. Two Plume Chasing measurement setups. Scientific setup with extensive instrumentation for research purposes (left) and simple setup for the use of authorities (right).

emitters using the Plume Chasing method. The second setup (shown on the right Figure 118118; Table 7) with only one ICAD instrument (Airyx GmbH) was used for demonstration purposes and for the NO_x high-emitter identification of HDVs together with the Czech authorities.

The Plume Chasing measurements of HDVs were conducted on the D1 highway between Prague and Brno. A new emission software from Airyx GmbH (see Figure 120) was used to indicate with a traffic light system whether the vehicle under examination was a low, suspicious, or high NO_x emitter with green, yellow, or red, respectively. This allowed for simple recommendations to be given to the police waiting on the highway before the Do Bernartice police inspection location.

Table 7: Used instruments during the Prague measurement campaign.

Instruments (scientific setup)	Instruments (simple setup)	Measured Species
ICAD	ICAD	NO_x, NO_2, CO_2
Counter		PN (D_{50} @ 23 nm)
SMPS		PN_{90nm}
TEN		PN (D_{50} @ 23 nm)
Black Carbon Tracker		BC, CO_2
GPS	GPS	Location, Speed

Figure 120: The tablet is used to display real-time data and is connected to the ICAD instrument via WIFI.

3.3.2. Investigated HDVs and emission results

On the Czech highway D1, the majority of HDVs are of the Euro VI category (>80%), followed by ~15% Euro V HDVs (see Figure 120). The main brands of these vehicles are DAF, Mercedes, Volvo, Scania, and MAN, which make up more than 80% of the HDVs. These brands have a relatively similar share for both Euro V and VI, with Mercedes being the dominant brand for Euro V trucks. The country of origin of the trucks is mainly Czech (38%), followed by Polish (12%), Romanian (11%), Hungarian and Slovakian trucks.

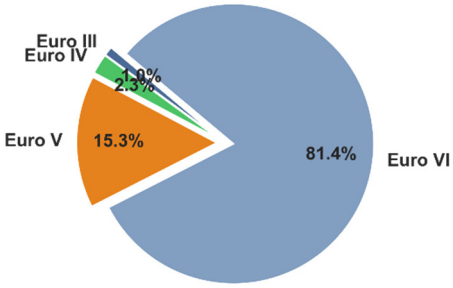

Figure 120: Euro classes of measured HDVs.

The NO_x, NO_2, PM, PN and PN_{90nm} emissions of HDVs measured by the Plume Chasing method for different Euro classes are presented in Figure 121. The emissions of all species are decreasing with increasing Euro class, except for the NO_x, NO_2 and PN concentration from Euro III to Euro IV. There a rise of average emissions can be observed for the Counter and TEN instrument. NO_x emissions decrease on average significantly from 2,845 mg/kWh for Euro V to 900 mg/kWh for Euro VI HDVs. The PN (SMPS, Counter) and PM (BCT) emissions show a 50% decrease of emissions from Euro V to Euro VI HDVs.

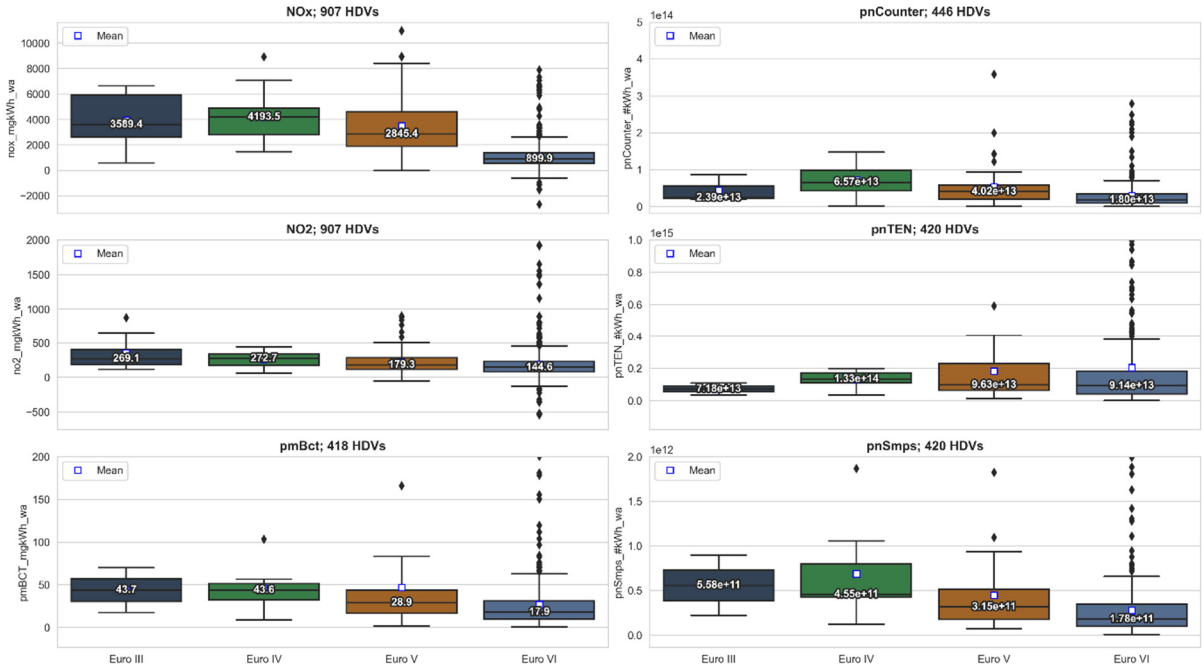

Figure 121. NO_x, NO_2, PM and PN and PN_{90nm} emissions of HDVs measured by Plume Chasing for different Euro classes.

3.3.3. HDV NO_x high-emitter identification with Plume Chasing and Police inspection

The study found that approximately 39% of the chased HDVs had high or suspicious emissions (Figure 122). The emission thresholds for high and suspicious emitters are summarized in Table 8. However, this percentage increased to 61% for Euro V HDVs (Figure 122, top right), indicating that this Euro class had a larger share of high emitters compared to Euro VI.

Table 8. Thresholds for Euro V and Euro VI HDVs.

	Euro V	Euro VI
Classification	mg/kWh	mg/kWh
low (up to)	<2500	<1200
suspicious (up to)	<3500	<2200
high (above)	>3500	>2200
Euro emission limit	<2000	<460
RDE conformity factor		1.5

Furthermore, the study also revealed that 52% of HDVs from countries such as Romania, Bulgaria, Bosnia and Herzegovina, Serbia, Slovenia, and Turkey had high or suspicious emissions. Notably, there was thus a larger share of suspicious and high emitters for HDVs from some countries in the southeast region.

The study also analyzed emissions during different times of the day and found that a larger share (70%) of HDVs had high or suspicious emissions during the night (after 18:00).

During inspections conducted with the Czech authorities (see Figure 124, left), 17 of the investigated HDV (24% suspicious, 76% high emitters) were inspected, with 41% of those being Euro V and 59% being Euro VI. The inspections were led by NO_x consulting, Martin Kristensen.

For all inspected vehicles, a reason for the high emissions was identified (see Figure 123). It was observed that vehicles with very high emissions were more likely to be manipulated compared to those with only suspicious emissions. Several emulators could be found (see e.g., Figure 124, right). A software issue was found in Volvo trucks due to a missing mandatory update of OE software, which reveals a lack of legislation on mandatory updates if trucks are not maintained at a manufacturer workshop. Euro V vehicles had a higher share of manipulations, while Euro VI had more defects/errors and software issues.

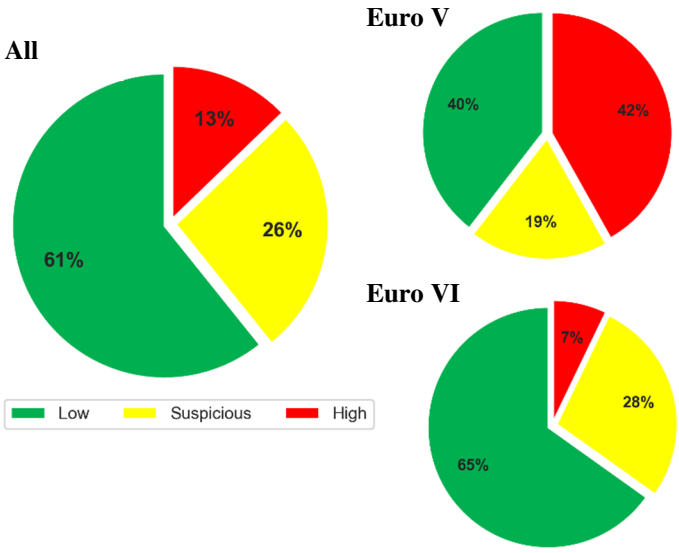

Figure 122: Percentage of low (green), suspicious (yellow) and high (red) emitters of all (left), Euro V (top right) and Euro VI (bottom right) HDVs.

The results of the investigations demonstrate that the emission inspection with Plume Chasing is well suited to efficiently identify illegally defective and manipulated HDV SCR systems for further inspection. It is a simple tool for inspection authorities to reliably identify manipulated and defective HDVs.

Figure 124: High NO_x emitter inspection of HDVs by Czech police (left); emulator that was found during inspection of high NO_x emitters identified by the Plume Chasing method (right).

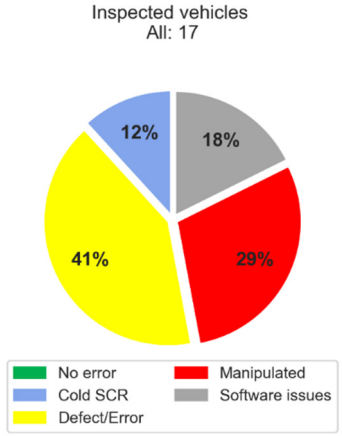

Figure 123: Results of HDV inspections together with the authorities.

3.3.4. Impact of high emitter HDVs

As inspections have proven that the Plume Chasing is reliable in identifying illegally defective and manipulated NO_x systems of HDVs, the impact of these vehicles on total emissions has been analysed. The observed emissions are statistically analysed and the histograms of occurrence together with the cumulative distribution can be found in Figure 126 and Figure 125 for Euro V and VI, respectively. From these, it is calculated that clean / low emitters with a correctly working emission reduction system show 1,589 mg/kWh and 598 mg/kWh NO_x for Euro V and VI, respectively. High emitters feature 5,508 mg/kWh and 3,939 mg/kWh, respectively, which is an average increase by factors of 3.4 and 6.6 relative to the low emitters but can be up to 20 times higher in individual cases. The classified suspicious emitters show 2,879 mg/kWh and 1,544 mg/kWh NO_x emissions, respectively. The average HDV emissions due to these high and suspicious emitters are significantly increased in comparison to the low emitters. For Euro V this results in an increase of the average fleet by +118%, and for EURO VI it increases by +84%. In other words, defective and manipulated HDVs cause approximately a doubling of the HDV NO_x emissions.

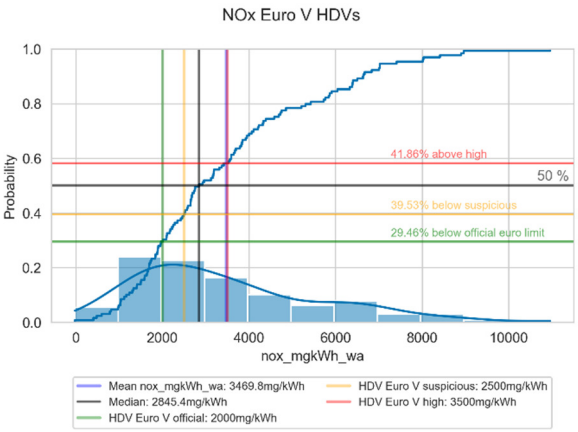

Figure 126: Histogram of Euro V HDV NO_x emissions; blue line indicates the accumulated emission from low to high emitters. Only 39.53% are found as low (clean) emitters.

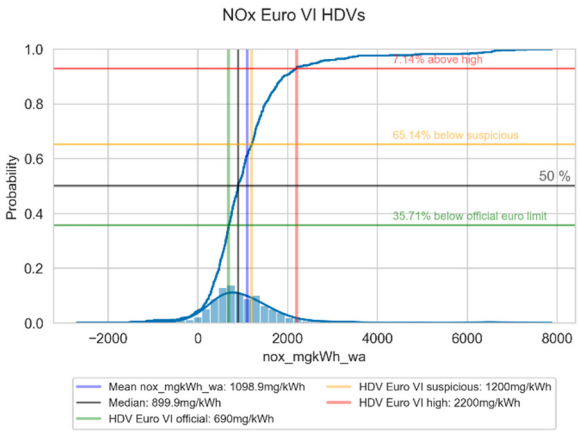

Figure 125: Histogram of Euro VI HDV NO_x emissions; blue line indicates the accumulated emission from low to high emitters. 65.14% are found as low (clean) emitters.

3.3.5. Different Particle Instruments for Plume Chasing

Different particle instruments were used in the scientific Plume Chasing measurement configuration (Table 7). Two diffusion chargers (particle counter, TEN AEM; counter, AVL DiTest) for measuring PN and one photoacoustic instrument (Black Carbon Tracker (BCT), TUG, developed within the CARES project) for measuring BC were compared. We used an SMPS (Electrostatic Classifier 3082 and TSI 3775 CPC) measuring 90 nm particles as identified currently best reference instrument for identifying defective Diesel Particulate Filters (DPFs) (see Deliverable 1.1 and 1.2) and compared the other instruments to it. One of our goals was to find for the Plume Chasing application a cheaper and easier-to-operate particle instrument for screening, in comparison to the SMPS.

An excerpt from a time series showing the measurements of the different tested instruments can be seen in Figure 127. The scatter plots in Figure 128 compared the PN and PM emissions of individual HDVs for the three different tested instruments (Counter, TEN, BCT) to the PN of the SMPS. If the SMPS detected high emissions for a chased vehicle, all other instruments also detected them. Thus, we can conclude that all tested instruments are capable of observing a high emitter, even if the TEN and the counter from AVL DiTest were not developed for this application. However, in several situations, the TEN instrument detected high counts that were not seen by the other instruments (see Figure 127 blue line with peaks A, B, C and Figure 128, upper left corner of middle panel). The reasons for those false positive misidentifications of high emitters need further studies. It should be considered that the TEN instrument and the counter from AVL DiTest were developed for PTI measurements directly at the exhaust with much higher particle concentrations compared to Plume Chasing, where also additional environmental factors and pollution sources play a role. Based on these results, it cannot be concluded that the overestimation of PN of the TEN instrument in this Plume Chasing configuration has any effect on its application of PTI measurements. Overestimation of the TEN device can be due to multiple reasons, this will be further researched in the future.

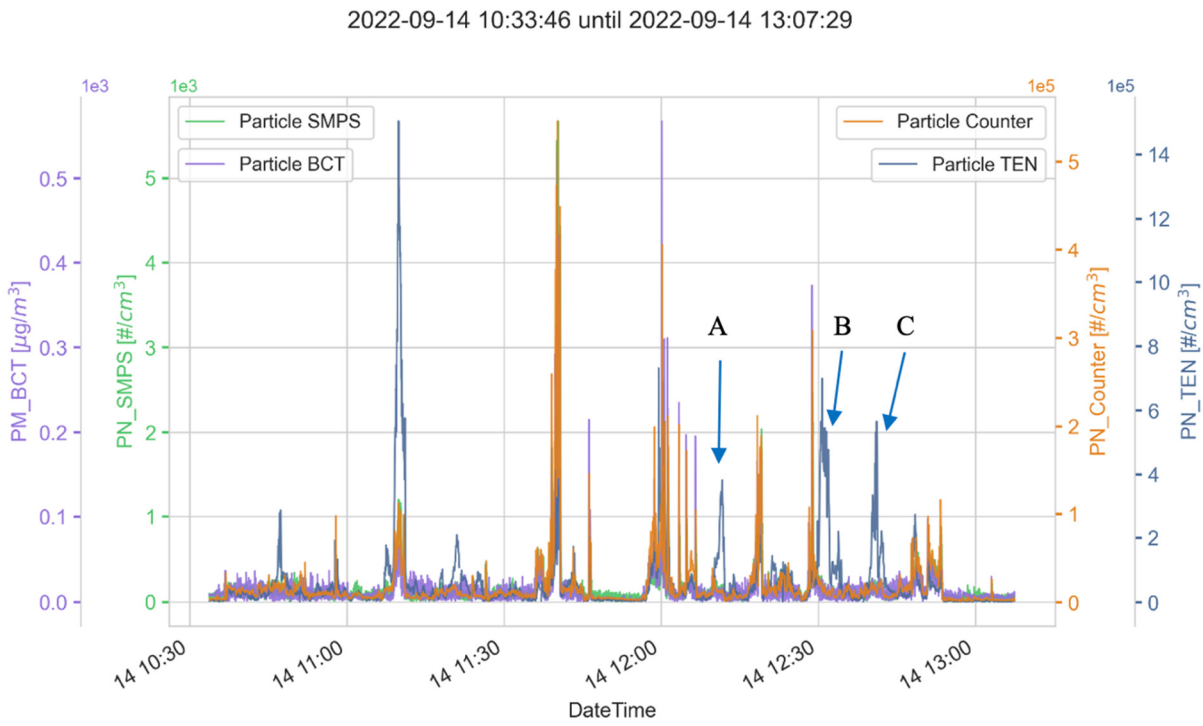

Figure 127. Time series of the Plume Chasing PN instruments (SMPS in green, Counter in orange, TEN in blue) and PM instrument (BCT in purple) for 14th Sept 2022, 10:34-13:07.

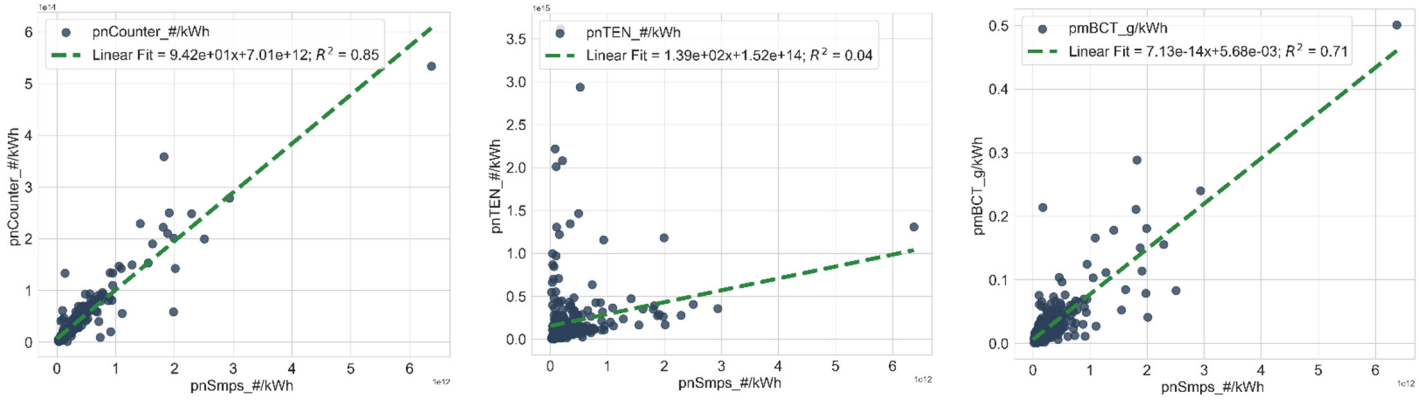

Figure 128. Comparison between PN of Counter and TEN as well as PM of BCT with PN of SMPS for 327 HDVs. Note that larger spread in the correlation of the TEN and SMPS instrument is focused on the false positive side. Spread in correlation can be due to numerous reasons (e.g., larger size range compared to SMPS) and will be the topic of further research.

4. Cross-campaign emission comparison

4.1. Commercial open-path instruments

Cross-campaign comparison of distance-specific NO_x and PM emissions are shown in Figure 129 and Figure 130. Overall, the results demonstrate that vehicles measured in all three cities are emitting NO_x at comparable levels and that the two different commerical remote sensing systems do not have big discrepancies between how they measure NO_x emisisons. Both median and mean NO_x emissions from diesel vehicles measured in all three cities showed a good agreement. Notably, diesel vehicles have achieved comparable NO_x emission performance with petrol vehicles with RDE testing (Euro 6d-TEMP and Euro 6d). Those from petrol vehicles, however, reaffirmed the likely presence of vehicles with defective or tampered three-way catalysts in the Prague measurements, largely indicated by higher mean and median NO_x emissions from petrol vehicles certified to Euro 5 and below (Figure 129). The CARES remote sensing data also generated emission factors from LPG vehicles commonly found in Milan and Krakow, which showed higher NO_x emissions than their petrol counterparts.

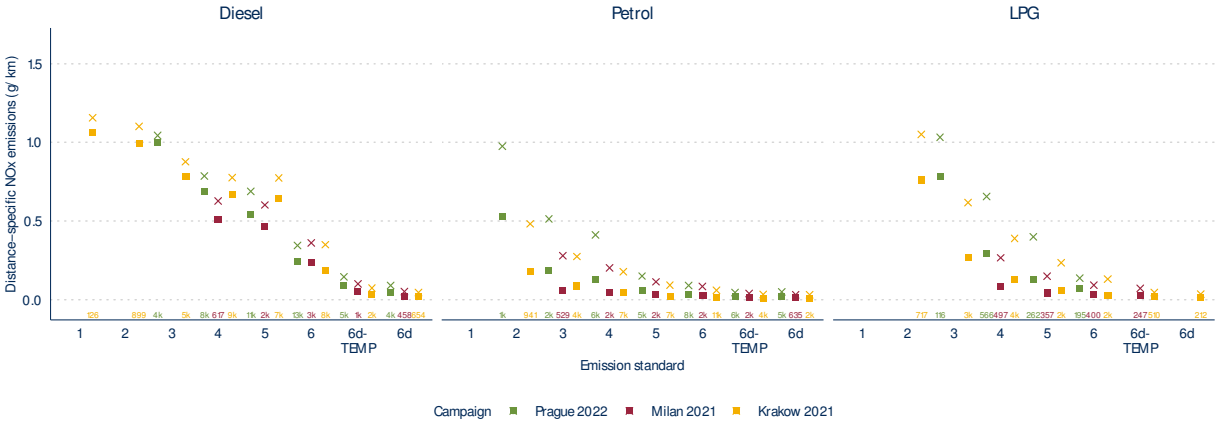

Figure 129. Comparison of distance-specific NO_x emissions of passenger vehicles by fuel type and emission standard from the three city measurement campaigns measured by open-path systems. Square. Whiskers, and cross indicate median value, interquartile range, and mean value, respectively.

Distance-specific mean PM emissions from vehicles measured in all three cities showed similar levels. In general, looking at the mean values diesel vehicles from all three cities show a large improvement in PM emission performance from Euro 5, from which standard diesel particulate filters were introduced. In all three cities, the mean PM emissions are higher than the median PM emissions, highlighting a presence of a small fraction of high-emitting vehicles within each standard group. The highly elevated PM emissions from the petrol vehicles measured in Krakow are evident when compared with the vehicles measured in Milan and Prague, the reason for which is explained in the campaign-specific section.

The interquartile ranges of the EDAR measurements collected in Milan, however, demonstrated that the Milan measurements are concentrated around zero (0) while a few high PM readings pull up the average. This indicates that the EDAR systems may not be able to accurately capture low levels of

tailpipe PM emissions under a certain threshold and warrants further assessment of its performance.

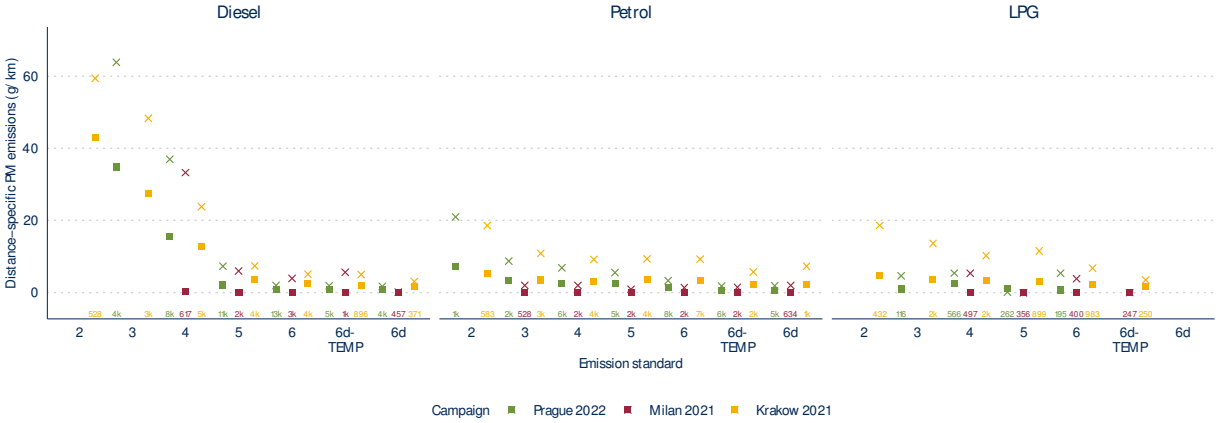

Figure 130. Comparison of distance-specific PM emissions of passenger vehicles by fuel type and emission standard from the three city measurement campaigns measured by open-path systems. Square. Whiskers, and cross indicate median value, interquartile range, and mean value, respectively.

4.2. Point sampling

In Figure 131 to Figure 134, direct comparisons of the three different city measurement campaigns for BC and NO_x emissions of diesel and petrol passenger cars are depicted. For all campaigns, similar trends can be observed, with BC emissions strongly decreasing with the introduction of the DPF (post Euro 4) or the introduction of more stringed type approval standards for Euro 6d-TEMP and Euro 6d NO_x emissions. However, differences can be seen between the emission distributions of the different campaigns, which are described in the sections of the individual campaigns.

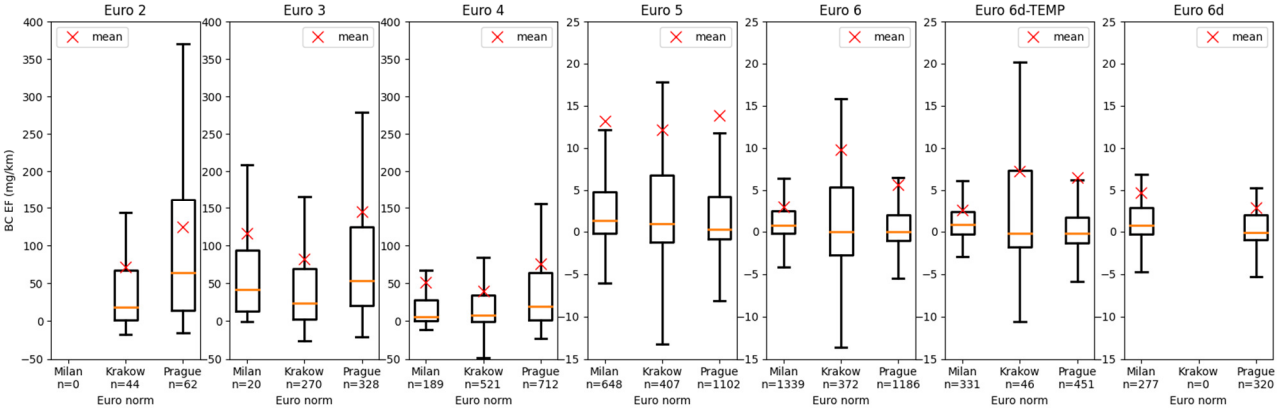

Figure 131. Comparison of distance-specific BC emissions of diesel passenger vehicles by emission standards from the three city measurement campaigns measured by the PS system. Y-scale adjusted between Euro2-4 and Euro 5-6d emission standards.

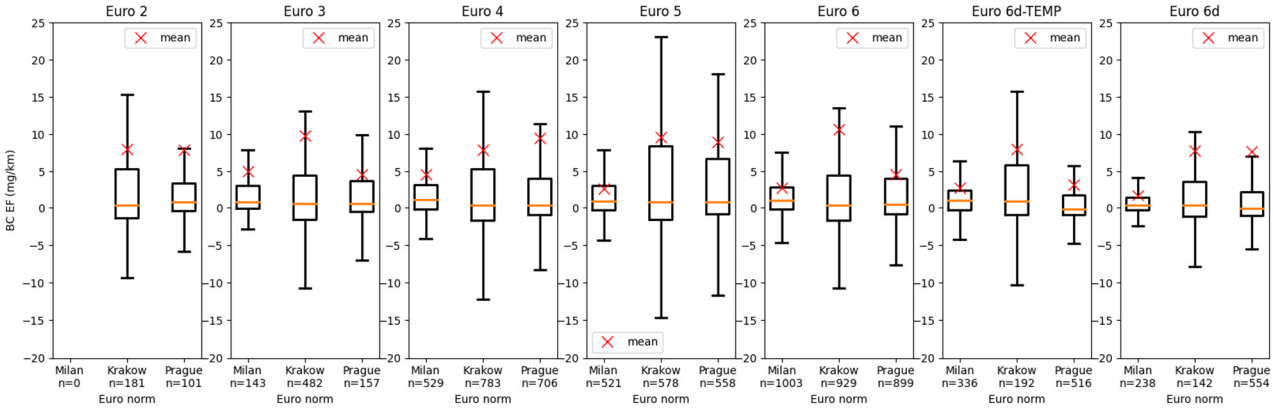

Figure 132. Comparison of distance-specific BC emissions of petrol passenger vehicles by emission standards from the three city measurement campaigns measured by the PS system.

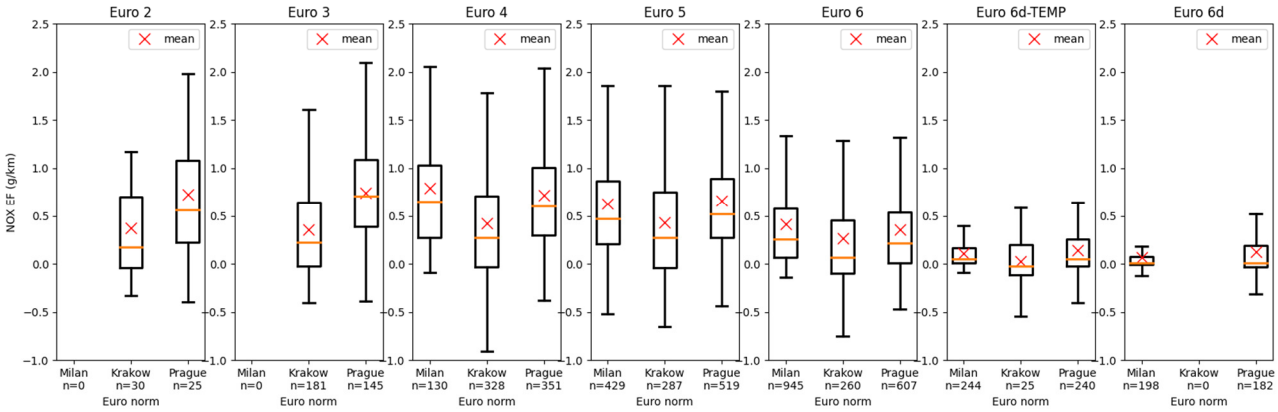

Figure 133. Comparison of distance-specific NO_x emissions of diesel passenger vehicles by emission standards from the three city measurement campaigns measured by the PS system.

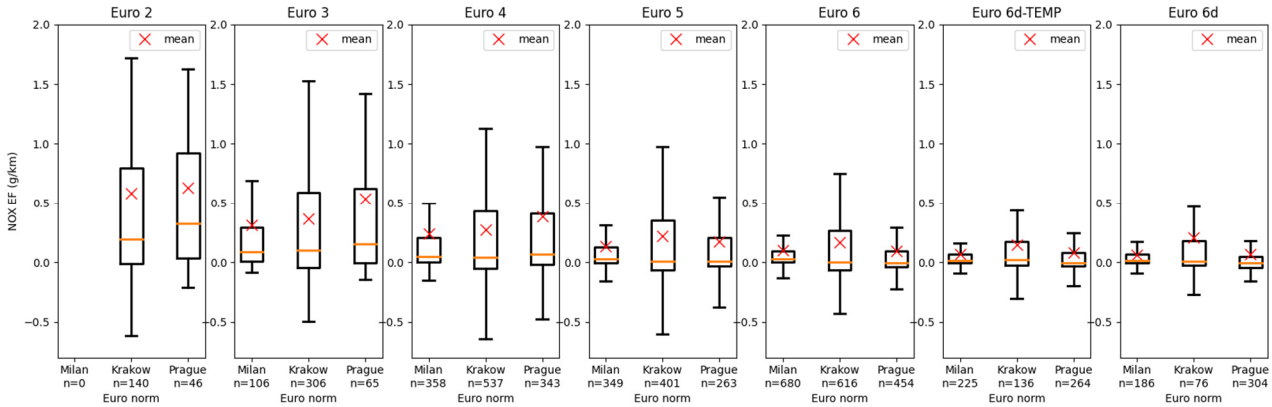

Figure 134. Comparison of distance-specific NO_x emissions of petrol passenger vehicles by emission standards from the three city measurement campaigns measured by the PS system.

Table 9 in the Appendix summarizes mean and median NO_x, BC / PM emissions from commercial open-path and point sampling instruments.

5. Conclusion

Although the initial schedule was impacted by COVID-19 restrictions, testing campaigns successfully took place in Milan, Krakow and Prague and demonstrated the feasibility of multiple remote emissions sensing (RES) technologies in real-traffic situations: commercial cross-road and overhead open-path techniques, point sampling, and plume chasing. Overall, more than over 300,000 data points were collected across three campaigns. The emission results were compared between those techniques as well as with PEMS. The Milan campaign also provided the opportunity to evaluate advanced air quality sensors and the effect of street cleaning on PM concentrations.

In Milan, the potential of remote sensing in the emission assessment of plug-in hybrid vehicles was demonstrated. Despite the small number of LPG- and CNG-powered cars, the results suggested that their emissions are not lower than their petrol equivalents. Point sampling of speciated VOCs further revealed that LPG fuel type emits multiple times higher VOCs (VOC/CO2) than standard gasoline type, likely contributed largely by evaporative emissions. These results are particularly relevant for Milan, as the current low-emission zone exempts LPG and CNG vehicles from its restrictions. Point sampling of speciated VOCs showed that the highest VOC/CO_2 ratio originated from motorcycles and mopeds, approximately four times higher than goods vehicles and 5 times higher than passenger cars. Mobile measurements indicated that these vehicle types could play a key role in spatial emissions of NO_x and VOCs.

All techniques confirmed that pre-Euro 5 diesel are the highest emitters for NO_x and PM. From Euro 5 onwards diesel vehicles show a significant reduction in PM, PN and BC emissions. However, their mean emission appears to have largely exceeded the type-approval limits due to a small share of vehicles likely malfunctioning or tampered. Euro 6d-TEMP and 6d light-duty vehicles observed in all three cities showed the lowest emission across all pollutants, indicating the improvement in regulations with the introduction of real-driving emissions (RDE) testing.

The comparison of the EDAR system with PEMS and point sampling shows good correlation for gaseous pollutants (NO_x, THC), but not for particles. PEMS and point sampling showed good agreement for NO_x and PN.

Air quality sensors were found to be in good agreement with reference instruments. Hotspots were linked to the passages of high-emitting vehicles, as captured by the advanced air quality sensors. Ammonia concentrations in the city were found to be higher than expected, possibly linked to an underestimation of ammonia emissions from road vehicles. Intensive street cleaning was correlated with lower PM concentrations due the reduction of resuspension.

In Krakow, PM emissions from petrol vehicles in winter were found to be higher than in other campaigns by both Point Sampling and the cross-road OPUS instrument.

In Prague, average NO_x emissions from older petrol cars were remarkably higher than in other campaigns. Point sampling measurements showed the highest PM absolute values for diesel Euro 2-4 classes across campaigns. Those results call for the need for a rigorous monitoring and inspection of passenger vehicles to detect individual high emitting vehicles.

Plume Chasing was applied to measure the NO_x, PN and BC emissions of about 2,000 individual vehicles . Those included mainly trucks but plume chasing also successfully measured busses and light-duty vehicles. It successfully identified high NO_x-emitting HDVs in real-time, as verified by direct inspections conducted by the police at the roadside. The inspections mainly revealed illegal defective or manipulated emission systems. This demonstrates that Plume Chasing can reliably identify and preselect HDVs for further inspections, making vehicle control much more efficient. The analysis of the emission data showed that the high emitters increase the total HDV fleet NO_x emissions by approx. 100% (+118% for Euro V, +84% for Euro VI), highlighting the importance of better controlling these vehicles. Furthermore, the application of various particle instruments for Plume Chasing demonstrated the potential for using current PN / PM technologies for defective DPF screening.

6. Appendix

Table 9: Mean and median NO_x, BC / PM emissions from commercial open-path and point sampling instruments measured in Milan, Krakow, and Prague.

Campaign: Milan (mean / median)								
Instrument	PS	RS-HEAT	PS	RS-HEAT	PS	RS-HEAT	PS	RS-HEAT
Fuel type	Diesel	Diesel	Petrol	Petrol	Diesel	Diesel	Petrol	Petrol
Emission type / Euro norm	BC (mg/km)	PM (mg/km)	BC (mg/km)	PM (mg/km)	NOx (g/km)	NOx (g/km)	NOx (g/km)	NOx (g/km)
Euro 2			1.4 / 0.7					
Euro 3	116.8 / 42.2		5.1 / 0.8	1.9 / 0.0	0.53 / 0.46		0.31 / 0.09	0.28 / 0.06
Euro 4	51.1 / 6.0	33.3 / 0.2	4.6 / 1.1	1.9 / 0.0	0.79 / 0.65	0.63 / 0.51	0.24 / 0.05	0.2 / 0.04
Euro 5	13.2 / 1.3	5.9 / 0.1	2.7 / 0.9	0.9 / 0.0	0.63 / 0.47	0.60 / 0.46	0.13 / 0.03	0.11 / 0.04
Euro 6	2.9 / 0.8	3.9 /0.0	2.8 / 1.0	1.3 / 0.0	0.42 / 0.26	0.36 / 0.24	0.10 / 0.03	0.09 / 0.03
Euro 6d-TEMP	2.5 / 0.8	5.6 / 0.0	2.8 / 0.9	1.4 / 0.0	0.11 / 0.05	0.10 / 0.05	0.07 / 0.02	0.04 / 0.02
Euro 6d	4.7 / 0.7	0.1 / 0.0	1.7 / 0.3	2.0 / 0.0	0.07 / 0.01	0.05 / 0.02	0.06 / 0.01	0.03 / 0.02

Campaign: Krakow (mean / median)								
Instrument	PS	RS-OPUS	PS	RS-OPUS	PS	RS-OPUS	PS	RS-OPUS
Fuel type	Diesel	Diesel	Petrol	Petrol	Diesel	Diesel	Petrol	Petrol
Emission type / Euro norm	BC (mg/km)	PM (mg/km)	BC (mg/km)	PM (mg/km)	NOx (g/km)	NOx (g/km)	NOx (g/km)	NOx (g/km)
Euro 2	71.2 / 19.0	59.4 / 43.1	7.9 / 0.3	18.5 / 5.2	0.37 / 0.18	1.10 / 0.99	0.58 / 0.19	0.48 / 0.18
Euro 3	82.3 / 23.6	48.4 / 27.3	9.9 / 0.5	10.8 / 3.5	0.36 / 0.22	0.88 / 0.79	0.36 / 0.10	0.27 / 0.09
Euro 4	39.2 / 7.5	23.8 / 12.6	7.9 / 0.3	9.1 / 3.1	0.42 / 0.28	0.78 / 0.67	0.27 / 0.04	0.18 / 0.05
Euro 5	12.1 / 1.0	7.4 / 3.7	9.6 / 0.7	9.3 / 3.5	0.43 / 0.27	0.77 / 0.64	0.22 / 0.01	0.09 / 0.02
Euro 6	9.7 / -0.1	5.0 / 2.6	10.6 / 0.3	9.2 / 3.4	0.26 / 0.07	0.35 / 0.18	0.17 / 0.00	0.06 / 0.01
Euro 6d-TEMP	7.2 / -0.2	4.9 / 2.0	8.0 / 0.9	5.7 / 2.2	0.03 / -0.02	0.07 / 0.03	0.15 / 0.02	0.03 / 0.01
Euro 6d		3.0 / 1.8	7.8 / 0.4	7.3 / 2.2		0.05 / 0.02	0.21 / 0.01	0.03 / 0.01

Campaign: Prague (mean / median)								
Instrument	PS	RS-OPUS	PS	RS-OPUS	PS	RS-OPUS	PS	RS-OPUS
Fuel type	Diesel	Diesel	Petrol	Petrol	Diesel	Diesel	Petrol	Petrol
Emission type / Euro norm	BC (mg/km)	PM (mg/km)	BC (mg/km)	PM (mg/km)	NOx (g/km)	NOx (g/km)	NOx (g/km)	NOx (g/km)
Euro 2	124.3 / 63.7		7.9 / 0.8	21.0 / 7.1	0.72 / 0.57		0.63 / 0.32	0.97 / 0.53
Euro 3	145.3 / 54.1	63.9 / 34.7	4.6 / 0.5	8.7 / 3.4	0.74 / 0.71	1.04 / 1.00	0.54 / 0.15	0.51 / 0.19
Euro 4	76.4 / 19.6	36.9 / 15.6	9.4 / 0.4	6.8 / 2.4	0.71 / 0.60	0.79 / 0.69	0.39 / 0.07	0.41 / 0.13
Euro 5	13.8 / 0.3	7.3 / 2.2	8.9 / 0.7	5.5 / 2.5	0.66 / 0.52	0.69 / 0.54	0.17 / 0.01	0.15 / 0.06
Euro 6	5.6 / 0.0	1.9 / 0.9	4.6 / 0.4	3.3 / 1.5	0.36 / 0.22	0.35 / 0.24	0.09 / -0.01	0.09 / 0.03
Euro 6d-TEMP	6.5 / -0.2	1.9 / 0.9	3.2 / -0.1	1.7 / 0.6	0.14 / 0.05	0.15 / 0.09	0.08 / 0.00	0.05 / 0.02
Euro 6d	2.8 / -0.1	1.7 / 0.8	7.6 / -0.1	1.9 / 0.6	0.13 / 0.01	0.09 / 0.05	0.07 / -0.01	0.05 / 0.02